**Transcriptomic analysis of thyroid hormone effects on *Rana [Lithobates] catesbeiana* tadpole tissues with special emphasis on the innate immune system**

by

Shireen Hanna Partovi
B.Sc. Biotechnology, Utah Valley University, 2014

A Thesis Submitted in Partial Fulfillment
of the Requirements for the Degree of

MASTER OF SCIENCE

in the Department of Biochemistry and Microbiology

# Supervisory Committee

**Transcriptomic analysis of thyroid hormone effects on *Rana [Lithobates] catesbeiana* tadpole tissues with special emphasis on the innate immune system**

by

Shireen Hanna Partovi
B.Sc. Biotechnology, Utah Valley University, 2015

**Supervisory Committee**

Dr. Caren C. Helbing (Department of Biochemistry and Microbiology)
**Supervisor**

Dr. Caroline Cameron (Department of Biochemistry and Microbiology)
**Departmental Member**

Dr. Juergen Ehlting (Department of Biology)
**Outside Member**

# Abstract

**Supervisory Committee**
Dr. Caren C. Helbing (Department of Biochemistry and Microbiology)
**Supervisor**
Dr. Caroline Cameron (Department of Biochemistry and Microbiology)
**Departmental Member**
Dr. Juergen Ehlting (Department of Biology)
**Outside Member**

Amphibian metamorphosis is facilitated solely by thyroid hormones (THs), L-thyroxine ($T_4$) and 3,5,3'-triiodothyronine ($T_3$). TH modulates the remodeling of many different organs and systems in the body of developing tadpoles, including the immune system. Previous research found evidence of $T_4$ action on direct-response genes in outer ring deiodinase-poor premetamorphic tadpole tail fin and liver without the required conversion to $T_3$ described by current TH dogma. The mechanisms of environmental endocrine disrupting chemicals (EDCs) may be better understood by expanding our understanding of the transcriptomic effects of both forms of THs and how they relate to estrogen signaling. Furthermore, analysis of TH-modulation of the immune system may enable a greater understanding of the devastating effects of amphibian pathogens such as Ranavirus. Premetamorphic *Rana (Lithobates) catesbeiana* tadpoles were exposed to physiological concentrations of $T_4$, $T_3$, or 17-beta-estradiol ($E_2$) through water bath immersion. qPCR analysis was performed to assess the response of canonical TH-responsive genes *thra, thrb,* and *thibz* to these hormones in the liver and tail fin tissues of bullfrog tadpoles. $E_2$ treatment did not elicit a response in these gene transcripts in either tissue. $T_3$ treatment in the tail fin elicited an overall stronger response than $T_4$, while $T_4$ treatment in the liver recapitulated results consistent with non-genomic mechanisms of $T_4$ signaling for *thrb* and *thibz* transcripts. Illumina Hiseq2500 was used to sequence RNA

isolated from hormone-treated premetamorphic tadpole liver and tail fin tissues to assess differential transcriptomic responses and identify TH-responsive immune system-associated transcripts. The impact of TH-treatment on the general immune system in the liver and tail fin transcriptomes was also analyzed using RNA-seq data. We found that $E_2$ modulates at least some shared TH pathways in the liver, but none in the tail fin and that the tail fin transcriptome is more affected by $T_3$, while the liver transcriptome is more affected by $T_4$. Additionally, evidence of immune system modulation by both THs was found in both the liver and tail fin transcriptomes.

Antimicrobial peptides (AMPs) are an important component of the amphibian immune response. Details regarding the regulation, synthesis, and expression of AMPs remain obscure, although evidence of TH-modulation of specific AMPs has been identified, as well as evidence of increased expression of AMPs throughout metamorphosis. Frog skin is a prolific source of AMPs that may prove useful in the quest for alternative antimicrobial agents in the face of antibiotic resistance. Identification of new AMPs is hindered by the practical limitations of classical protein-based discovery approaches. By using known AMP characteristics and common AMP properties, we developed a high throughput bioinformatics approach predicated on the use of *R. catesbeiana* genome resources. We mined these resources and identified novel and known AMPs that exhibited verified antimicrobial activity against various bacterial organisms.

This thesis sought to elucidate the differential and modulatory effects of both forms of TH on a transcriptomic level and in the context of immunity, and to examine the utility of the bullfrog transcriptome and genomics resources in identifying and characterizing novel bullfrog-derived AMPs and elucidating aspects of AMP expression.

# Table of Contents

# List of Tables

# List of Figures

# Acknowledgments

I want to thank my supervisor, Dr. Caren Helbing, for her direction, support, and dedication to my project. This work would not have been possible without her persistent guidance. I would also like to thank my committee members Dr. Caroline Cameron and Dr. Juergen Ehlting for their advice and oversight regarding my thesis.

I am endlessly grateful for the past and present members of the Helbing lab. I want to thank Jessica Round and Emily Koide for being a constant source of positivity, insight, friendship, and for keeping me laughing through the ebb and flow of a Master's program. I would like to acknowledge Sara Ohora and Austin Hammond for their expertise, training sessions, and friendship, all of which I am incredibly grateful for. Krysta Gmitroski, Branden Walle, and Tristan Zaborniak: thank you for the helpful discussions, encouragement, and kindness. And finally, a huge thank you to Kevin Jackman, for your patience, support, for the endless confusing, exhausting, enlightening conversations about our projects, and for joining me on this crazy journey.

# Dedication

For my cat (the nice one, not the grey one).

# List of Abbreviations

Use of capitalization and italics for gene transcripts and proteins follow the scheme derived from http://www.xenbase.org/gene/static/geneNomenclature.jsp, http://www.informatics.jax.org/mgihome/nomen/gene.shtml, and https://www.genenames.org/about/guidelines

Amphibia: Transcript = *thibz*, protein = thibz.

Rodents: Transcript = *Thrb*, protein = THRB

Humans: Transcript = *THRB*, protein = THRB

| | |
|---|---|
| AMP | Antimicrobial peptide |
| APD | Antimicrobial Peptide Database |
| BART | Bullfrog Annotation Resource for the Transcriptome |
| BLAST | Basic local alignment search tool |
| BLAT | BLAST-like alignment tool |
| CBP | CREB-binding protein |
| cDNA | Complementary DNA |
| CHO | Chinese hamster ovary cells |
| CNS | Central nervous system |
| CRF | Corticotropin releasing factor |
| Ct | Cycle threshold |
| D1/dio1 | Type I iodothyronine deiodinase |
| D2/ dio2 | Type II iodothyronine deiodinase |
| D3/dio3 | Type III iodothyronine deiodinase |
| DBD | DNA-binding domain |
| DNA | Deoxyribonucleic acid |

| | |
|---|---|
| DO | Dissolved oxygen |
| E2 | Estradiol |
| ER | Estrogen ($E_2$) receptor |
| EDC | Endocrine disrupting compound |
| eef1a | Eukaryotic translation elongation factor 1 |
| GO | Gene ontology |
| HMM | Hidden Markov model |
| HPT | Hypothalamus – pituitary – thyroid axis |
| IP | Intraperitoneal injection |
| LAT1/2 | Large neutral amino acid transporters 1 and 2 |
| MAD | Median absolute deviation |
| MAPK | Mitogen activated protein kinase |
| MBC | Minimum bactericidal concentration |
| MCT10 | Monocarboxylate transporter 10 |
| MCT8 | Monocarboxylate transporter 8 |
| MHA | Mueller-Hinton agar |
| MHB | Mueller-Hinton broth |
| MHC | Major histocompatibility complex |
| MIC | Minimum inhibitory concentration |
| MIQE | Minimum information for publication of quantitative real-time PCR experiments |
| mRNA | Messenger RNA |
| NaOH | Sodium hydroxide |

| | |
|---|---|
| NCBI | National Center for Biotechnology Information |
| N-CoR | Nuclear corepressor |
| NIS | Sodium/iodide transporter |
| OATP-F | Organic anion transporter family member 1C1 |
| OATPP4C1 | Organic anion transporter family member 4C1 |
| OE | Olfactory epithelium |
| ORF | Open reading frame |
| ORF | Open reading frame |
| PESC | Pacific Environmental Science Centre |
| PCA | Principle component analysis |
| PCR | Polymerase chain reaction |
| PI3K | Phosphatidylinositol 3-kinase |
| qPCR | Real-time quantitative polymerase chain reaction |
| RIN | RNA integrity number |
| RNA | Ribonucleic acid |
| RNA-seq | High-throughput RNA sequencing |
| rpl8 | Ribosomal protein L8 |
| rps10 | Ribosomal protein S10 |
| $rT_3$ | Reverse $T_3$ |
| RXR | Retinoic acid receptor |
| SEM | Standard error of the mean |
| SMRT | Silencing mediator of retinoid and thyroid hormone receptors |
| SRC | Steroid-receptor-coactivator family |

| | |
|---|---|
| tnfa | Tumor necrosis factor alpha (α) |
| $T_2$ | 3,3’-diiodothyronine |
| $T_3$ | 3,5,3’ -triiodothyronine |
| $T_4$ | Thyroxine |
| TALEN | Transcriptional activator-like effector nuclease |
| Tg | Thyroglobulin |
| TBG | Thyroxine-binding globulin |
| TH | Thyroid hormone |
| thibz | Thyroid hormone-induced basic leucine zipper-containing protein |
| thra | Thyroid hormone receptor alpha (α) |
| thrb | Thyroid hormone receptor beta (β) |
| TK | Taylor and Kollros developmental stage |
| TMS | Tricaine methanesulfonate |
| TPO | Thyroid peroxidase |
| TR | Thyroid hormone receptor, either isoform |
| TRα | Thyroid hormone receptor alpha |
| TRβ | Thyroid hormone receptor beta |
| TR | Thyroid hormone receptor |
| TRE | Thyroid hormone response element |
| TRH | Thyrotropin response hormone |
| TSA | Transcriptome shotgun assembly |
| Tyr | Tyrosine |
| xbp1 | X-box binding protein 1 |

## Thesis Format and Manuscript Claims

This thesis is presented in the format of a manuscript. The first chapter provides a general background and introduces the rationale for the thesis and outlines thesis objectives. Chapters two and three are written in a manuscript style and contain an Abstract, Introduction, Materials and Methods, Results, and Discussion. The fourth chapter concludes the major findings of the data chapters and provides suggestions for future directions in related fields of inquiry.

Chapter 2: **Shireen H. Partovi**, Rachel C. Miliano, Bonnie Robert, Nik Veldhoen, Mary Lesperance, Gregory G. Pyle, Graham van Aggelen, and Caren C. Helbing. 2017. Transcriptomic analysis of *Rana [Lithobates] catesbeiana* tadpole tail fin and liver tissues following exposure to thyroid hormones and estrogen. **In preparation**. Caren C. Helbing, Greg G. Pyle, Graham van Aggelen, and Nik Veldhoen designed the exposures. Shireen H. Partovi performed RNA isolation, qPCR analysis, and prepared and analyzed RNA samples for RNA sequencing. Bonnie Robert and Mary Lesperance designed the bioinformatics pipeline and performed RNA sequencing analyses. Shireen H. Partovi and Caren C. Helbing wrote the manuscript.

Chapter 3: **Shireen H. Partovi**, S. Austin Hammond, Simon Houston, Nik Veldhoen, Caroline E. Cameron, Inanç Birol, and Caren C. Helbing. 2017. Characterization and functional analysis of antimicrobial peptides within the *Rana (Lithobates) catesbeiana* transcriptome through a bioinformatics pipeline. **In preparation**. Caren C. Helbing, Inanc Birol, S.Austin Hammond, and Nik Veldhoen built *R. catesbeiana* genomics

resources. Inanc Birol, S. Austin Hammond, and Caren C. Helbing established the bioinformatics pipeline for identifying novel AMPs. Shireen H. Partovi analyzed putative AMPs computationally and characterized known and novel peptides. Shireen H. Partovi and Simon Houston performed functional analyses on putative AMPs for MIC/MBC determination. Caroline E. Cameron offered support and insight necessary for successful completion of the functional analysis. Shireen H. Partovi, S. Austin Hammond, and Caren C. Helbing wrote the manuscript.

# 1 Introduction

## 1.1 Thyroid hormone (TH)

### 1.1.1 TH: importance, synthesis, and regulation

TH signaling plays a crucial role in normal growth, metabolism, and development in vertebrates and acts on nearly every cell in the body (Mullur et al., 2014; Nussey and Whitehead, 2001). It is also involved in cardiovascular, nervous, immune, and reproductive system development (Choksi et al., 2003). Normal TH function is particularly important in development during the mammalian perinatal period due to its involvement in neuronal cell differentiation, skin keratinization, and hemoglobin switching (Shi, 2009). Disruption to TH signaling, particularly during development, may lead to deleterious consequences such as mental retardation, rapid heart rate, and poor weight gain in humans (Glinoer, 1997).

TH is produced in the thyroid gland, which is the largest endocrine organ in the human body (Zhang et al., 2017). TH production and release controlled by the hypothalamic – pituitary – thyroid axis (HPT) (**Figure 1.1**). First, environmental stimuli are registered by the central nervous system (CNS), which then communicates with the hypothalamus (Nussey and Whitehead, 2001). The hypothalamus then stimulates the pituitary gland with either thyrotropin response hormone (TRH) in vertebrates, including mammals, or corticotropin releasing factor (CRF) in amphibians (Denver, 2013; Nussey and Whitehead, 2001; Ortiga-Carvalho et al., 2016). This action leads to the secretion of thyroid stimulating hormone (TSH), which then regulates iodide uptake from the bloodstream via the ATPase dependent sodium-iodide symporter (NIS) (Brent, 2012; Nussey and Whitehead, 2001).

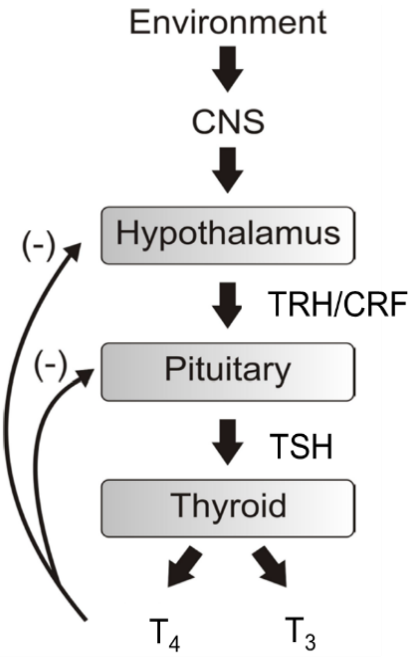


**Figure 1.1 Hypothalamus-pituitary-thyroid axis. Adapted from Nussey and Whitehead (2001).**

Iodide is oxidized and activated by thyroid peroxidase (TPO) in the presence of hydrogen peroxide and transported to the apical surface of the follicular cells, where it is incorporated into the tyrosine (Tyr) residues of thyroglobulin (Tg), a large glycoprotein (Nussey and Whitehead, 2001). Iodination of Tyr residues results in monoiodinated and diiodinated residues in Tg molecules (Yen, 2001). An enzymatic coupling reaction between pairs of iodinated Tyr molecules occurs to produce the two bioactive forms of TH: L-thyroxine ($T_4$), which is comprised of two diiodotyrosine residues, and 3,5,3'-triiodothyronine ($T_3$), which is formed by one diiodotyrosine and one monoiodotyrosine (Nussey and Whitehead, 2001). Iodinated Tg molecules are stored in follicular cells until secretion occurs (Yen, 2001).

Once proteolytically cleaved from Tg, newly synthesized THs enter the blood stream where a large percentage bind to plasma proteins transthyretin, thyroxine-binding

globulin (TBG), and albumin, and a smaller amount (approximately 0.03%) (Yen, 2001) exist freely in circulation (Nussey and Whitehead, 2001). The release of THs in turn exerts negative feedback upon the HPT axis to moderate the amount of circulating TH in the body by downregulating the release of TSH (Nussey and Whitehead, 2001).

Free THs enter target tissues via various TH transporters expressed in specific tissues, such as monocarboxylate transporter 8 (MCT8 aka SLC16A2; solute carrier family 16 member 2) and MCT10 aka SLC16A10 (solute carrier family 16 member 10), organic anion transporters M1 (OATP4C1 aka SLC04C1; solute carrier organic anion transporter family member 4C1) and F (OATP-F aka SLC01C1; solute carrier organic anion transporter family member 1C1), and large neutral amino acid transporters (LAT1 and LAT2) that have a demonstrated ability to transport TH (Friesema et al., 2005; Kinne et al., 2011; Visser et al., 2007). Once in the cell, $T_4$ can be converted to $T_3$ via intracellular type I (Dio1) and type II (Dio2) 5'deiodinases (**Figure 1.2**). This occurs through 5'-deiodination of the outer ring of $T_4$ (Yen, 2001).

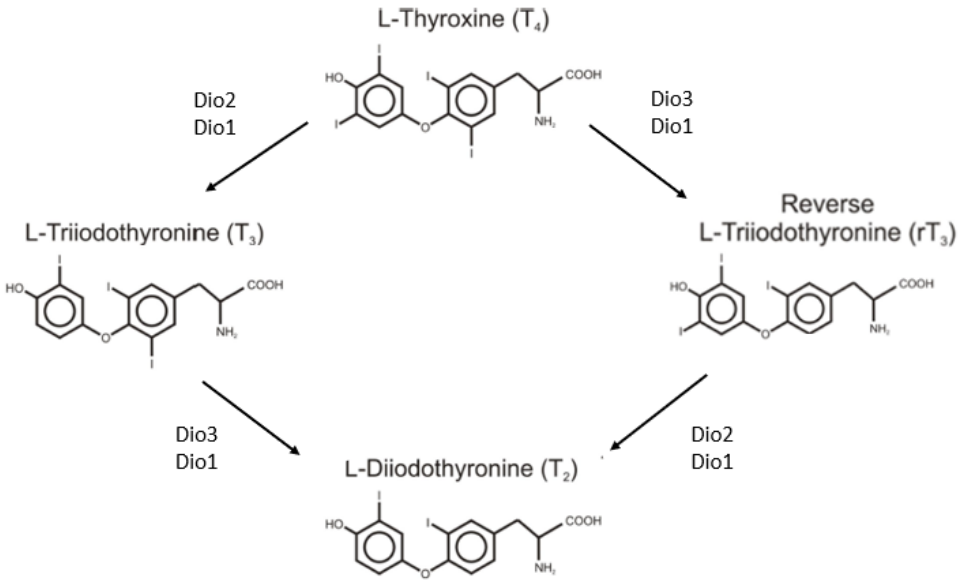


**Figure 1.2 Structures of THs and interconversion of deiodinases. Adapted from Yen (2001).**

Conversion by Dio1 occurs in peripheral tissues such as the liver and kidney, after which $T_3$ is released into the bloodstream and constitutes the majority of circulating TH, while Dio2 is found in tissues like the brain, pituitary, and adipose tissue and primarily serves to convert $T_4$ to $T_3$ intracellularly (Yen, 2001). Deiodinase 3 (Dio3) is located in the plasma membrane of various tissues and serves to inactivate $T_4$ and $T_3$ by converting them to reverse $T_3$ ($rT_3$) and 3,3'-diiodothyronine ($T_2$) (Gereben et al., 2008). Additional deiodinations can occur by Dio1 and Dio2 to produce these inactive intermediates (Gereben et al., 2008; Yen, 2001).

Some tissues do not contain Dio1 or Dio2, such as the liver and tail fin in premetamorphic *Rana catesbeiana* tadpoles (Maher et al., 2016), which results in a lack of conversion of $T_4$ to $T_3$. $T_4$ is traditionally thought to function as a prohormone, but recent evidence suggests that it can directly affect gene expression in the absence of deiodinases (Maher et al., 2016). Additionally, previous experimentation involving knockout mice lacking 5' deiodinase activity revealed only moderate biological disruption (Galton et al., 2009, 2014), suggesting that conversion of $T_4$ to $T_3$ is not as critical for TH signaling as initially thought.

### 1.2 Transcriptional regulation by TH

TH modulation of gene expression primarily occurs through interaction with the two main isoforms of TH receptors (TRs), alpha (thra) and beta (thrb), that bind to TH response elements (TREs), which are composed of two half-site DNA sequences often found in the promoters of target genes (Cheng et al., 2010; Paquette et al., 2014), although these sequences can also be located downstream from the coding region (Yen, 2001). These two TR genes are conserved in all vertebrate species and are members of the nuclear hormone receptor superfamily (Shi, 2009). TRs contain an amino-terminal

A/B domain, a central DNA-binding domain (DBD) that contains two zinc fingers, a nuclear localization signal domain, and a carboxyl terminal ligand-binding domain, all of which are conserved in all nuclear hormone receptors (Yen, 2001).

Although it has been determined that TRs can function as monomers or homodimers, *in*

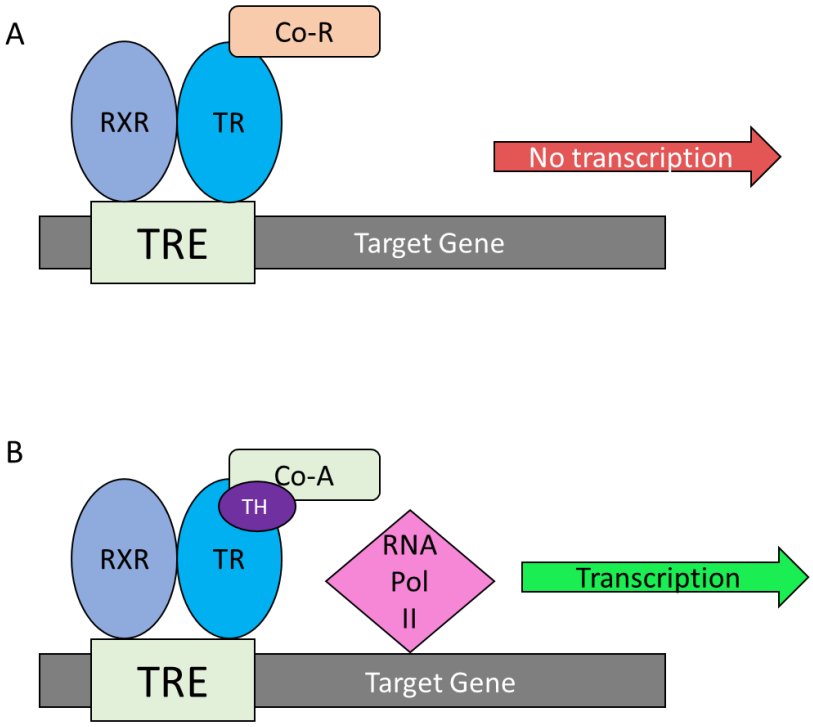


**Figure 1.3 Transcriptional regulation in the absence (A) and presence (B) of TH. Co-R, corepressor complex; co-A, coactivator complex; RXR, retinoic acid receptor; TR, thyroid hormone receptor; TRE, thyroid hormone response element; RNA Pol II, RNA polymerase II. Adapted from Yen (2001).**

*vitro* evidence suggests that heterodimerization with 9-*cis*-retinoic acid receptors (RXRs), which are part of the same nuclear superfamily as TRs, greatly increases the binding of TRs to TREs to facilitate transcription (Song et al., 2011; Yen, 2001).

In the absence of TH (**Figure 1.3A)**, TRs typically heterodimerize to RXRs, bind to TREs, and recruit corepressor proteins such as N-CoR (nuclear corepressor) and SMRT

(silencing mediator of retinoid and thyroid hormone receptors) (Shi, 2013). These proteins recruit histone deacetylases, resulting in the repression of transcription through chromatin disruption and a closed chromatin state that is not conducive to the initiation of transcription in TH-responsive genes. (Shi, 2013)

In the presence of TH **(Figure 1.3B**), these corepressors are released and coactivators, such as members of the steroid-receptor-coactivator family (SRC) (Shi, 2013; Yen et al., 2003), CREB-binding protein (CBP), and p300 complex with the TR-RXR heterodimer (Shi, 2013). Histone acetyltransferases are then recruited, resulting in an open chromatin state that is permissive to gene transcription through acetylation of local histones in the promoter region (Oetting and Yen, 2007; Shi, 2013). RNA-polymerase II and additional transcriptional components interact with this complex, resulting in the expression of these TH-responsive target genes (Yen, 2001).

Recent evidence suggests that TR isoforms exhibit differing responses to $T_3$ and $T_4$ in varied cell types that may be related to differential cofactor recruitment; TRα1 exhibited a greater affinity for $T_4$ than TRβ1 in Chinese hamster ovary (CHO), HeLa, and 3T3L1 (mouse) cells, and coactivators SRC1 and thyroid hormone receptor-associated protein 220 (TRAP220) were recruited to TRα1 at nearly equal rates by both forms of TH, whereas 5-fold more $T_4$ than $T_3$ was required to induce SRC1 binding by TRβ1 (Schroeder et al., 2014). These findings suggest that $T_4$ and $T_3$ may play different transcriptional roles in various tissue types and conditions that are not explained by current TH signaling dogma and may involve differential cofactor recruitment.

### 1.3 Non-genomic regulation by TH

Mechanisms of TH action that are not initiated by TH binding to intranuclear TRs are considered non-genomic (Cheng et al., 2010). These mechanisms have been determined

through the displacement of radiolabeled $T_4$ by tetraiodothyroacetic acid, integrin RGD recognition site peptides, and integrin-specific antibodies, which revealed the interaction of TH with cell surface receptor integrin αvβ3 at the plasma membrane and the initiation of crucial events such as cell proliferation in glioma cell lines (Davis et al., 2006) and angiogenesis in kidney fibroblast cells (CV-1) (Bergh et al., 2005). This non-genomic activity is thought to occur through activation of mitogen activated protein kinase (MAPK) pathways (Cheng et al., 2010). Involvement of MAPK was determined through activation of the MAPK pathway through $T_4$ administration, as well as inhibition of $T_4$ binding that blocked the proangiogenic action of $T_4$ (Bergh et al., 2005). This integrin also displays a higher affinity for $T_4$ than $T_3$ (Hammes and Davis, 2015), which suggests the possibility for additional differences regarding signaling pathways and the transcriptomic effects of both forms of TH. Additional non-genomic methods identified in previous research include the initiation of TH action at transiently expressed isoforms of TH receptors located in the cytoplasm that effect downstream expression of specific genes through interaction with the p85 regulatory subunit of phosphatidylinositol 3-kinase (PI3K) in human skin fibroblasts (Cao et al., 2005), and a $T_3$-mediated increase in Na-K-ATPase (sodium pump) activity in adult rat lung alveolar cells (MP48) through MAPK and PI3K pathways (Lei et al., 2008). Currently, however, the most understood mechanism of TH action is through transcriptional regulation.

### 1.4 TH-mediated amphibian metamorphosis

Amphibian metamorphosis is a quintessential example of TH-mediation of development, in which progression from the larval stage to the juvenile phenotype of anurans is facilitated solely by TH (Shi, 2000). Amphibians, which are classified as such

by a change in their habitat and mode of living that occurs throughout development, are grouped into three separate orders: Anura (frogs and toads), Urodela (newts and salamanders), and Caecilia (worm-like animals), with anurans representing the largest group of amphibians (Shi, 2000).

Anuran metamorphosis is the most studied and most dramatic metamorphosis of amphibians. Extensive internal and external remodeling occurs throughout metamorphosis and includes multiple systems and most organs, such as the skin, respiratory organs, liver, immune system, and brain (Brown and Cai, 2007). Developmental progression from an aquatic larvae to a juvenile frog is divided into three distinct periods that are marked by varying levels of TH: premetamorphosis, prometamorphosis, and metamorphic climax (**Figure 1.4**) (Shi, 2000). These periods of

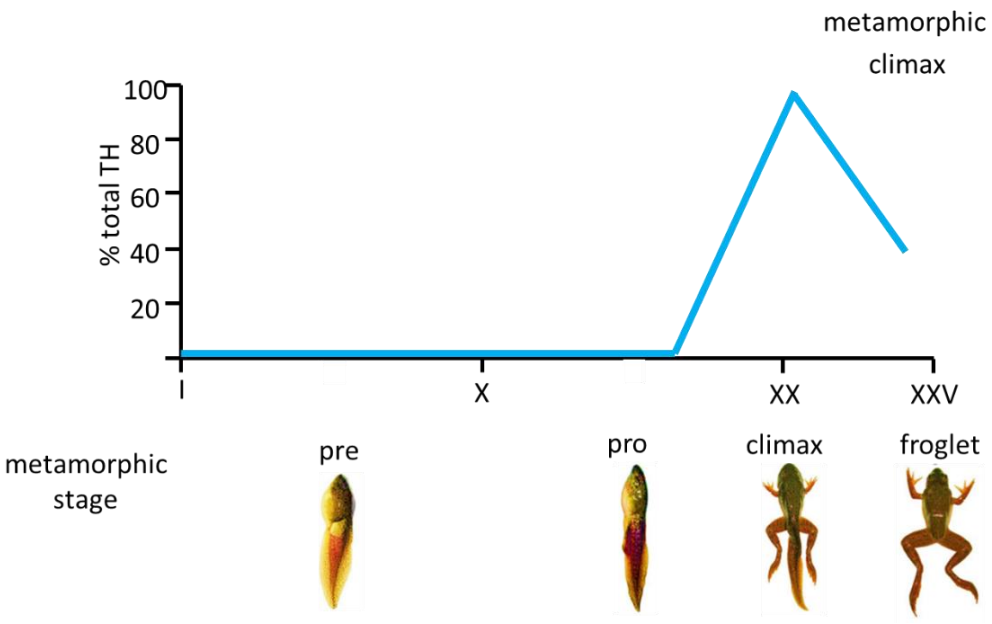


**Figure 1.4 Plasma TH levels throughout metamorphosis in *R. catesbeiana* tadpoles. % total TH refers to amount of circulating TH throughout metamorphosis. The roman numerals refer to TK staging (Taylor and Kollros, 1946).**

growth in the North American bullfrog (*Rana catesbeiana*) are staged according to the Taylor and Kollros (TK) staging system (Taylor and Kollros, 1946) or Gosner (Gs)

staging system (Gosner, 1960). These stages are characterized by distinct morphological changes that occur as the animal progresses through metamorphosis. For consistency, I will refer to the TK staging system in this thesis.

Premetamorphosis (TK stages I – IX) begins with the free-swimming tadpole and is marked by the absence of circulating TH, although the TH gland is present, and involves early tadpole growth (Shi, 2000). Limited development of the hind limbs also occurs during this time. Prometamorphosis (XI – XIX) is marked by extensive growth of the hind limbs and toe digitation, as well as increasing concentrations of circulating endogenous TH (Shi, 2000). The most drastic morphological changes occur during metamorphic climax (XX – XXV), which is characterized by the highest endogenous levels of TH in metamorphosis **(Figure 1.4**). The tail and gills of the tadpole completely resorb at around the same time as one another, and limbs and lungs become fully developed in preparation for a terrestrial life (Gilbert, 2006; Shi, 2000). Tail resorption, which marks the end of metamorphosis, occurs when aggregations of condensed chromatin and cytoplasm fragment and form apoptotic bodies that are digested by macrophages (Shi, 2000). The tadpole liver undergoes biochemical changes that facilitate the transition from ammonotelism to ureotelism that is necessary for the survival of the juvenile frog (Shi, 2000). Tadpole skin is drastically remodeled from an assortment of apical and basal cells that undergo apoptosis or differentiate into adult stem cells, respectively, to reconstitute the adult epidermis that is equipped for the terrestrial life of the frog (Ishizuya-Oka et al., 2010). Additionally, the intestine undergoes even more drastic morphological changes at this stage. The tadpole intestine is comprised of a monolayer of larval epithelial cells, surrounded by thin layers of connective tissue and

muscles (Shi et al., 2011). This structure shortens and develops into a more complex organ comprised of extensive connective tissue and muscles necessary for the carnivorous diet of the frog (Shi, 2000; Shi et al., 2011).

Anuran metamorphosis can be precociously induced to initiate these complex morphological changes through the addition of exogenous TH to the rearing water or through intraperitoneal (IP) injection of test tadpoles (Brown and Cai, 2007; Maher et al., 2016; Shi, 2009, 2000). Because these metamorphic changes occur in a free-living organism rather than a uterine-enclosed mammalian embryo (Shi, 2013), frogs are an ideal model for the study of TH-mediated postembryonic development. Additionally, characteristics of anuran metamorphosis are similar to both morphological and molecular features of postembryonic development in mammals, such as the switch from fetal to adult hemoglobin genes, skin keratinization, an increase in serum albumin levels, and the remodeling and development of the nervous system (Shi, 2009). The transition from a larval aquatic environment to a terrestrial environment for the frog also bears similarities to that of mammalian postembryonic development where fetal development occurs in amniotic fluid (Shi, 2000, 2013).

Furthermore, recent studies (Choi et al., 2015; Wen and Shi, 2015) regarding unliganded TRα in postembryonic development of *Xenopus tropicalis* have led to novel discoveries of the critical roles of this receptor in the absence of TH in developing vertebrates. Transcriptional activator-like effector nucleases (TALENs) were designed to mutate the TRα gene in *X. tropicalis* fertilized eggs that were then used to produce TRα knockdown tadpoles (Choi et al., 2015; Wen and Shi, 2015). TH-response genes in knockdown tadpoles increased in transcript abundance in the absence of TH but did not

respond to exogenous TH treatment, indicating that unliganded TRα plays a role in regulating the initiation of metamorphosis by repressing TH-response genes (Choi et al., 2015; Wen and Shi, 2015). Knockdown tadpoles also demonstrated enhanced growth, likely due to the observed increased expression of growth hormone genes in these animals, as well as accelerated initiation of metamorphosis (Wen and Shi, 2015). These findings elucidate the critical importance of unliganded TRα during postembryonic vertebrate development that have proved challenging to ascertain in mammalian systems due to the supply of maternal TH to the fetus as well as the uterine-enclosed nature of mammalian embryos (Yen, 2015). Collectively, these characteristics exemplify the use of frogs in studying aspects of TH-modulated development in vertebrates.

Previous gene expression studies in frogs have mostly focused on the African Clawed Frog, *Xenopus laevis*, and the effect of $T_3$ on TH-responsive gene transcripts rather than $T_4$. Over the years, several different studies have placed emphasis on determining the gene expression changes associated with TH-induced metamorphosis in *X. laevis* to establish the gene expression programs involved in various processes. Investigation into the remodeling of tissue types in *X. laevis* tadpoles found that early TH-responsive genes are expressed in areas of the body undergoing cell proliferation, as well as tissues undergoing remodeling, while the expression of late TH-responsive genes are higher in areas such as the tail that undergo complete resorption (Berry et al., 1998). Additionally, increased expression of the type III deiodinase was observed in developing tissues near the end of their completed metamorphic changes (Berry et al., 1998). Identification of direct TH response genes in *X. laevis* and *Xenopus tropicalis* tadpoles was determined by inhibition of protein synthesis followed by microarray analysis and genome-wide

sequence analysis. This methodology led to the identification of 188 up-regulated genes and 249 down-regulated genes as a result of $T_3$ treatment in the absence of new protein synthesis, which revealed the earliest gene expression programs that initiate the complex process of metamorphosis (Das et al., 2009). Additionally, because most studies have maintained a focus on direct TH response genes, a recent study performed genome-wide chromatin immunoprecipitation assays on the intestines of premetamorphic *X. tropicalis* tadpoles revealed nearly 300 genes bound by TR *in vivo*, most of which were found to be regulated by $T_3$ (Fu et al., 2017).

Studies on gene expression in developing *R. catesbeiana* tadpoles determined that a TH-induced increase in the expression of a liver-specific transcription factor CEBPα initiates the expression of genes carbamyl phosphate synthetase-1 and ornithine transcarbamylase, both of which are necessary for the conversion of urea from ammonia in an adult frog (Atkinson et al., 1998). Additionally, the first transcriptomic study involving $T_3$ exposure in *R. catesbeiana* tadpoles demonstrated similarities between the premetamorphic liver transcriptomes of *R. catesbeiana* and *X. laevis* as well as marked differences in receptor/signal transduction pathways and a prominent observed difference in the immune system response to $T_3$ between the two species (Birol et al., 2015). However, a comparative transcriptomic analysis of $T_3$ and $T_4$ is missing from the current body of literature and would fill in the gap of knowledge that exists where differential aspects of TH signaling are concerned.

### 1.5 TH modulation of the amphibian immune system

The immune system of amphibian larvae is remodeled extensively during TH-mediated metamorphosis, although the most drastic changes occur in anurans (Rollins-Smith, 1998). The immune system in vertebrates is divided into two categories: innate immunity

and adaptive immunity, and considerable cross-talk occurs between these responses (Boehm, 2012). Innate immunity is characterized by non-specific, rapid responses involving key components such as antimicrobial peptides, lysozymes, leukocytes, and the complement system that function as the primary defense against pathogens (Zimmerman et al., 2010). These acute defense mechanisms of the innate immune system are not predicated on previous exposure to these pathogens. Adaptive immune responses, on the other hand, may take weeks to fully develop and require prior exposure to pathogen antigens (Zimmerman et al., 2010). This arm of the immune system involves cell-mediated immunity that employs lymphocytes known as T cells that regulate antibody production, and humoral immunity, which utilizes B cells: lymphocytes that produce antibodies upon recognition of an antigen (Zimmerman et al., 2010).

The amphibian immune system shares similar features exhibited in mammals, including primary and secondary lymphoid organs like the thymus and spleen, soluble innate immune factors (complement and cytokines), and B and T cells (Colombo et al., 2015). The most thoroughly investigated anuran immune system remains that of *X. laevis* (Colombo et al., 2015; Robert and Ohta, 2009), while information regarding the immune system and associated modulating factors of true frog species such as *R. catesbeiana* is touched on only briefly in current literature. Previous research on *X. laevis* provides evidence of a larval immune system that relies on innate immune responses due to an immature adaptive immune system and dramatically reorganizes throughout metamorphosis, resulting in a mature immune system in the adult frog that is equipped to defend against pathogens and various environmental stressors through both innate and

adaptive immunity (Brown and Cai, 2007a; De Jesús Andino et al., 2012; Robert and Ohta, 2009; Rollins-Smith, 1998).

Metamorphosing *X. laevis* tadpoles experience an increase in glucocorticoids that matches that of TH, and correlative reduction in the number of tadpole lymphocytes that is thought to prevent the destruction of developing adult-specific antigens and molecules like adult hemoglobin and urea cycle enzymes (Rollins-Smith, 1998). Precocious induction of metamorphosis with TH has been show to result in an 80% loss of tadpole lymphocytes (Rollins-Smith et al., 1988). These are replaced by adult lymphocytes post-metamorphosis. Furthermore, in contrast to the limited expression in tadpoles, constitutive expression of major histocompatibility complex (MHC) class II molecules occurs pervasively on antigen presenting cells, lymphocytes, thymocytes, and mature T cells in adults (Robert and Ohta, 2009; Rollins-Smith, 1998).

Although extensive research has been conducted on aspects of the developing immune system of *X. laevis*, information regarding the development of the immune system of true frog species such as *R. catesbeiana* is limited. Previous research has demonstrated that the immune system of *X. laevis*, which diverged from true frogs over 200 million years ago (Hammond et al., 2017; Helbing, 2012), differs from the immune system of true frog species. Comparative studies of MHC genes in *X. laevis* and three other frog families, including Ranidae (true frogs), found evidence of genetic diversity in the number of expressed loci in the MHC I gene in *X. laevis* as compared to the other families (Kiemnec-Tyburczy et al., 2012). Moreover, analysis of premetamorphic *R. catesbeiana* and *X. laevis* liver transcriptomes following treatment with $T_3$ revealed a stark difference in the number of elevated immune-associated transcripts in the complement, coagulation,

acute phase response, and antigen-presentation signaling pathways, with *R. catesbeiana* liver samples exhibiting a more extensive upregulated response (Birol et al., 2015).

These findings suggest a fundamental difference in TH modulation of the immune system in the developing forms of *R. catesbeiana* as compared to *X. laevis,* which lives a completely aquatic life and does not transition to a terrestrial environment as a frog (Helbing, 2012). Further investigation of TH-mediated immune system development in *R. catesbeiana* is necessary to develop a greater understanding of this phenomenon in Ranidae, the largest frog family (Helbing, 2012), as well as other more closely related frog families that cannot be accomplished with the resources available for *Xenopus.* This is of particular importance from a conservation standpoint as populations of amphibians are currently at risk of devastation by emerging pathogens that cause chytrid fungal and Ranavirus infection (Rosa et al., 2017).

Chytrid fungal infection, caused by the fungus *Batrachochytrium dendrobatidis,* is a prevalent cause of amphibian death around the world and is characterized by initial colonization and disruption of the skin (Van Rooij et al., 2015). Immune responses are critical in clearing *B. dendrobatidis* from the host, with most studies focusing on *Xenopus laevis*; innate immune defenses against this pathogen involve antimicrobial peptides (AMPs), antifungal metabolites secreted by skin microbiota, and lysozyme, whereas possible adaptive immune defenses against *B. dendrobatidis* are currently unclear (Van Rooij et al., 2015). Recent *B. dendrobatidis* transcriptomic analyses in *Atelopus zeteki* (Panamanian golden frog), *Hylomantis lemur* (lemur leaf frog), and in culture provide novel information regarding the interplay between *B. dendrobatidis* and different hosts and how these findings contrast with gene expression changes observed in culture.

*B. dendrobatidis* differential gene expression varied in each host and differed from those identified in culture, with 390 genes exhibiting higher expression levels in *A. zeteki* compared to *H. lemur,* and 722 *B. dendrobatidis* genes exhibiting higher expression levels in the host treatments than in culture, suggesting that the environment of different host species results in modulation of the *B. dendrobatidis* transcriptome (Ellison et al., 2017).

Ranaviruses, double-stranded DNA viruses, are now considered the second most common amphibian pathogen in the world; half of the amphibian deaths in the United States over a five-year span were attributed to Ranavirus (Grayfer et al., 2012). Frog Virus (FV3) is considered the best-characterized member of the Iridoviridae family. Although investigation of the amphibian immune response to this virus has been conducted mostly on *X. laevis*, the findings shed light on interactions with an amphibian host and this pathogen. Previous research suggests that *Xenopus* larvae are less capable of dealing with Ranavirus infections than adult frogs due to an immature adaptive immune response in tadpoles that, in contrast, appears to be potent and effective in adults and employs CD8 T-cell and antibody responses (Grayfer et al., 2012). Additionally, evidence suggests that peritoneal leukocytes in *X. laevis* adults significantly increase in number as early as one day after infection, followed by an increase in natural killer cells and T-cells just a few days later (Morales et al., 2010). Furthermore, FV3 infections of adult *X. laevis* resulted in rapid gene expression increases of pro-inflammatory cytokines such as tumor necrosis factor α and interleukin-1β (Morales et al., 2010) compared to moderate and delayed gene expression increases in *X. laevis* tadpoles (De Jesús Andino et al., 2012), suggesting that an efficient innate immune response is critical for viral

clearance in these animals. Furthering our understanding of components of the innate immune system is necessary to find effective means for dealing with the grave threat posed by these infections.

### 1.6 Antimicrobial Peptides (AMPS) in frog skin

AMPs, which are found in both prokaryotes and eukaryotes, are naturally occurring oligopeptides that are composed of approximately 5-100 amino acids with demonstrated antimicrobial activity against bacteria, viruses, fungi, and parasites (Bahar and Ren, 2013). In animals, AMPs are often expressed in tissues and organs that are exposed to the external environment and therefore at direct risk of interacting with pathogens, although they can be found in other tissues as well (Bahar and Ren, 2013). Immunomodulatory functions of AMPs have also been discovered, such as the ability to alter host gene expression, induce chemokine production, and modulate components of the adaptive immune response (Bahar and Ren, 2013; Hiemstra and Zaat, 2013; Nijnik and Hancock, 2009; Pan et al., 2014).

These peptides are considered an essential component of the innate immune response in frogs, likely the first line of defense in cases of injury or infection (Bahar and Ren, 2013; Hiemstra and Zaat, 2013), and are abundantly expressed in frog skin (Bahar and Ren, 2013; Conlon, 2011). Adult frog skin in particular is a rich source of AMPs (Conlon and Mechkarska, 2014). AMPs are produced and stored within specialized granular or poison glands located in the dermis of frog skin that are then released onto the surface of the skin in response to injury or infection by pathogens (Conlon and Mechkarska, 2014; Hiemstra and Zaat, 2013). AMPs are typically produced as precursors that are cleaved at specific, conserved residues by proprotein convertases to produce the C-terminal mature peptide

with functional, antimicrobial properties (Aittomäki et al., 2017; Hiemstra and Zaat, 2013; Rosa et al., 2017; Valore and Ganz, 2008).

AMPs are classified into four separate groups based on their secondary structures: β-sheet, α-helix, extended coil, and loop, with α-helical AMPs representing the largest category (Bahar and Ren, 2013; Hiemstra and Zaat, 2013). Antibacterial AMPs, most of which are cationic (Bahar and Ren, 2013) are the most studied AMPs. The majority of frog AMPs are α-helical in nature and are composed of positively charged amino acid residues, resulting in a net cationic charge that enables electrostatic attraction to negatively charged microbial cell membranes while avoiding interaction with eukaryotic membranes (Bahar and Ren, 2013; Conlon, 2011; Hiemstra and Zaat, 2013). Additionally, AMPs contain a large proportion of hydrophobic and hydrophillic residues. This imbues the peptides with amphipathic properties that enable interaction with microbial cell membranes (Bahar and Ren, 2013; Hiemstra and Zaat, 2013). Although the exact mechanisms still remain unclear, antibacterial AMPs are thought to kill bacteria by a number of different methods, including the inhibition of DNA replication and protein synthesis, as well as disruption of microbial cell membrane integrity (Bahar and Ren, 2013; Hiemstra and Zaat, 2013; Nijnik and Hancock, 2009).

However, the most common characteristic of identified AMPs appears to be their ability to interact with and damage the cell membrane. AMPs with antibacterial activity are electrostatically attracted to lipopolysaccharides (LPS) on the outer membrane of Gram-negative bacteria and to the teichoic and teichuronic acids on the cell wall of Gram-positive bacteria, after which the peptides are able to traverse the microbial membranes by several different methods (Guilhelmelli et al., 2013). The “barrel-stave” model is

characterized by the formation of transmembrane pores via direct insertion into the core of the membrane, the “toroidal” model involves insertion of several peptide molecules into the membrane which form a bundle that disrupts the distribution of the lipid monolayers, whereas the “carpet” model is characterized by a detergent-like coating of AMPs across the membrane surface until disintegration of the membrane is achieved (Guilhelmelli et al., 2013). Not surprisingly, it remains unclear what inherent AMP properties are responsible for antimicrobial activity against specific pathogens due to the vast repertoire of action employed by these molecules (Bahar and Ren, 2013), although an analysis of the Antimicrobial Peptide Database reveals that more AMPs exhibit specific action against Gram-positive bacteria than Gram-negative bacteria (Malanovic and Lohner, 2016).

It is now evident that bacteria are capable of mounting resistance mechanisms against AMPs, although it was initially thought that use of these molecules did not facilitate the development of bacterial resistance due to the wide variety of employed antimicrobial activities. Both Gram-positive and Gram-negative bacteria can modify their cell wall components to reduce the net negative charge of their surfaces to avoid detection by AMPs and the resultant electrostatic attraction; Gram-negative bacteria can increase the charge of the LPS molecules by bringing intracellular positively charged molecules to the cell surface, while Gram-positive bacteria incorporate D-alanine residues to the teichoic acids on their cell walls (Guilhelmelli et al., 2013). Some bacteria are even capable of down-regulating the expression of AMP genes (Guilhelmelli et al., 2013).

The general structures of AMPs may vary. However, frog peptides are typically composed of an N-terminus signal peptide region that enables transport of AMPs into a

specific region of the granular gland for proteolytic cleavage, and a prosequence that, upon additional stimulus-based proteolytic cleavage, yields the mature active peptide (Boland and Separovic, 2006; Cardoso, 2014) (**Figure 1.5**). Antimicrobial properties are conserved within AMP families due to common primary sequence similarities maintained between peptides of the same family (Conlon and Mechkarska, 2014; Waghu et al., 2016). AMP prosequences are typically conserved within families, while the cleaved

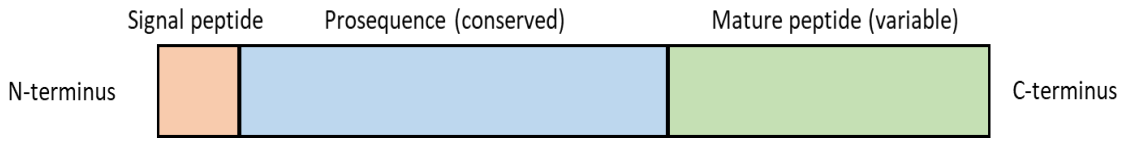


**Figure 1.5 General structure of frog AMPs. Adapted from Clark et al (1994).**

active mature sequences vary considerably and represent the functional peptide (Dutton, 2002; Hiemstra and Zaat, 2013; Vanhoye et al., 2003). In fact, even minor variations in AMP sequences and consequent structures can lead to differences in antimicrobial activities (Khamis et al., 2015). Conservation can also occur in the signal peptide region within families.

Properties of frog AMPs are diverse. They exhibit demonstrated potent antimicrobial activity against Gram-positive and negative bacteria (Conlon, 2012), fungi (Holden et al., 2015), viruses (Rollins-Smith, 2009; VanCompernolle et al., 2005), and even protozoa (Mangoni et al., 2005), and each frog species produce a unique set of AMPs with diverse activity against a broad range of pathogens suited for their respective environments (Bahar and Ren, 2013; Hiemstra and Zaat, 2013; Rollins-Smith, 2005). It is suspected that the main mechanism of antimicrobial activity of frog AMPs, like the majority of these molecules, is related to the electrostatic attraction and subsequent disruption of the

cell membrane (Rollins-Smith, 2005). AMPs from the magainin family, first isolated from *X. laevis* in the 1980s, remain the best-characterized and most intensively studied frog peptides, although they exhibit low to moderate antimicrobial activity (Conlon and Mechkarska, 2014). However, because of the abundance of AMPs present in frog skin and their overall demonstrated potency, frog AMPs are gaining interest as possible antimicrobial therapeutics due to the current global threat presented by antibiotic resistance (Batista et al., 2001; Ge et al., 2014; Luca et al., 2013).

The circumstances involved in the regulation of the production and expression of frog AMPs are still relatively unknown. Exposures to bacterial, viral, and fungal pathogens increase the synthesis of frog AMPs (Mangoni, 2001; Pietiäinen et al., 2009; Yang et al., 2012), suggesting that granular gland cells may recognize pathogen receptors (Rollins-Smith, 2009). Previous research involving glucocorticoid (stress response) exposures in Northern Leopard frogs (*Rana pipiens*) observed an increase in AMP expression (Tatiersky et al., 2015).

Expression of a handful of AMP transcripts in the context of TH-dependent natural metamorphosis has been observed in a few studies that looked specifically at mRNA abundance levels of isolated and identified AMPs. Exogenous TH-induction of AMP mRNA has been examined to a lesser degree with even fewer test peptides examined, with one study focusing on these results in adult frogs that may contain a different repertoire of AMPs than tadpoles based on the environmental and whole-body transformations that occur in the transition from tadpole to adult.

Analysis of the natural developmental expression of a Temporin precursor in Japanese mountain brown frog (*R. ornativentris*) skin using semi-quantitative RT-PCR detected

preprotemporin-1O mRNA at the onset of metamorphosis, with an observed increase during metamorphosis as TH levels increase and peak expression levels at metamorphic climax, where TH levels reach a maximum (Ohnuma et al., 2009). Following induction with 2 nM $T_3$ for 48 h, adult brown frogs exhibited a 1.5-fold increase in preprotemporin-1O mRNA abundance relative to untreated control frogs, although this treatment was not repeated in tadpoles (Ohnuma et al., 2009). Northern blot analysis of *X. laevis* tadpole mRNA revealed increased expression of the two most abundant members of the magainin AMP family in tadpoles throughout natural metamorphosis with a peak near metamorphic climax, as well as Northern blot-demonstrated precocious induction of magainin mRNA expression in premetamorphic tadpoles following treatment with 5 nM $T_3$ (Reilly et al., 1994). This same expression pattern was observed for Ranalexin, an AMP isolated from the skin of *R. catesbeiana*. Northern blot analysis of bullfrog RNA revealed Ranalexin mRNA expression at the onset of metamorphosis, but not during premetamorphosis where circulating TH is absent, with sustained expression through metamorphosis and in adulthood (Clark et al., 1994). Additionally, using RT-PCR, Brevinin-1SY mRNA from *R. sylvatica* also exhibited increased abundance levels towards the later stages of development (Katzenback et al., 2014).

Although these findings are of interest and introduce possible insight into regulatory aspects of AMPs through transcript-based analyses, the current state of literature regarding AMP expression, regulation, and identification is still lacking, particularly in true frog species such as *R. catesbeiana* that express high potency AMPs in abundance. Further investigation into the characteristics of these defense peptides may shed light on a critical component of innate immunity.

## 1.7 Objectives

The main objectives of this thesis are:

*1)* To examine differential TH responses in premetamorphic *R. catesbeiana* liver and tail fin tissue transcriptomes through RNA-seq and evaluate TH-modulation of immune system transcripts in the liver and tail fin

*2)* To identify, characterize, and functionally analyze putative AMPs based on peptide homology using *R. catesbeiana* genomic resources

The first data chapter addresses the first objective and the second data chapter addresses the second.

# 2 Transcriptomic analysis of *Rana [Lithobates] catesbeiana* tadpole tail fin and liver tissues following exposure to thyroid hormones and estrogen


## Abstract

Amphibian metamorphosis is dependent on the action of thyroid hormones (THs), L-thyroxine ($T_4$) and 3,5,3'-triiodothyronine ($T_3$). Recent evidence showed that $T_4$ can act directly on direct-response genes in tissues that lack 5' deiodinase activity, such as the premetamorphic tadpole tail fin and liver, rather than requiring conversion to $T_3$. Understanding the common and differential effects of THs and how they relate to estrogen signaling is important in identifying mechanisms of environmental endocrine disrupting chemicals. We exposed premetamorphic *Rana (Lithobates) catesbeiana* tadpoles to physiological concentrations of $T_4$, $T_3$, or 17-beta-estradiol ($E_2$) for 48 h. Illumina Hiseq2500 was used to sequence RNA isolated from hormone-treated premetamorphic tadpoles to assess differential transcriptomic responses in the liver and tail fin and to identify TH-responsive immune system-related transcripts. We found that $E_2$ modulates at least some shared TH pathways in the liver, but none in the tail fin. Overall, the tail fin transcriptome is more affected by $T_3$, while the liver transcriptome is more affected by $T_4$. Additionally, evidence of immune system modulation by both THs was found in the liver and tail fin transcriptomes. qPCR analysis was also performed to assess the response of canonical TH-responsive genes to these hormones in the liver and tail fin tissues. $E_2$ treatment did not elicit a response in these gene transcripts in either tissue. $T_3$ treatment in the tail fin elicited an overall stronger response, while $T_4$ treatment in the liver recapitulated interesting results consistent with non-genomic mechanisms of $T_4$ signaling for *thrb* and *thibz*.

## 2.1 Introduction

Thyroid hormone (TH) plays a crucial role in the modulation of normal metabolism, growth, and development in vertebrates (Mullur et al., 2014). In amphibians, TH is solely responsible for the initiation of metamorphosis (Gilbert et al., 1996; Shi, 2000), which facilitates drastic changes to the body plan and physiology that results in the transition from aquatic larvae to the juvenile frog (Gilbert, 2000; Miyata and Ose, 2012). TH controls metamorphosis primarily by binding to TH nuclear receptors α (TRα) and β (TRβ) that activate or repress early response genes when bound to TH response elements (TREs) located in the promoter region (Gilbert et al., 1996; Mullur et al., 2014; Shi, 2000).

The two main biological forms of TH exist as L-thyroxine ($T_4$), which is produced in the thyroid gland, and 3,5,3'-triiodothyronine ($T_3$). The conventional dogma of TH action describes $T_4$ as a prohormone that is converted by 5' deiodinases to the more bioactive form $T_3$ in target tissues (Mullur et al., 2014). However, recent evidence has demonstrated that $T_4$ is also capable of acting directly on TRs of certain genes in tissues that lack 5' deiodinase activity (Maher et al., 2016 and references therein). Evaluation of this finding on a transcriptomic level may provide novel information for better understanding differential TH mechanisms and tissue-specific effects, as well as shed light on the impacts of endocrine disrupting chemicals (EDCs) that are dependent upon perturbation of either $T_4$ or $T_3$.

During premetamorphosis, the thyroid gland of tadpoles is inactive, which results in a lack of circulating TH in the body (Tata, 2006). However, TRα and TRβ are present in tissues at low levels during these stages (Grimaldi et al., 2013; Tata, 2006). Exposure to exogenous THs therefore induces precocious metamorphosis in premetamorphic tadpoles

as demonstrated in several studies (Brown and Cai, 2007; Maher et al., 2016; Tata, 2006), making these young animals an ideal model for the study of TH action. Moreover, they present an opportunity to study the effects of estrogens as well since these animals have not yet undergone sexual differentiation. 17-β estradiol ($E_2$) receptors (ERs) and TH receptors (TRs) bind a similar DNA consensus site in their hormone responsive element sequences (Vasudevan et al., 2002). Consequently, the ability of $E_2$ and TH to interact through both hormone receptors has been demonstrated (Fujimoto, 2004; Zhao et al., 2005). The extent to which this occurs on a transcriptomic level has not yet been explored.

Previous research found evidence of $T_3$-induced modulation of immune system associated transcripts in the liver transcriptome of premetamorphic *Rana (Lithobates) catesbeiana* tadpoles through *de novo* transcriptome assembly (Birol et al., 2015). However, the effect of $T_4$ treatment in this tissue is not known. Additionally, analysis of TH-modulation of immune-related transcripts in the tail fin has not been completed. Epithelial tissue in amphibians employs both innate and adaptive immune responses and exhibits more complex defense barriers than those observed in aquatic organisms (Huang et al., 2016). Additionally, granular glands of the skin contain antimicrobial peptides (AMPs) that serve as the first line of defense against pathogens (Bahar and Ren, 2013) and have promising therapeutic potential (Jantaruk et al., 2017). Evaluation of TH-modulation of the liver and tail fin may provide insight into differential EDC sensitivities in certain genes and tissues and a greater understanding of the interplay between THs and immunity.

The purpose of the present study was three-fold: (1) To examine differential $T_4$ and $T_3$ responses in 5' deiodinase-poor liver and tail fin tissue transcriptomes through RNA-seq, (2) to assess the impact of $E_2$ treatment on classical TH-responsive genes and the transcriptome, and (3) to evaluate TH-modulation of immune system transcripts in the liver and tail fin.

We used Illumina Hiseq2500 to sequence RNA isolated from $E_2$, $T_4$, and $T_3$ treated premetamorphic *R. catesbeiana* tadpoles to assess differential transcriptomic responses in the liver and tail fin. RNA-seq results were used to examine the transcriptomic response of all three hormones in both tissues and to identify immune system-related transcripts that were TH-responsive. Quantitative polymerase chain reaction (qPCR) was used to confirm the established response of classical TH-responsive genes to TH and compare those findings with that of $E_2$, and to validate the RNA-seq results by testing the new immune system tools on the same set of samples.

## 2.2 Materials and methods

### 2.2.1 Experimental animals, Exposure, and Tissue Isolation

Premetamorphic (Taylor and Kollros (TK) stages I-VI: (Taylor and Kollros, 1946)) *R. catesbeiana* tadpoles of mixed sex were caught locally by Westwind Sealab Supplies in Victoria, British Columbia (BC, Canada) and housed at the University of Victoria Outdoor Aquatics Unit. Animals were housed in 100 gallon covered fiberglass tanks containing recirculated dechlorinated municipal water at 15±1°C with pH 6.8 and 96-98% dissolved oxygen (DO) and fed daily with Spirulina flakes (Nutrafin Max, Rolf C. Hagen, Montreal, PQ, Canada). Animals were then sent to Pacific Environmental Science Centre in North Vancouver, BC and housed in a covered outdoor facility prior to chemical treatments and received Nutrafin A6762C Max spirulina meal tablets at a ratio of ½ tablet per tadpole every Monday, Wednesday, and Friday. Tanks were plumbed with

on-site well water that was tempered to 15 ± 1°C with a 16 h light/8 h dark photoperiod. Tadpoles were brought indoors 96 h before the experiment and housed at 20.3-21.8°C (temperatures varied per hormone treatment) in 60 L tanks with a density of 10 tadpoles per tank with a16 h light/8 h dark photoperiod. Tadpoles were fed at this time and no further food was given prior to testing.

During the hormone exposures, premetamorphic tadpoles were housed in aerated 20 L aquaria at a ratio of 10 L per tadpole, with two tadpoles per aquarium and 12 tadpoles per treatment condition. Animals were immersed in water between 20-21$^{o}$C for 2d to each of three concentrations of $T_3$ (0.1, 1, 10 nM; Sigma-Aldrich, Oakville, ON; Catalog #T2752, CAS 55-06-1), $T_4$ (0.5, 5, 50 nM; Sigma, Catalog # T2501, CAS 6106-07-6), or $E_2$ (0.1, 1, 10 nM; Sigma, Catalog # E4389, PubChem Substance ID 329799056), and NaOH vehicle control (800 nM; TH control) or well water ($E_2$ control) as previously described in a companion study (Heerema et al., 2017). Biologically-relevant $T_4$ doses were matched to $T_3$ doses based on a comparative analysis of the biological activity and binding affinity of $T_4$ and $T_3$ to TRs (Maher et al., 2016). Tadpole morphology details and water quality parameters for each exposure group are reported in (Jackman et al., 2017).

The care and treatment of animals was in accordance with guidelines established by the Canadian Council on Animal Care and approved by the Animal Care Committee of the University of Victoria. Tadpoles were euthanized in buffered tricaine methanesulfonate (1000 mg/L; TMS, Aqua Life, Syndel Laboratories, Nanaimo, BC, Canada). The liver and tail fin tissue were isolated from each animal and placed in RNAlater solution (Ambion, Foster City, CA, USA) as per manufacturer's instructions for preservation. The

preserved tissues were stored at -20$^{o}$C and shipped to the University of Victoria on ice for RNA isolation.

### 2.2.2 Total RNA Isolation and cDNA Preparation

Tissue samples were randomized prior to processing and extraction of RNA. Portions of liver and tail fin tissue were individually placed in 700 µL of TRIzol and mechanically mixed via Retsch MM301 Mixer Mill (Thermo Fisher Scientific, Ottawa, Canada) at 20 Hz for two three-minute intervals separated by a 180° rotation. RNA was extracted according to the protocol described in Heerema et al., 2017. Liver and tail fin RNA was subsequently dissolved in 40 µL diethyl pyrocarbonate-treated water (Sigma Aldrich) and used for cDNA synthesis via a High-Capacity cDNA Reverse Transcription Kit with RNAse Inhibitor as per the manufacturer's manual (Applied Biosystems Foster City, CA, USA).

### 2.2.3 Quantitative Real-Time Polymerase Chain Reaction (qPCR)

Prior to RNA-sequencing of select model chemical samples, qPCR analysis was completed using validated primers for TH receptor α (*thra*), TH receptor β (*thrb*), and TH-induced basic region leucine zipper-containing transcription factor (*thibz*) due to their established TH-associated responses as described previously (Maher et al., 2016). Three additional gene transcripts were used in the qPCR assay as input normalizers: ribosomal protein S10 (*rps10*), ribosomal protein L8 (*rpl8*), and eukaryotic translation elongation factor 1 α (*eef1a*) (Veldhoen et al., 2014). Covariation among the average cycle threshold ($C_t$) values for the three normalizer genes (*rpl8*, *rps10*, *eef1a*) was analyzed using RefFinder (http://www.leonxie.com/referencegene.php) and BestKeeper (Pfaffl et al., 2004) to confirm precision in generating a geometric mean used to normalize sample input variation in the qPCR data all gene transcripts. All cDNA samples were analyzed in quadruplicate on either an MX3005P qPCR system (Agilent Technologies Canada Inc.,

Mississauga, ON, Canada) or a CFX Connect real-time system (Bio-Rad Laboratories Ltd., Mississauga, ON, Canada). All samples for a given gene transcript were run using the same system to eliminate bias. All qPCR reactions included 10 mM Tris–HCl (pH 8.3 at 20 °C), 50 mM KCl, 3 mM MgCl2, 0.01% Tween-20, 0.8% glycerol, 40,000-fold dilution of SYBR Green I (Life Technologies Corp., Carlsbad, CA, USA), 83.3 nM ROX (Life Technologies), 5 pmol forward and reverse primer, 200 mM dNTPs (Bioline USA Inc., Taunton, MA, USA), 2 μL of 20-fold diluted cDNA, and 1 unit of Immolase DNA polymerase (Bioline USA Inc.) as described previously (Heerema et al., 2017).

Following RNA-seq, immune system targets tumor necrosis factor α (*tnfa;* F – 5'-CTTCAATGTCCTGCGAGAG, R – 5'-CAAGTCTGATGCCACCATAG) and x-box binding protein 1 (*xbp1*; F – 5'-TCACCTCCGTCATGTTACC, R – 5'-CTGTGCGGCTACTCTGTT) were chosen from RNA-seq data for primer design according to their strength of response to THs (fold change (≥ 2.0), p-value (≤ 0.05). TNFα is a pro-inflammatory cytokine that is secreted by activated macrophages and is involved in acute phase response of the innate immune response (Fagerberg et al., 2014). XBP1 is a transcription factor that regulates MHC class II genes and other immune related genes (Fagerberg et al., 2014). Immune-associated contigs were identified through Gene Ontology analysis using UniProt IDs as described in (Hammond et al., 2017). Parameters for primer design and validation were followed according to the MIQE-compliant quality control measures employed for qPCR assay development discussed in previous literature (Veldhoen et al., 2014). Based on the results of the three-tier quality control (QC) validation, the primer for *xbp1* was run on the model chemical exposure sample set for liver, and primer for *tnfa* was run on the tail fin sample set

according to the methods described above for qPCR. SYBR green detection was used for qPCR analysis of both targets. Parameters for *tnfa* and *xbp1* qPCR were one cycle of 9 minutes at 95 °C, followed by 40 cycles of 15 s at 95 °C, 30 s at 60 °C, and 45 s at 72 °C.

### 2.2.4 Illumina HiSeq (RNA-seq)

Liver and tail fin RNA samples were analyzed for quality and concentration using a Bioanalyzer 2100 (Agilent, Mississauga, Ontario, Canada). Five vehicle and five high concentration RNA samples for each tissue with a RIN ≥ 8 from each of 10 nM $E_2$, 10 nM $T_3$, and 50 nM $T_4$ exposed tadpoles along with their matched controls (60 samples total) were chosen and shipped at -20 °C to the Michael Smith Genome Sciences Centre in Vancouver, BC for strand-specific mRNA library construction and sequencing using the HiSeq2500 (Illumina, San Diego, California, USA) paired-end platform to generate 2x75 base pair reads described previously (Hammond et al., 2017).

Following sequencing, the resultant raw reads were aligned using an in-house bioinformatics alignment script (aln2BART) to a bullfrog reference annotated transcriptome (BART) derived from 132 *R. catesbeiana* tadpole samples and six tissue types expanded from that described in Hammond et al., (2017). The contigs that comprise BART were aligned using the BLAST-like Alignment Tool (Kent, 2002) or parallelized BLAT (pblat; icebert.github.io/pblat/) to identify highly similar sequences; only the longest of each set of similar sequences was retained (Hammond et al., 2017). Bioinformatic alignment of raw reads to BART, which contains nearly two million contigs, was done to yield counts of read alignments to contigs. Generated counts, quantified through bioinformatics scripts, were fed through DESeq2 (Love et al., 2014), which normalizes raw read counts by library depth, to determine statistical significance between control and treatment samples by using a false discovery rate (FDR) corrected p-

value of 0.05, followed by annotation of contigs using the human Uniprot and TSA database. Uniprot IDs assigned to each contig were run through Gene Ontology (geneontology.org) to determine contig groupings (Hammond et al., 2017) and through GO Panther-Slim (geneontology.org) to produce representative charts of affected biological processes. GO IDs were then used as input for REVIGO (revigo.irb.hr) to produce treemaps of differentially expressed biological processes following hormone treatments.

### 2.2.5 Statistical Analyses

Statistical analyses for data obtained from qPCR assays were performed as indicated previously (Heerema et al., 2017). Nonparametric Kruskal-Wallis and Mann-Whitney U tests were performed using R (R Core Team, 2017). Fold changes were calculated and statistical significance was set at $p \leq 0.05$. RNA-seq data was analyzed using DESeq2 (Love et al., 2014) to identify differentially expressed contigs.

## 2.3 Results

### 2.3.1 Evaluation of classical TH-responsive gene transcripts

*Thra, thrb,* and *thibz* have often been used as indicators of TH response due to their established hormone-associated upregulation (Maher et al., 2016; Heerema et al., 2017), while their response to $E_2$ treatment was unknown. We sought to establish that the animals responded to $T_4$ and $T_3$ treatment as expected and evaluate the response of these gene transcripts to $E_2$ treatment. qPCR was run on liver and tail fin model chemical cDNA samples from three concentrations of $T_3$ (0.1, 1, 10 nM), $T_4$ (0.5, 5, 50 nM), or $E_2$ (0.1, 1, 10 nM), and NaOH vehicle (800 nM) or well water controls.

In the tail fin, $T_3$ exposure resulted in significant increases in the abundance of *thra* at the high concentration (2-fold; $p < 0.001$; **Figure 2.1**) relative to the control (NaOH), while $T_4$ and $E_2$ exposure did not elicit a response. The low concentration of $E_2$ resulted

in a slight increase in *thrb* transcript abundance (2-fold; $p = 0.001$; **Figure 2.1**). $T_4$ exposure increased *thrb* abundance at the medium and high concentrations, while $T_3$ exposure increased abundance at all three concentrations. $E_2$ exposure did not elicit a significant response in *thibz,* but both $T_4$ and $T_3$ increased *thibz* transcript abundance at the medium and high concentrations (**Figure 2.1**). Comparison of the relative responses of all transcripts to $T_4$ and $T_3$ showed a significantly higher response to $T_3$ compared to $T_4$ in *thra* and *thibz* at all three concentrations, and in *thrb* at the medium and high concentrations. Comparisons between $T_4$ and $T_3$ exposures at the low concentration in *thrb* were not statistically significant. RNA-seq analysis of *thrb* and *thibz* transcript abundance revealed differences and similarities in the reported fold changes: $T_4$ exposure resulted an 8-fold increase in *thrb* transcript abundance and a 12-fold increase following $T_3$ exposure, while *thibz* transcript abundance increased 94-fold following $T_4$ exposure and 147-fold following $T_3$ exposure. Slight differences in fold change between the two quantification methods is likely due to the lack of strand-specificity employed by qPCR.

In the liver, all three concentrations of $E_2$ did not elicit a response in *thra, thrb,* or *thibz. Thra* and *thrb* transcript abundance increased following exposure to all three concentrations of $T_4$, and only the medium and high concentrations of $T_3$ (**Figure 2.2**). $T_4$ and $T_3$ exposure elicited a significant increase in *thibz* transcript abundance at the medium and high concentrations for both hormones (**Figure 2.2)**. Comparison of the relative responses of all three transcripts to $T_4$ and $T_3$ showed a significantly higher response to $T_4$ at the medium concentration in *thrb* and *thibz* transcripts ($p < 0.001$ and $p < 0.001$, respectively). RNA-seq analysis of *thrb* and *thibz* transcript abundance revealed that $T_4$ exposure resulted a 15-fold increase in *thrb* transcript abundance and an 11-fold

increase following $T_3$ exposure, while *thibz* transcript abundance increased 117-fold following $T_4$ exposure and 35-fold following $T_3$ exposure. Again, the fold change differences observed between RNA-seq and qPCR are likely due to the differences inherent in the methods with regards to strand-specificity.

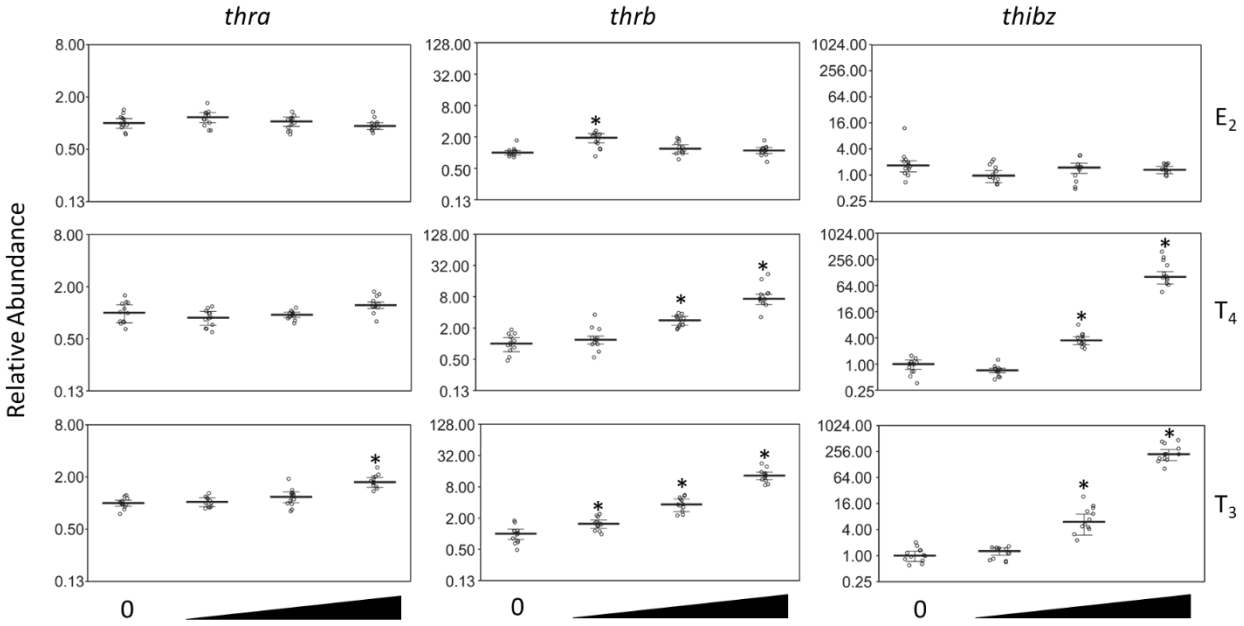


**Figure 2.1 Premetamorphic *R. catesbieana* tadpole tail fin transcript abundance for TH receptor α (*thra*), TH receptor β (*thrb*), and TH-induced basic region leucine zipper-containing transcription factor (*thibz*) after 48 h exposure to either 800 nM NaOH vehicle ('0') or increasing physiologically-relevant concentrations of $E_2$ (0.1, 1.0, 10 nM), $T_4$ (0.5, 5.0, 50 nM), or $T_3$ (0.1, 1.0, 10 nM) as measured by qPCR. The bevel represents increasing concentrations for each respective hormone. The wide bar represents the median, the whiskers represent the median absolute deviation, and the open circles represent the data points of individual animals. An asterisk denotes a significant difference relative to the vehicle ($p \leq 0.05$).**

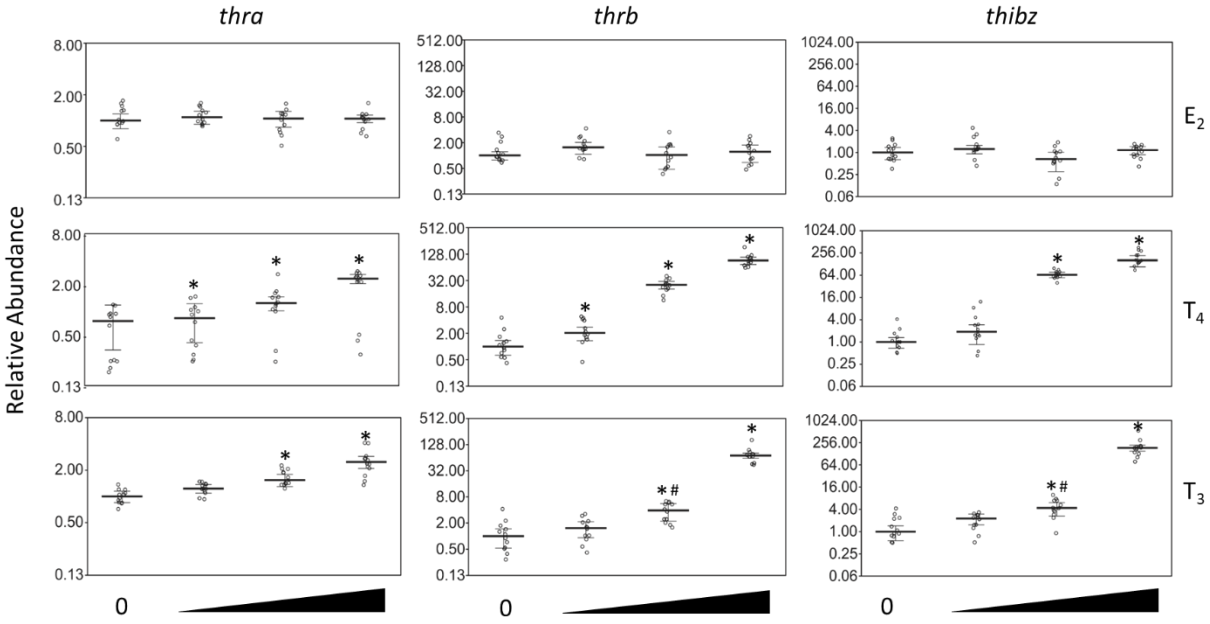


**Figure 2.2 Premetamorphic *R. catesbieana* tadpole liver transcript abundance for TH receptor α (*thra*), TH receptor β (*thrb*), and TH-induced basic region leucine zipper-containing transcription factor (*thibz*) after 48 h exposure to either 800 nM NaOH vehicle ('0') or increasing physiologically-relevant concentrations of $E_2$ (0.1, 1.0, 10 nM), $T_4$ (0.5, 5.0, 50 nM), or $T_3$ (0.1, 1.0, 10 nM) as measured by qPCR. A pound sign denotes significance between the medium concentration of $T_3$ and the corresponding concentration of $T_4$. Refer to Figure 2.1 legend for additional details.**

### 2.3.2 RNA-seq Analyses

Comparison of tail fin and liver transcriptomes following RNA sequencing illuminates vast differences in differentially expressed contigs following $E_2$, $T_4$, and $T_3$ treatment in these two tissues. Tail fin samples generated an average of 94- 102 million reads with an average of 99.7% of all reads aligning to contigs, while liver samples generated an average of 90 – 98 million reads with an average of 99.7% of all reads aligning (**Appendix A**).

Principle component analysis (PCA) plot depictions of tail fin and liver data show strong separation of control and treatment samples for all three hormone treatments, with PC1 representing a range of 64-81% of variation in tail fin samples, and 70-79% of variation in the liver samples (**Figure 2.3**).

Volcano plot depictions of $E_2$ exposure in the tail fin indicate a small number of differentially expressed contigs exhibited low magnitude fold change increases (less than 2.5-fold), with just two contigs exhibiting fold change decreases (around 2.5-fold and 1-fold; **Figure 2.4**). Volcano plot depictions of tail fin data show a lesser volume of differentially expressed contigs with high magnitude fold changes following $T_4$ treatment (around 8-fold down, 32-fold up; **Figure 2.4**) as compared to $T_3$ treatment (around 8-fold down, 32-fold up; **Figure 2.4**). In the liver, these plots indicate a far greater strength of response following $E_2$ treatment than either $T_4$ or $T_3$, with fold change magnitudes reaching over 1024 for upregulated transcripts (around 8-fold in downregulated transcripts; **Figure 2.4**).

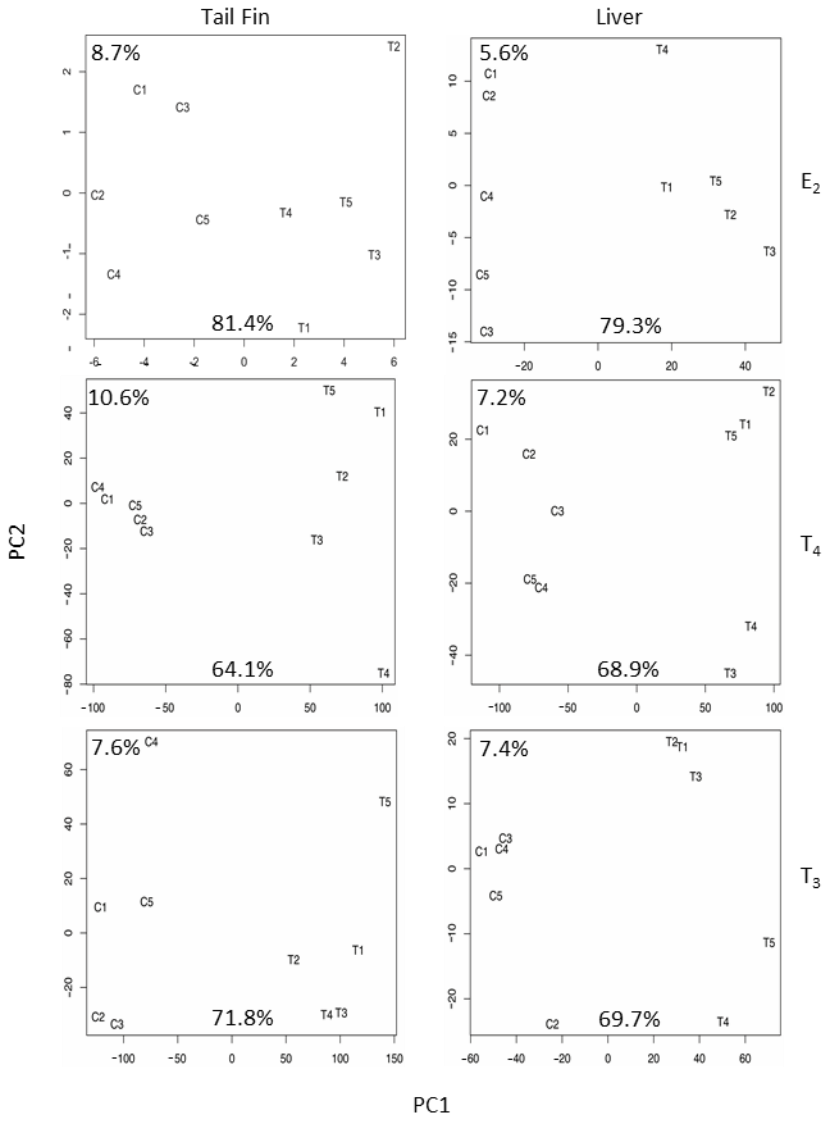


**Figure 2.3 PCA plots of premetamorphic tadpole tail fin and liver differentially expressed contigs from control, $E_2$, $T_4$, and $T_3$ treatments. X-axis represents principle component 1 and the y-axis represents principle component 2. C1-C5 are untreated control biological replicates, T1-T5 are biological replicates exposed to 10 nM $E_2$, 50 nM $T_4$, or 10 nM $T_3$. The percent variation of PC1 and PC2 are indicated in the bottom center and top left corner of each graph, respectively.**

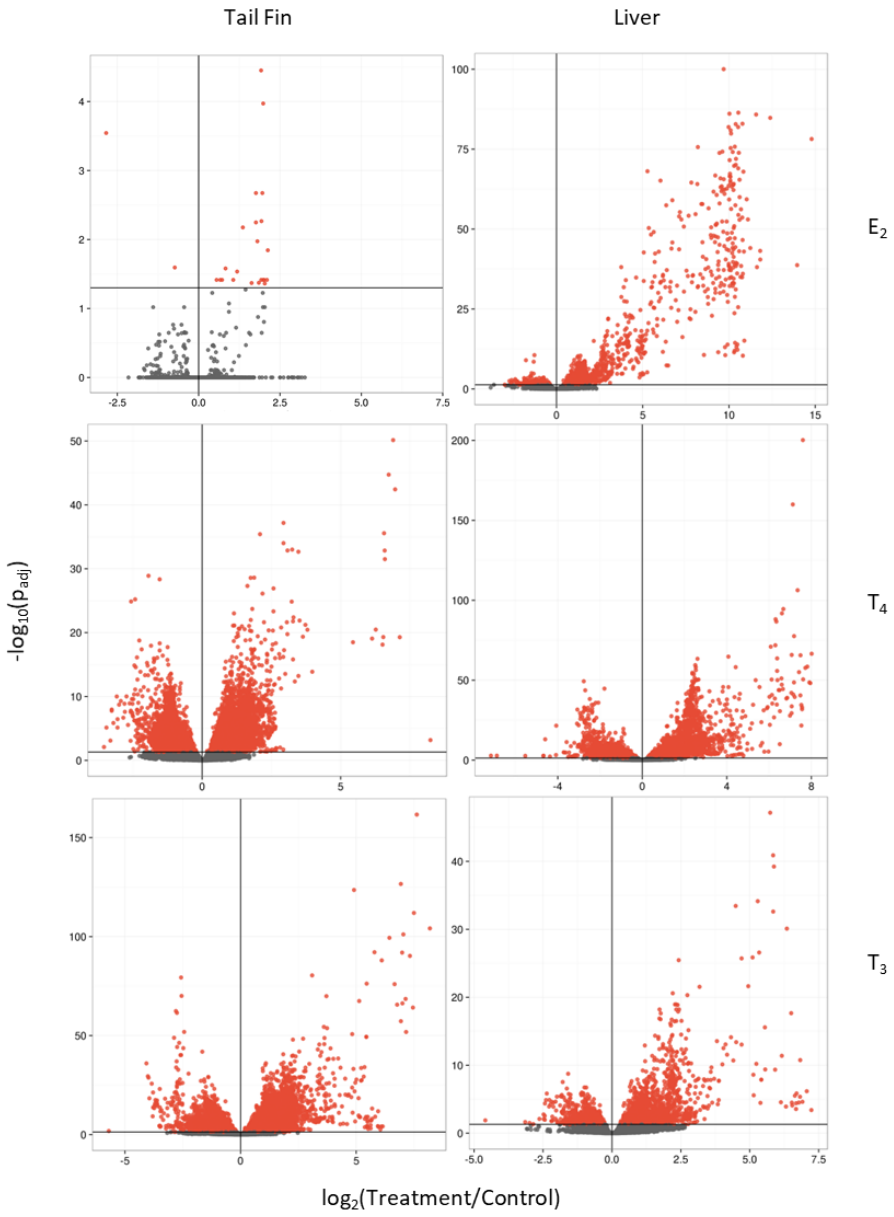


**Figure 2.4 Volcano plots of premetamorphic tadpole tail fin and liver differentially expressed contigs from control, 10 nM $E_2$, 50 nM $T_4$, or 10 nM $T_3$ treatments. The x-axis represents logarithmic fold change down (left of '0') or up (right of '0'), the y-axis represents adjusted p-values ($p_{adj} \leq 0.05$). Each dot on the plot represents a differentially expressed contigs as determined by DESeq2 analysis. Red dots are statistically significant, grey dots are not significant ($p_{adj} < 0.05$). NA, not available.**

$T_4$ treatment resulted in differentially expressed contigs reaching fold changes of 256, with the majority of upregulated contigs clustering around 16-fold (around 8-fold downregulated), compared to most contigs exhibiting 6-fold or less increase or decrease in abundance following $T_3$ treatment (**Figure 2.4**).

Tail fin heat maps show a very similar distribution of up and down regulated contigs following $T_4$ and $T_3$ treatment, while $E_2$ exposure resulted in more contigs increasing in abundance, despite the scant number of differentially expressed contigs identified (**Figure 2.5**). Liver heat maps depicting the results of $E_2$ exposure indicate an increase in transcript abundance in the majority of differentially expressed contigs (**Figure 2.5**). $T_4$ treatment shows a qualitatively similar distribution of transcript abundance increases and decreases, while $T_3$ treatment appears to show that majority of these transcripts increase in abundance, rather than decrease.

Venn diagram depictions of RNA-seq data show that $E_2$ exposure in the tail fin resulted in just 25 statistically significant differentially expressed contigs, while $T_4$ exposure resulted in 11,348 contigs, and $T_3$ exposure resulted in 17,051 contigs (**Figure 2.6**). 3 contigs were identified across all three treatments, and 8165 common $T_4$ and $T_3$ treated contigs were identified.

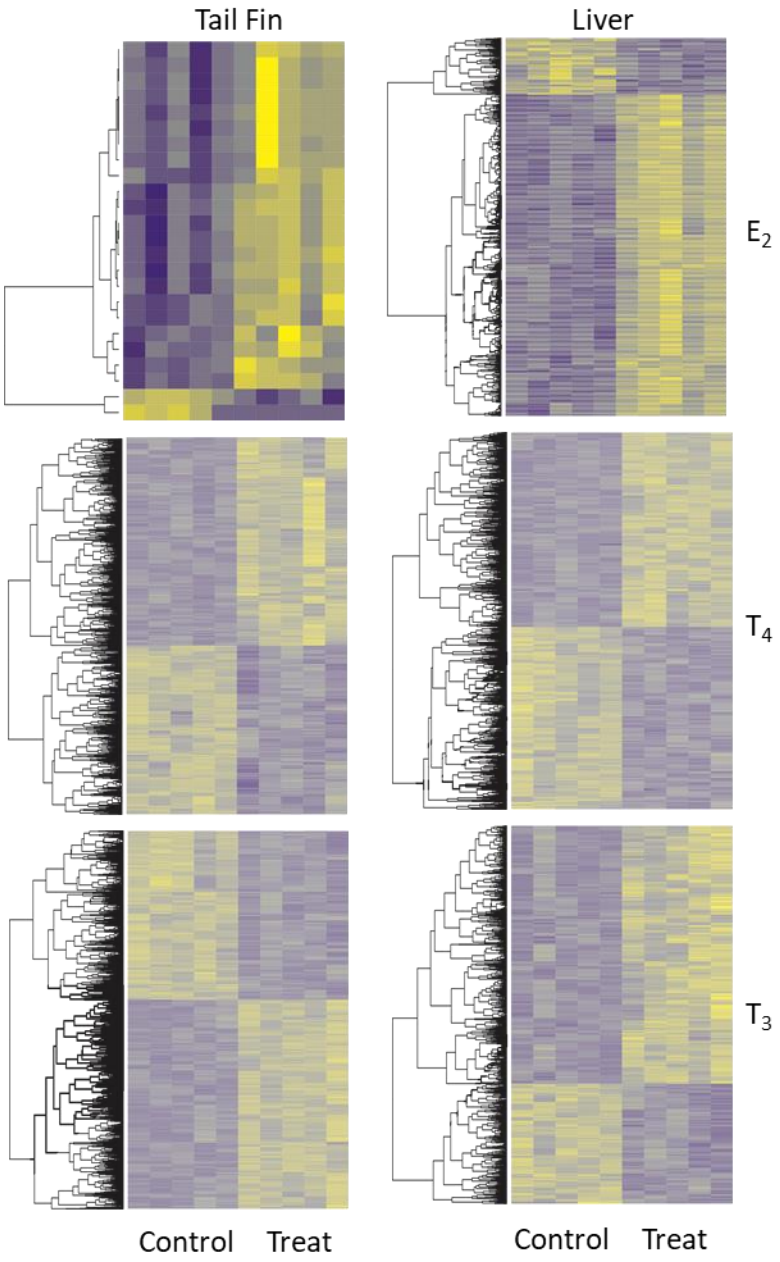


**Figure 2.5 Heat maps of premetamorphic tadpole tail fin and liver differentially expressed contigs from control, $E_2$, $T_4$, and $T_3$ treatments. The x-axis represents experimental samples. Each column represents a biological replicate (n=5 per control or treatment ('Treat') condition). The treatments are either 10 nM $E_2$, 50 nM $T_4$, and 10 nM $T_3$. The y-axis represents a z-score (blue: -2; yellow: +2) mediated cluster analysis of statistically significant differentially expressed contigs (p-value<0.05).**

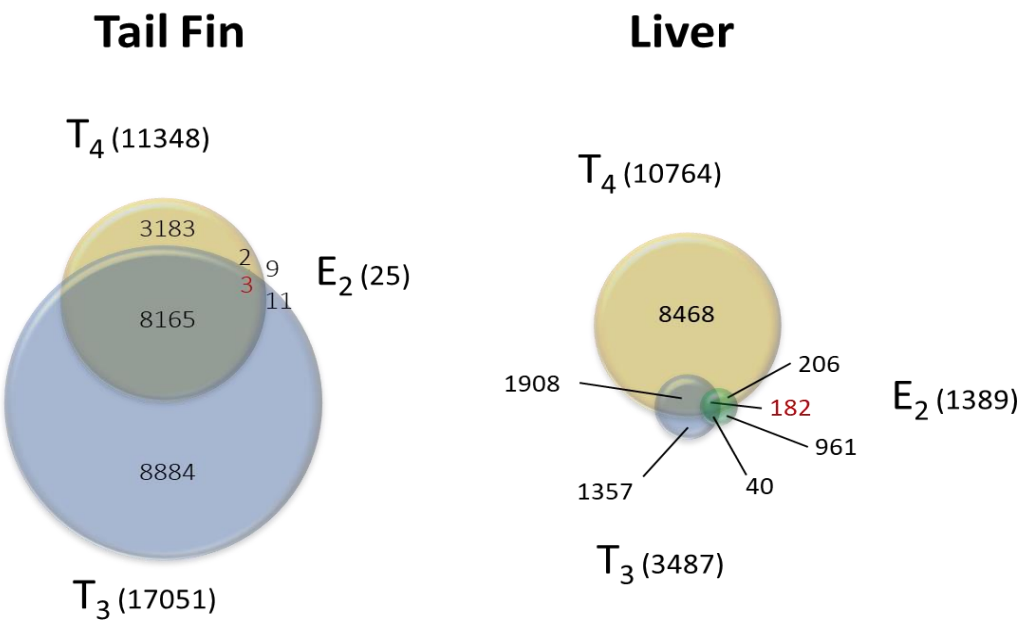


**Figure 2.6 Venn diagram comparison of statistically significant (p-value<0.05) differentially expressed contigs identified in $E_2$ (10 nM), $T_4$ (50 nM), and $T_3$ (10 nM) treatments in the liver and tail fin of premetamorphic *R. catesbeiana* tadpoles following RNA-seq. Red numbers indicate significance in all three treatments. Circles were scaled to indicate the difference in total contigs represented in each hormone exposure group**.

In the liver, $E_2$ exposure resulted in 1,389 differentially expressed contigs, while $T_4$ treatment resulted in 10,764 differentially expressed contigs, compared to just 3,487 following $T_3$ treatment (**Figure 2.6**). 182 differentially expressed contigs common to all three treatments were identified. 1,908 contigs common to both $T_4$ and $T_3$ were identified in the liver.

98% of all tail fin contigs were annotated successfully (**Table 2.1**), while 99% of all liver contigs were annotated successfully (**Table 2.2**). Of the differentially expressed contigs, GO-analysis was limited to human Uniprot annotations, which represent 72-73% of successfully annotated contigs in the tail fin and about 73% in the liver, but nonetheless provide useful characterizations of identified contigs (**Table 2.1** and **2.2**, respectively).

**Table 2.1 Summary of tail fin RNA-seq results following 3,5',3-triiodothyronine ($T_3$), thyroxine ($T_4$), and 17β- estradiol ($E_2$) exposures**

| | Total contigs | | | Significant contigs | | |
|---|---|---|---|---|---|---|
| Treatment | Overall | Annotated | Annotated with human Uniprot | Overall | Annotated | Annotated with human Uniprot |
| 10 nM $E_2$ | 55859 | 54532 (98%)[a] | 40033 (72%)[a] | 25 (0.04%)[a] | 22 (88%)[b] | 20 (80%)[b] |
| 50 nM $T_4$ | 55864 | 54772 (98%)[a] | 40282 (72%)[a] | 11348 (20%)[a] | 11011 (97%)[b] | 8501 (75%)[b] |
| 10 nM $T_3$ | 61698 | 60520 (98%)[a] | 44876 (73%)[a] | 17051 (28%)[a] | 16614 (97%)[b] | 12932 (76%)[b] |

[a]Percent values relative to overall total contigs

[b]Percent values relative to overall significant contigs

**Table 2.2 Summary of liver RNA-seq results from the 3,5',3-triiodothyronine ($T_3$), thyroxine ($T_4$), and 17β-estradiol ($E_2$) exposure sets. Percent values relative to overall.**

| | Total contigs | | | Significant contigs | | |
|---|---|---|---|---|---|---|
| Treatment | Overall | Annotated | Annotated with human Uniprot | Overall | Annotated | Annotated with human Uniprot |
| 10 nM $E_2$ | 44964 | 44529 (99%)[a] | 32213 (72%)[a] | 1389 (3%)[a] | 1380 (99%)[b] | 821 (59%)[b] |
| 50 nM $T_4$ | 45026 | 44593 (99%)[a] | 32666 (73%)[a] | 10764 (24%)[a] | 10678 (99%)[b] | 8289 (77%)[b] |
| 10 nM $T_3$ | 44311 | 43874 (99%)[a] | 32256 (73%)[a] | 3488 (8%)[a] | 3464 (99%)[b] | 2585 (74%)[b] |

[a]Percent values relative to overall total contigs

[b]Percent values relative to overall significant contigs

$E_2$ treatment data in the tail fin was not sufficient to generate biological process REVIGO Gene Ontology treemaps. Treemaps of $T_4$ and $T_3$ treated differentially expressed contigs further exemplify the differences evident in the tail fin transcriptome following exposure to these two forms of TH. Major categories for $T_4$ exposure included negative regulation of cellular processes, vesicle-mediated transport, response to organic substance, single-multicellular organism process and neutrophil activation (**Figure 2.7A**), while $T_3$ treatment affected negative regulation of biological process, mRNA metabolism, protein localization, cellular metabolism, and response to organic substance (**Figure 2.7B**). In the liver, $E_2$ treatment affected response to endoplasmic reticulum (ER) stress, epoxygenase p450 pathway, and retrograde vesicle-mediated transport Golgi to ER (**Figure 2.8A**). In contrast, both $T_4$ and $T_3$ exposure most affected monocarboxylic acid metabolism, vesicle-mediated transport, translational initiation, negative regulation of biological process, and organic substance metabolism (**Figures 2.8B** and **2.8C**, respectively).

Although $E_2$ treated tail fin data was not sufficient for gene ontology analysis, GO Panther-Slim biological process bar charts of difference of TH treatments in the tail fin reveal a substantial difference in biological process components affected by $T_4$ and $T_3$. $T_4$ treatment resulted in less differentially expressed biological process categories than $T_3$ treatment (**Appendix B**), although they do share several pathway components, such as immune response (downregulation) and protein transport (upregulation).

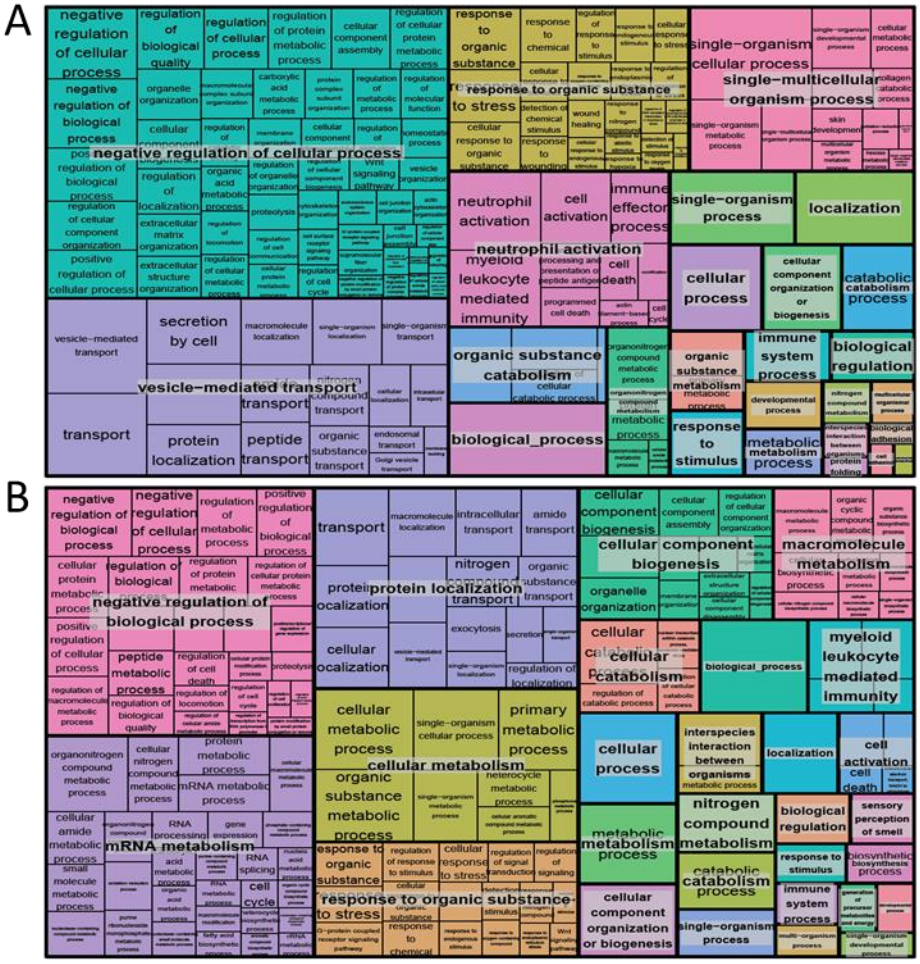


**Figure 2.7 Biological process REVIGO gene ontology treemap of A) $T_4$-treated and B) $T_3$-treated differentially expressed tail fin contigs. $E_2$-treated contig treemaps are not included due to the low number of DE contigs that inhibited the completion of this analysis.**

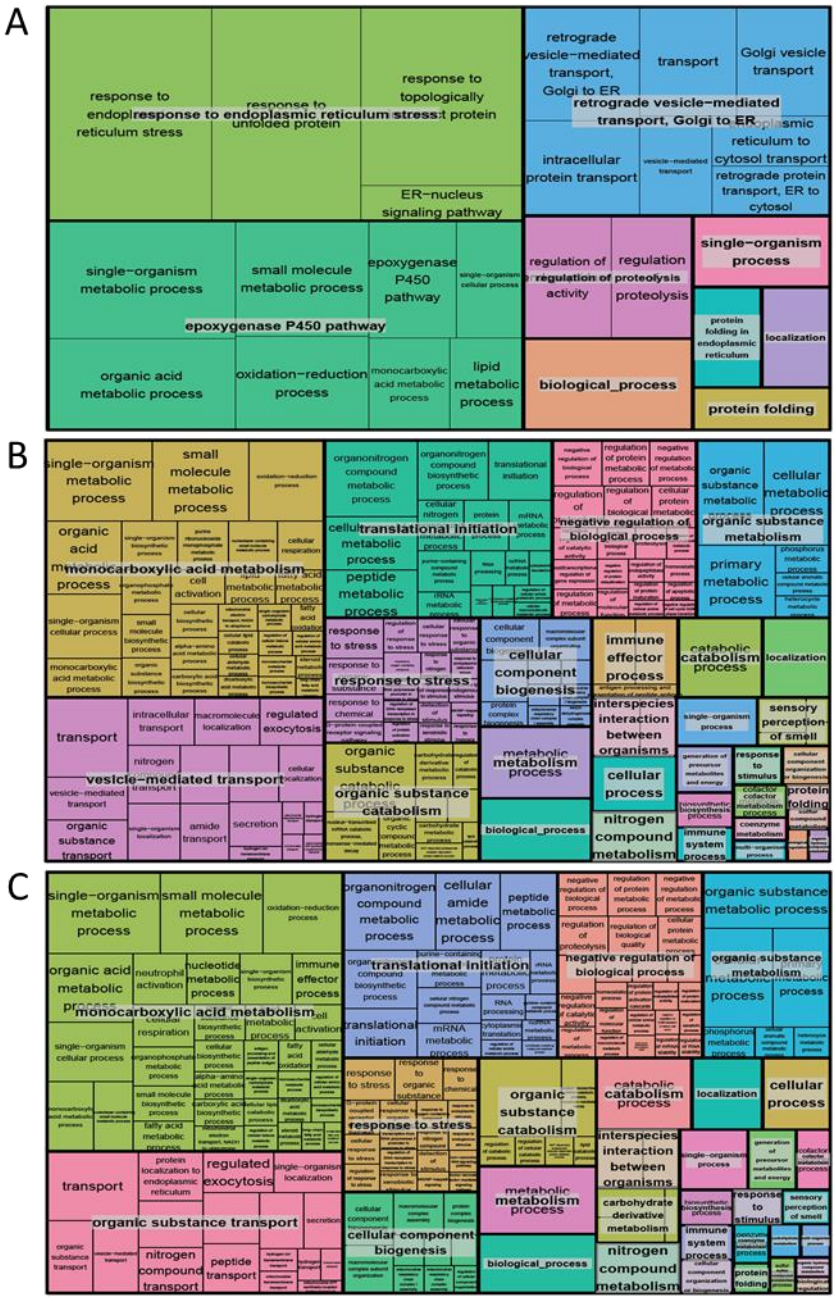


**Figure 2.8 Biological process REVIGO gene ontology treemap of A) $E_2$-treated, B) $T_4$-treated and C) $T_3$-treated differentially expressed liver contigs.**

Interestingly, several categories such as B-cell mediated immunity and defense response to bacteria are downregulated in response to $T_3$ treatment, but are not even present in $T_4$ treated contigs (**Appendix B**). In the liver, $E_2$ treated contigs represent only six biological process categories: catalytic activity, oxidoreductase activity, peptidase and peptidase inhibitor activity, and serine-type endopeptidase and peptidase activity (**Appendix C**). All are increased in response to $E_2$ treatment. In contrast to the tail fin, $T_4$ and $T_3$ treatments in the liver resulted in very similar GO Panther-Slim biological process bar charts of difference (**Appendix C**); downregulation of cytokine signaling and regulation of nucleobase pathways in $T_3$ treated samples appears to be the only qualitatively observable difference between the two hormone treatments in this context.

We selected two novel immune system candidates (*tnfa* and *xbp1*) for more extensive qPCR analysis. In the tail fin, $T_4$ treatment resulted in increased *tnfa* transcript abundance at the high concentration (1.4-fold; $p = 0.003$; **Figure 2.9**), while $T_3$ treatment resulted in increased abundance at both the medium and high concentrations (1.5-fold; $p = 0.01$ and 2.7-fold, $p < 0.001$, respectively; **Figure 2.9**). $E_2$ treatment did not elicit a response. RNA-seq analysis of *tnfa* revealed similar fold changes; $T_4$ treatment yielded a fold change of 2.5, and $T_3$ treatment yielded a fold change of 2.6 (data not shown).

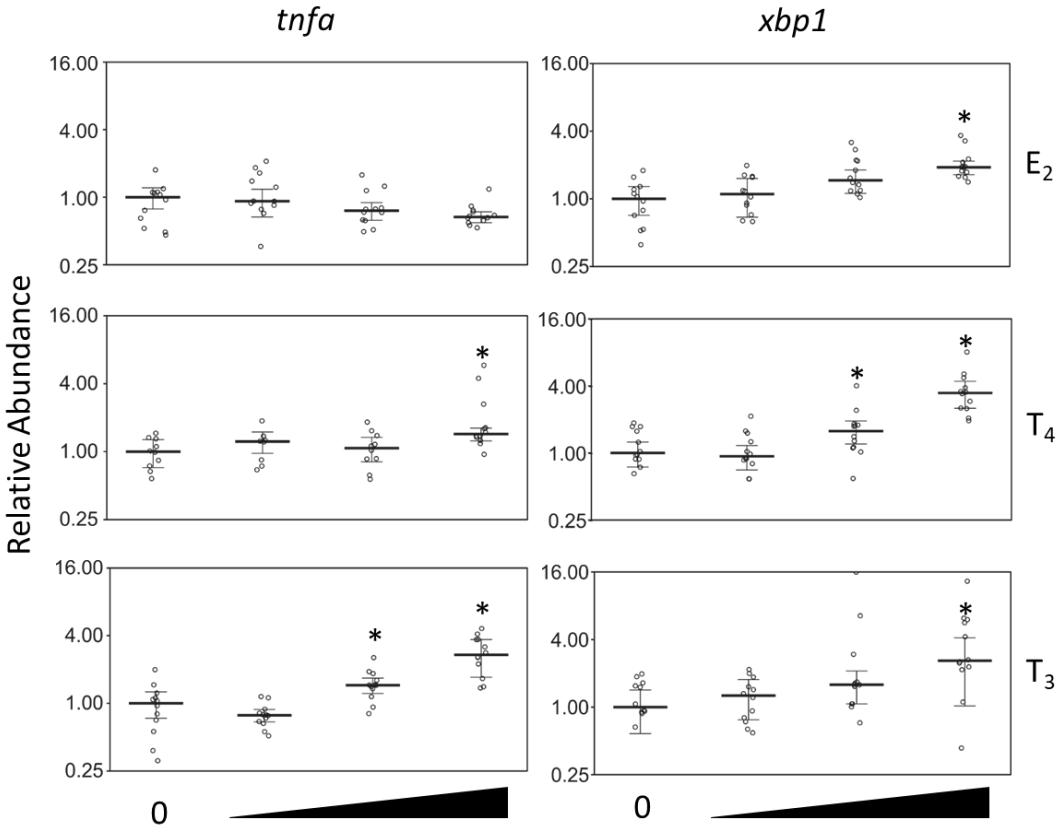


**Figure 2.9 Premetamorphic *R. catesbeiana* tadpole transcript abundance for A) tumor necrosis factor α (*tnfa*) in tail fin and B) X-box binding protein 1 (*xbp1*) in liver after 48 h exposure to either vehicle ('0') or increasing physiologically relevant concentrations of $E_2$ (0.1, 1.0, 10 nM), $T_4$ (0.5, 5.0, 50 nM), or $T_3$ (0.1, 1.0, 10 nM) as measured by qPCR. Refer to Figure 2.1 legend for details.**

In the liver, $E_2$ treatment resulted in increased *xbp1* transcript abundance at the high concentration (3-fold; p = 0.001; **Figure 2.9**). $T_4$ treatment increased *xbp1* mRNA levels at the medium and high concentrations (1.5-fold; p = 0.007 and 1.9-fold; p < 0.001, respectively; **Figure 2.9**), while the only the high concentration of $T_3$ treatment increased transcript abundance, although to a greater magnitude (3-fold; p = 0.001; **Figure 2.9**). RNA-seq analysis of *xbp1* revealed a fold change of 2.8 following $E_2$ exposure, 2.0 following $T_4$ exposure, and 2.4 following $T_3$ exposure (data not shown).

## 2.3 Discussion

The present study establishes and reveals distinct differences in transcriptomic profiles of *R. catesbeiana* tadpole tail fin and liver tissue following treatment with the two forms of TH, $T_4$ and $T_3$. RNA-seq evaluation of deiodinase status of both tissues confirmed the absence of expressed *dio1* or *dio2* within our present study, which was also demonstrated in Birol et al. (2015) for the liver. Both tissues exhibited distinctive response profiles to the two hormones, providing an intriguing insight into differential tissue responsiveness to the two major forms of THs.

qPCR results of canonical TH-responsive genes in the tail fin reveal that $T_3$ treatment resulted in a stronger response in all mRNA profiles analyzed at nearly every concentration tested relative to the vehicle. RNA-seq examination of the transcriptomic response to TH exposures provides further evidence that $T_3$ may play a more extensive role than $T_4$ in modulating the tail fin transcriptome; more statistically significant differentially expressed $T_3$ treated contigs were identified than $T_4$ treated contigs following sequencing, $T_3$ produces a greater magnitude fold change response in treated contigs, and gene ontology analysis revealed a divergence between $T_3$ and $T_4$ modulated biological categories. These findings, coupled with qPCR analysis, suggest that while $T_4$

is capable of affecting gene expression, the degree to which that action occurs does not recapitulate the previously demonstrated 5-fold difference in biological activity and affinity between $T_4$ and $T_3$ (Maher et al., 2016). However, the methods of exposure differ between the foundational study (intraperitoneal injection) and the present study (water bath immersion for 48 h). Previous research that used tail regression as an endpoint observed that use of the injection method for both $T_4$ and $T_3$ exposures resulted in a larger percentage decrease in tail length compared to immersion after 5 days (Frieden and Westmark, 1961), indicating that immersion requires more time to elicit the same response as injection. Because the exposure methods in the present study and Maher et al., (2016) both occurred over a 48 h period, it is possible that the discrepancy noted between the tail fin responses to $T_4$ and $T_3$ in these studies is a result of differential kinetics of the injection and immersion methods.

The study by Frieden and Westmark (1961) also observed that $T_3$ exposure resulted in a larger percentage decrease in tail length than $T_4$ (Frieden and Westmark, 1961). Additionally, monocarboxylate transporter 10 (MCT10), a transporter with a reported preference for $T_3$ (Visser et al., 2007), was identified in the tail fin transcriptome (the present study, data not shown). Previous work with *R. catesbeiana* tadpole tail fin nuclei also found more $T_3$ nuclear binding sites than $T_4$ (Yoshizato et al., 1975). These factors provide additional insights into the differential response of the two THs in this tissue.

Despite the difference in TH exposure methods stated previously, qPCR results of canonical TH-responsive genes in the liver recapitulate the results observed in Maher et al., (2016) that indicated that multiple modes TH binding are possible within the same tissue. *Thra* differs from *thrb* and *thibz* in that it has not been identified as a “direct

response" gene in TH signaling pathways (Hammond et al., 2016). In both studies, $T_4$ and $T_3$ produced similar responses in *thra* transcript abundance across all three concentrations, suggesting that a direct mode of $T_4$ action is possible in certain gene transcripts. On the other hand, *thrb* and *thibz* transcripts in the present study show a stronger response at the medium concentration of $T_4$ than that of $T_3$, which was also observed in (Maher et al., 2016) at intermediate $T_4$ treatment doses. It was postulated therein that a possible explanation for this gene-specific phenomenon involves non-genomic $T_4$ signaling via a transmembrane integrin αvβ3 (Davis et al., 2009; Freindorf et al., 2012). In the present study, both integrin components were identified in the liver transcriptome but were not differentially affected (data not shown), suggesting that this mechanism could be at play in the liver tissue.

Additionally, RNA-seq examination of $T_4$ and $T_3$ response patterns suggest that $T_4$ may play a more extensive role than $T_3$ in modulating transcriptomic events in the liver. Over 10,000 statistically significant differentially expressed contigs were identified in the livers of animals treated with $T_4$, compared to just 3,487 contigs following $T_3$ treatment; only 1908 contigs were found to respond to both hormones. Analysis of the magnitude of response of differentially expressed contigs indicates that $T_4$ treatment results in greater fold changes on average than $T_3$ treatment. However, gene ontology analysis and REVIGO treemaps summarizing affected contigs suggests that both hormones modulate similar pathways, despite the differences noted above. This suggests that although $T_4$ and $T_3$ modulate similar pathways and produce similar responses in certain gene transcripts, it is possible that a preference for $T_4$ occurs in other situations.

Previous evaluation of the role of $T_4$ as an active hormone in premetamorphic tadpoles found that $T_4$ is capable of exerting a physiological effect without 5'-deiodinase-mediated conversion to $T_3$; $T_4$ uptake in the liver greatly exceeded that of $T_3$ within the first hours of treatment by injection, and equimolar administration of both hormones resulted in at least twice as much $T_4$ in the liver cytosol and nuclei (Galton and Cohen, 1980). However, of the known TH transporters, only large neutral amino acid transporters (LAT1 and LAT2), transmembrane proteins that transport THs into cells and exhibit a slight preference for $T_3$ over $T_4$ (Kinne et al., 2011), were identified in the liver transcriptome through RNA-seq (the present study), which does not explain the observed differential response to $T_4$ in this tissue. Further examination of this liver-specific observation is warranted with a particular focus on non-genomic signaling pathways.

Furthermore, we demonstrated that classical TH-responsive genes *thra, thrb,* and *thibz* were refractory to $E_2$ treatment at physiological doses in either tissue. This is notable for evaluating the presence of endocrine disrupting chemicals (EDCs) in that detection of a perturbation of *thra, thrb,* and *thibz* transcript levels indicates TH disruption, rather than disruption due to xenoestrogen.

We also found that $E_2$ elicits different responses in the tadpole tail fin and liver transcriptomes. Contigs identified by RNA-seq as differentially expressed following $E_2$ exposure in the liver are far more abundant than those identified in the tail fin. Interestingly, contigs from $E_2$-treated tadpoles showed the greatest magnitude of response compared to all other conditions analyzed in both tissues, although the number of differentially expressed contigs was far lower when compared to the TH responses in the

liver. This indicates that the liver, not the tail fin, may be a useful tissue to investigate for $E_2$-related responses such as potential xenoestrogen exposure in the context of EDCs.

Additionally, RNA-seq data from the present study suggests that $E_2$ modulates at least some transcriptomic events that are shared with $T_4$ and $T_3$ in the liver, but not in the tail fin. 182 contigs were found common to all three hormone treatments in the liver out of 15,640 differentially expressed contigs, while no common sequences were identified in the tail fin. Overall, however, there is little overlap in the $E_2$ and TH response profiles, indicating that cross-talk between these hormones in this context is less evident than has been previously reported. Previous work examining hormone cross-regulation in the brain of *R. pipiens* tadpoles found that 50 nM $T_3$ treatment led to a significant increase in ERα transcript abundance (Hogan et al., 2008). However, differential expression of ERs due to TH treatment was not observed in RNA-seq results in the present study, although ERα presence was confirmed in the liver transcriptome (data not shown). Additionally, ERα expression in the tail fin was extremely low (data not shown), which may account for the difference in tissue responsiveness to $E_2$ observed between the tail fin and liver.

The recently published bullfrog genome predicts over 22,000 protein-coding genes (Hammond et al., 2017), while BART contains over two million contigs. These contigs represent the most intact transcripts made possible by the transcriptome assembly and BLAT redundancy reduction process, which was performed to remove as many duplications as possible while retaining distinct transcript sequences. As a result, the contig numbers reported in the current study may include isoforms of different transcripts, possible duplications, or fragments of transcripts, which would explain the discrepancy noted in the number of protein-coding genes and the number of contigs

reported. This could possibly affect the GO analyses conducted in the present study in that more than one contig may share the same annotation, which would suggest a greater enrichment of a specific transcript type in the context of hormone induction.

The present study also demonstrates through qPCR analysis of novel validated immune transcripts, as well as examination of RNA-seq data through gene ontology, that elements of the immune system do appear to be modulated by THs. Previous research has demonstrated *tnfa* gene expression changes as a result of $T_3$ in various experimental conditions, such as $T_3$ exposure rainbow trout immune cells (Quesada-García et al., 2016), although the effect of $T_4$ was not demonstrated therein. However, TH-induced gene expression changes in *xbp1* are novel, with a focus on estrogen-associated gene expression changes in the current body of literature (Sengupta et al., 2010). This suggests that these new immune-associated tools could provide new information regarding TH-modulated immunity under a variety of experimental conditions in developing tadpoles. Tail fin gene ontology analysis revealed that both $T_4$ and $T_3$ treatment affected neutrophil activation and myeloid leukocyte mediated immunity, as well as general immune system processes. Furthermore, in addition to the immune system modulation by $T_3$ that was first reported in liver tissue (Birol et al., 2015), we have shown that $T_4$ is also capable of modulating these critical events in this tissue. Immune effector and system processes were affected by $T_4$ treatment, while $T_3$ also affected general immune system processes.

The role of the immune system in metamorphosis has also been demonstrated previously in the context of TH-mediated apoptosis of tissues such as the tail fin that rely on macrophages and lymphocytes to remove larval-associated apoptotic bodies from tissues in order for development to progress normally (Ishizuya-Oka et al., 2010;

Ishizuya-Oka, 2011). This, this evidence of TH-responsive immune system genes may be useful in the context of endocrine disruption in animals with developing immune systems in that the generation of an immune system-related qPCR toolbox may provide insight into possible disruption in the context of exposure to pathogens or EDCs. Amphibian populations around the world are rapidly declining due to the emergence of pathogens that cause Ranavirus and chytrid fungal infection (Rosa et al., 2017), and previous studies have reported immune modulatory effects of EDCs on vertebrates (Qiu et al., 2016; Regnault et al., 2016). Therefore, further investigation into TH-modulated immunity is necessary to understand the mechanisms of population devastation and possible immunosuppression due to environmental stressors.

In summary, the results presented herein show that the liver and tail fin, both 5'-deiodinase-poor tissues, respond differently to $E_2$ and THs in the context of canonical TH-responsive genes and their respective transcriptomes, and that elements of the immune system of a developing tadpole are modulated by THs. This work sets the foundation for further evaluation of tissue-specific responses to environmental contaminant effects on critical endocrine signaling systems.

# 3 Characterization and functional analysis of antimicrobial peptides within the *Rana [Lithobates] catesbeiana* transcriptome through a bioinformatics approach


## Abstract

Antimicrobial peptides (AMPs), small compounds that often exhibit broad spectrum antimicrobial activity, are garnering interest as potential therapeutics against antibiotic-resistant bacterial pathogens. Frog skin is a prolific source of high potency AMPs that may prove useful in the quest for alternative antimicrobial agents. However, identification of new AMPs remains arduous due to the practical limitations of classical protein-based discovery approaches. In the present study, we have developed a high throughput bioinformatics approach using known AMP characteristics and common AMP properties, confirmed identification of known AMPs from the North American bullfrog *(Rana (Lithobates) catesbeiana)* genome, and mined the genome to identify novel AMPs. Using this methodology, we have successfully identified two novel bullfrog AMPs that exhibited antimicrobial activity against *Mycobacterium smegmatis* via microtitre broth dilution assays. The results presented herein demonstrate the utility of bioinformatics and genomics resources in identifying and developing novel therapeutics to combat the public health crisis of antibiotic resistance.


## 3.1 Introduction

Antibiotic resistance amongst bacterial pathogens that cause prevalent global diseases has emerged as one of the most critical public threats facing the world today (Munita and Arias, 2016; Nathan and Cars, 2014; World Health Organization, 2014). An analysis conducted by the Centers for Disease Control and Prevention estimates that at least 23,000 deaths in the United States each year are attributed to infections caused by antibiotic-resistant organisms (Munita and Arias, 2016). In 2015, The World Health

Assembly endorsed a global action plan to combat antimicrobial resistance with strategic objectives that include optimizing the use of antimicrobial agents and sustainable investment in countering antimicrobial resistance (World Health Organization, 2015). Consequently, discovery and development of alternative antimicrobial pharmaceuticals is an urgent and global need. As an alternative to traditional antibiotic therapy, antimicrobial peptides (AMPs) are garnering interest as potential antimicrobial therapeutics (Jantaruk et al., 2017). AMPs are a diverse class of oligopeptides produced by all multicellular organisms as a defense against a broad spectrum of pathogenic organisms including bacterial, fungi, and viruses and are considered central components of the innate immune system (Bahar and Ren, 2013; Brandenburg et al., 2016; Hiemstra and Zaat, 2013).

Although overall AMPs exhibit remarkable primary and tertiary structural diversity, commonalities include the fact that they are typically shorter than 100 amino acids, maintain a positive net charge, and can be classified into four separate groups based on their secondary structures: β-sheet, α-helix, extended coil, and loop. Of these groups, α-helix AMPs are the most studied and most common (Bahar and Ren, 2013). The overall cationic nature of AMPs and distribution of hydrophobic residues enable these peptides to interact with and exhibit antimicrobial properties against pathogens and contribute to their overall function (Andersson et al., 2016; Bahar and Ren, 2013). Further, these properties associated with AMPs are conserved within AMP families due to common primary sequence similarities maintained between like peptides (Conlon and Mechkarska, 2014; Waghu et al., 2016).

AMPs are generally composed of an N-terminal signal peptide sequence, prosequence, and C-terminal mature peptide sequence. All AMPs are produced as precursors that are proteolytically processed by propeptide convertases to yield active, mature peptides (Aittomäki et al., 2017; Hiemstra and Zaat, 2013; Joo et al., 2016; Valore and Ganz, 2008).While AMP signal peptide and prosequences are typically conserved within families, the mature peptide sequences vary considerably and represent the functional portion of the antimicrobial peptide (Hiemstra and Zaat, 2013). As described in the current report, these characteristics can be exploited to identify and characterize novel AMPs from a large dataset (Waghu et al., 2016).

Furthermore, because of the unique and multifaceted mechanisms of antimicrobial action employed by AMPs, such as destruction of microbial membranes (Nguyen et al., 2011), inhibition of macromolecule synthesis (Haney et al., 2013), and peptide-induced modulation of the immune system (Otvos Jr., 2016), microbes are less likely to develop resistance against these peptides than conventional antibiotics. There are a few AMPs that are currently used in a clinical setting, and many more AMPs are undergoing clinical trials to ascertain their therapeutic potential (Andersson et al., 2016).

Frog skin is an abundant source of AMPs due to specialized granular glands in the dermis that synthesize and store these peptides, which are secreted onto the skin surface at the first sign of injury or microbial challenge (Bahar and Ren, 2013; Conlon and Mechkarska, 2014; Schadich et al., 2009). Adult frog skin in particular is a rich source of these peptides (Conlon and Mechkarska, 2014). From an evolutionary survival perspective having this rich repertoire of AMPs within frog skin makes sense, since frogs live in water and soil environments where pathogens are plentiful. The Antimicrobial

Peptide Database (APD; Wang, 2004), a curated, comprehensive database for AMPs, contains 978 active peptides originating from frog skin (out of 1043 amphibian peptides), a value that that represents 34% of the entire AMP database derived from all sources (http://aps.unmc.edu/AP/main.php). Furthermore, the utility and efficacy of some frog AMPs as potential therapeutics has been demonstrated previously (Batista et al., 2001; Ge et al., 2014; Luca et al., 2013).

Although development of AMPs originating from frog skin is a promising approach to counteract the global crisis of antibiotic resistance, limitations associated with traditional AMP identification methods of NMR and mass spectrometry, including the cost of implementation and low-throughput experimentation, have hindered the field of research. This emphasizes the need to develop an alternative approach for the identification of novel peptides with therapeutic potential.

Herein, we describe a high throughput bioinformatics approach for the identification and characterization of putative AMPs based on peptide homology using the rich genomic resources we have built for the North American bullfrog, *Rana (Lithobates) catesbeiana.* Through computationally-based methods, we identify two novel bullfrog AMPs that successfully demonstrate antimicrobial activity via an established microtitre broth dilution method (Hancock, 1999). These computational methods combined with valuable genomic resources may enable the identification and characterization of compounds with potent antimicrobial activity.

## 3.2 Materials and methods

### 3.2.1 *In silico Prediction and Characterization of Putative Antimicrobial Peptides*

Putative AMPs were initially identified in the bullfrog annotated reference transcriptome (BART version 2, NCBI TSA accession GFBS01000000) by homology to

known AMP sequences. The BART transcript sequences, all of which were *de novo* assembled with Trans-ABySS (Robertson et al., 2010) from strand-specific RNA-Seq libraries (Hammond et al., 2017), were *in silico* translated using Transdecoder (-m 20 -S; version 2.0.1) (https://github.com/TransDecoder/TransDecoder). Complete predicted open reading frames up to 100 amino acids long were retained. Hidden Markov models (HMMs) representing the salient features of AMPs, such as ORF length, cationicity, and specific distribution of residues from 35 protein families were downloaded from the Collection of Antimicrobial Peptides database (http://www.camp.bicnirrh.res.in/pattern_hmm.php?q=HMM_fam; accessed March 3, 2016), and hmmer (Mistry et al., 2013) was used to identify BART peptide sequences with similarity to one or more HMM (default settings, significance considered at $E < 0.001$). These hits were then further refined using InterProScan (Jones et al., 2014) default settings with the Pfam database (Finn et al., 2016) of protein domain HMMs (version 29.0).

Sixty-five additional putative transcripts were further identified from a more extensive version of BART that was assembled from a variety of tadpole tissues and treatment conditions (Hammond et al., 2017). Transcripts were retrieved from BART using an annotation-based search for AMP-like transcripts within the bullfrog transcriptome using key words such as ‘antimicrobial’ and ‘precursor’ to analyze a larger volume of potential AMPs. Annotations were derived from BLASTX alignments of BART contigs to the EMBL Uniprot protein database (Kulikova et al., 2007). The annotation of the top high quality hit (e-value$\leq 10^{-5}$) was applied.

A translated blast (TBLASTN; Altschul et al., 1990) using standard parameters was used to align all cDNA sequences of putative peptide queries against a representative selection of known antimicrobial peptides sequences from NCBI (National Center for Biotechnology Information; "Database resources of the National Center for Biotechnology Information," 2016) to initially characterize the sequences based on homology with known AMP families. Known sequences used in this analysis included representatives from ranatuerin, brevinin, ranalexin, esculentin, palustrin, catesbeianin, cathelicidin, odorranain, japonicin, and temporin families from a variety of anuran species. Sequences that did not align in any manner to any known AMP protein sequences in this characterization step were eliminated from consideration. Additional ORF determination of putative cDNA sequences was performed using Virtual Ribosome 2.0 (Wernersson, 2006) to ensure that proper reading frames and precursor sequences identified following TBLASTN were recapitulated.

Protein blasts (BLASTP; (Altschul et al., 1990) were performed against the NCBI nr database (accessed September 2017; "Database resources of the National Center for Biotechnology Information," 2016) using the protein sequences determined by the above analysis to identify the top protein alignments for further sequence characterization. Alignment e-value scores of $10^{-4}$ or lower were retained. Putative peptides that did not produce any alignments to known AMPs, did not begin with a methionine or valine residue, and did not include the canonical propeptide convertase Lys-Arg (KR) cleavage site (Chen et al., 2006; Dürr et al., 2006; Soloviev et al., 2008) or additional peptidase single-cut cleavage sites determined via ExPASy Peptide Cutter (http://web.expasy.org/peptide_cutter) were eliminated from consideration.

Clustal Omega (http://www.ebi.ac.uk/Tools/msa/clustalo/; Sievers et al., 2014) was used to produce alignments of each putative peptide and its best AMP alignment from the nr database as determined through BLASTP using the methodology described above. Additionally, a maximum likelihood tree was constructed using a Poisson model and nearest-neighbor-interchange heuristics with 500 bootstrap replicates via MEGA 7.0 (Kumar et al., 2016). Putative peptides, their best known AMP matches, and outgroup NCBI-derived peptides from brevinin, esculentin, temporin, and odorranain families were included to analyze the sequence-based relationships of the different peptides.

Peptide sequences were also analyzed via SABLE Protein prediction (http://sable.cchmc.org/) to assess secondary structures of the putative peptides and the presence of α-helices that typically compose AMPs, influence their biological function, and are conserved within AMP families (Bahar and Ren, 2013). The net charge, molecular weight, and isoelectric points (pI) of the mature peptides were determined to confirm their overall cationic nature using Protein Calculator v3.4 (http://protcalc.sourceforge.net/).

Additionally, transcript levels encoding these peptides in premetamorphic *R. catesbeiana* tadpole back skin, tail fin, olfactory epithelium, and liver tissues were determined through RNA-seq analysis of tadpole samples conducted in previous studies (Hammond et al., 2017; Jackman et al., 2017; Partovi et al., 2017). Strand-specific mRNA libraries were constructed and sequenced via Illumina HiSeq (Hammond et al., 2017) and aligned to the BART reference transcriptome (Hammond et al., 2017) to generate counts. All RNA-seq experiments had comparable sequencing depth and were normalized to the total number of reads per sample. To normalize the counts, the number of reads of each contig were divided by the total number of reads in the corresponding

sample and multiplied by 100 million. This was done to account for any variance in the sequencing depth to eliminate bias.

### 3.2.2 Microtitre Broth Dilution

Two identified known peptides (CCH-0008-T_R4012255: Ranatuerin-4; CCH-0008-T_S4110533: Ranatuerin-1) and two putative peptides (CCH-0008-T_S4162036; CCH-BS01-S16505513) from the BART bullfrog reference transcriptome were subjected to functional analysis to assess antimicrobial activity. Microtitre broth dilution methods were implemented for determination of the minimum inhibitory concentration (MIC) and minimum bactericidal concentration (MBC) of the four putative peptides using procedures adapted from the R.E.W. Hancock Laboratory for cationic AMPs (Hancock, 1999) and the CLSI methods for dilution antimicrobial susceptibility tests (Cockerill and Clinical and Laboratory Standards Institute, 2015).

To assess antimicrobial activity across a diverse range of bacterial species, gram negative rods (*Escherichia coli*: ATCC 9723H; *Pseudomonas aeruginosa*: ATCC 10148), gram positive cocci (*Staphyococcus aureus*: ATCC 6538P; *Streptococcus pyogenes*: unknown strain, hospital isolate), and *Mycobacterium smegmatis* ($MC^2155$; neither a true gram positive or gram negative bacterium) colonies were cultured overnight on Mueller Hinton agar plates (MHA; +5% sheep blood for *S. pyogenes*; Cockerill and Clinical and Laboratory Standards Institute, 2015) from frozen glycerol stock. Bacterial suspensions were prepared by placing 3-5 morphologically similar colonies from the grown plate into sterile glass culture tubes containing 2 mL of Mueller Hinton Broth (MHB; +5% lysed horse blood for *S. pyogenes*; Cockerill and Clinical and Laboratory Standards Institute, 2015). Microbial inoculums from bacterial suspensions were prepared through a

spectrophotometric adjustment of turbidity to 0.08-0.1 at 600 nm to achieve a turbidity equivalent to that of a 0.5 McFarland standard (1-2 x $10^8$ CFU/mL) (Hancock, 1999).

Peptides were synthesized by GenScript (Township, New Jersey, USA; https://www.genscript.com) using the mature sequences that followed the KR cleavage site. Peptide 5 from the *Treponema pallidum* protein Tp0751 (pallilysin) (Cameron et al., 2005) was also synthesized and used as a negative control. Peptides were dissolved in ultrapure water, filter sterilized and tested, and serially diluted to obtain a series corresponding to ten times the required testing conditions (Hancock, 1999) (2560 µg/mL, 1280 µg/mL, 640 µg/mL, 320 µg/mL, 160 µg/mL, 80 µg/mL, 40 µg/mL, 20 µg/mL, 10 µg/mL, 5 µg/mL). Peptide CCH-BS01-S14839083 was identified as a novel peptide, but failed to synthesize and was therefore not included in the broth microdilution assays.

Five 96-well microtitre plates (Fisher Cat. No. CS003790; Nepean, Ontario, Canada) were prepared with 100 µL of *E. coli*, *P. aeuruginosa*, *S. aureus*, *S. pyogenes*, or *M. smegmatis* bacterial suspension dispensed into each well of columns 1 through 11. Eleven microtitres of the 10x AMP dilution series for all four peptides were added to each well from column 1 (2560 µg/mL) to column 10 (5 µg/ mL) in all five plates. Column 11 functioned as a positive control for bacterial growth in the absence of AMPs. Column 12 in each plate contained 100 µL of MHB as a sterility control (+5% lysed horse blood for *S. pyogenes*; Cockerill and Clinical and Laboratory Standards Institute, 2015). Plates were incubated at 37°C for 16-24 hours within 15 minutes of adding the inoculum.

MIC values were visually determined by the unaided eye by comparing the amount of bacterial growth (turbidity) in wells containing AMPs with growth in the control wells that did not contain any amount of peptide. MBC values were determined by plating the

dilution/bacteria mixture representing the MIC and two of the more concentrated AMP dilutions onto non-selective MHA plates, followed by incubation for 24 hours at 37°C.

## 3.3 Results

### 3.3.1 Characteristics of Putative Antimicrobial Peptides

The HMM-based AMP prediction workflow yielded 11 putative AMP sequences. Six of the AMP candidates had significant similarity (e-value $\leq 2.8 \times 10^{-5}$) to "Frog antimicrobial peptide" or "Frog skin active peptide family signal and propeptide" Pfam domains. The other five candidate sequences had significant similarity to motifs from lysine and arginine-rich proteins with AMP-like secondary structures, and may represent false positive matches. These 11 putative sequences, combined with the 65 others identified from RNA-seq data, were subjected to characterization through homology and various structural and sequence-based analyses. From this list, nine AMPs were identified that represented known or novel AMPs. Sequence identification and active peptide characteristics for each peptide are noted in **Table 3.1**.

Clustal omega alignments of each putative peptide and their best known AMP match identified via BLASTP can be found in **Appendix D.** Six peptides (CCH-0008-T_R4012255 (A); CCH-0008-T_S4110533 (B); CCH-0013-CS4288341 (C); CCH-0008-T_R4012400 (D), CCH-0008-T_J4042717 (E), CCH-0008-T_S4147914 (F)) aligned with approximately 100% identity within the mature region of the peptide to three different AMP family categories: ranatuerin, catesbeianin, and palustrin (**Appendix D**).

**Table 1 Characteristics of putative AMP sequences. MW refers to molecular weight and pI refers to isoelectric point of the active peptide.**

| Sequence ID | Preprosequence | Putative Mature Sequence | Net Charge of Mature at pH 7 | MW Mature | pI Mature |
|---|---|---|---|---|---|
| CCH-0008-T_R4012255 | MFTLKKSLLLLFFLGTINLSLCEEERDAEEERRDNPDERDVEVEKR | FLPFIALAAKVFPSIICSVTKKC | +3 | 2497.14 | 9.39 |
| CCH-0013-C_S4288341 | MRKRMTMRRMMKKKKSEKERRERGKR | MMRVMRRKTKVIWEKKDFIGLYSID | +4 | 3144.85 | 10.16 |
| CCH-BS01-S14839083 | embargoed | embargoed | +2 | 3077.66 | 8.86 |
| CCH-0008-T_R4012400 | MFTLKKSLLLLFFLGTITLSLCEQERGADEDNGGEMTEEEVKR | GLFLDTLKGAKDVAGKLLEGLKCKITGCKP | +3 | 3117.80 | 9.19 |
| CCH-0008-T_J4042717 | MFFMSSPRRDADEVKEVKR | GFLDIIKNLGKTFAGHMLDKIKCTIGTCPPSP | +2 | 3417.10 | 8.82 |
| CCH-0008-T_S4147914 | MITVSSPRRDADGDEGEVEEVKR | GFLDIIKDTGKEFAVKILNNLKCKLAGGCPP | +2 | 3303.97 | 8.79 |
| CCH-0008-T_S4162036 | embargoed | embargoed | +5 | 2236.64 | 10.93 |
| CCH-0008-T_S4110533 | MSSFCEITNVALTISLSSPRRGADEEEGNGEKEIKR | SMLSVLKNLGKVGLGFVACKINKQC | +4 | 2651.28 | 9.70 |
| CCH-BS01-S16505513 | embargoed | embargoed | +1 | 3908.55 | 8.00 |

These peptides were then referred to as “known” candidates: Ranatuerin-1 (ACR46973.1), Ranatuerin-4 (ACO51651.1), Ranatuerin-2RC (ACR84073.1), Ranatuerin-3RC (PIO09118.1), Ranatuerin-2PRc (AFR43665.1), Palustrin-Ca (ACR84086.1), and Catesbeianin-1(ACQ65676.1). Of the nine putative peptides analyzed, only CCH-BS01-S16505513 did not align to any known AMPs in the nr database. CCH-0008-T_S4162036 (G) and CCH-BS01-S14839083 (C) alignments revealed variable amino acid sequence in the mature portion as compared to their known peptide match, indicating the possibility of novel functional proteins from the ranacyclin and ranatuerin families; in contrast to the known peptides alignments noted above, mature peptide CCH-0008-T_S4162036 aligned with 57% identity to Ranacyclin-Ca, and CCH-BS01-S14839083 aligned with 60% identity to Ranatuerin-2PRC (**Appendix D**). The designation of these peptides as known or novel was based on the standard in this field that frequently uses sequence homology within the signal and prosequences to identify AMPs from the same families (Liu et al., 2016) with the acknowledgement that even small sequence differences within the variable mature peptide region may lead to differences in antimicrobial activity that necessitate the designation of an AMP as novel (Bahar and Ren, 2013; Khamis et al., 2015).

Using MEGA 7.0 (Kumar et al., 2016), all peptide sequences were first aligned using ClustalW (**Appendix E**). This analysis was followed by the generation of a Maximum Likelihood tree using a Poisson model and nearest-neighbor-interchange heuristics with 500 bootstrap replicates with all nine putative transcriptome-derived peptides, BLASTP matched peptides, as well as outgroup peptides from brevinin, esculentin, temporin, and odorrainin families and was assembled to determine the categorization of the putative

peptides amongst known NCBI-derived AMP family representatives (**Figure 3.1**). The observed clustering of peptides based on their amino acid sequences reveals a separation of ranatuerin-like and outgroup peptides from catesbeianin-like peptides. CCH-BS01-S16505513 did not align with any known AMP and was therefore excluded from this analysis. CCH-0008-T_S4162036, on the other hand, aligned with Ranacyclin-Ca (**Figure 3.1**).

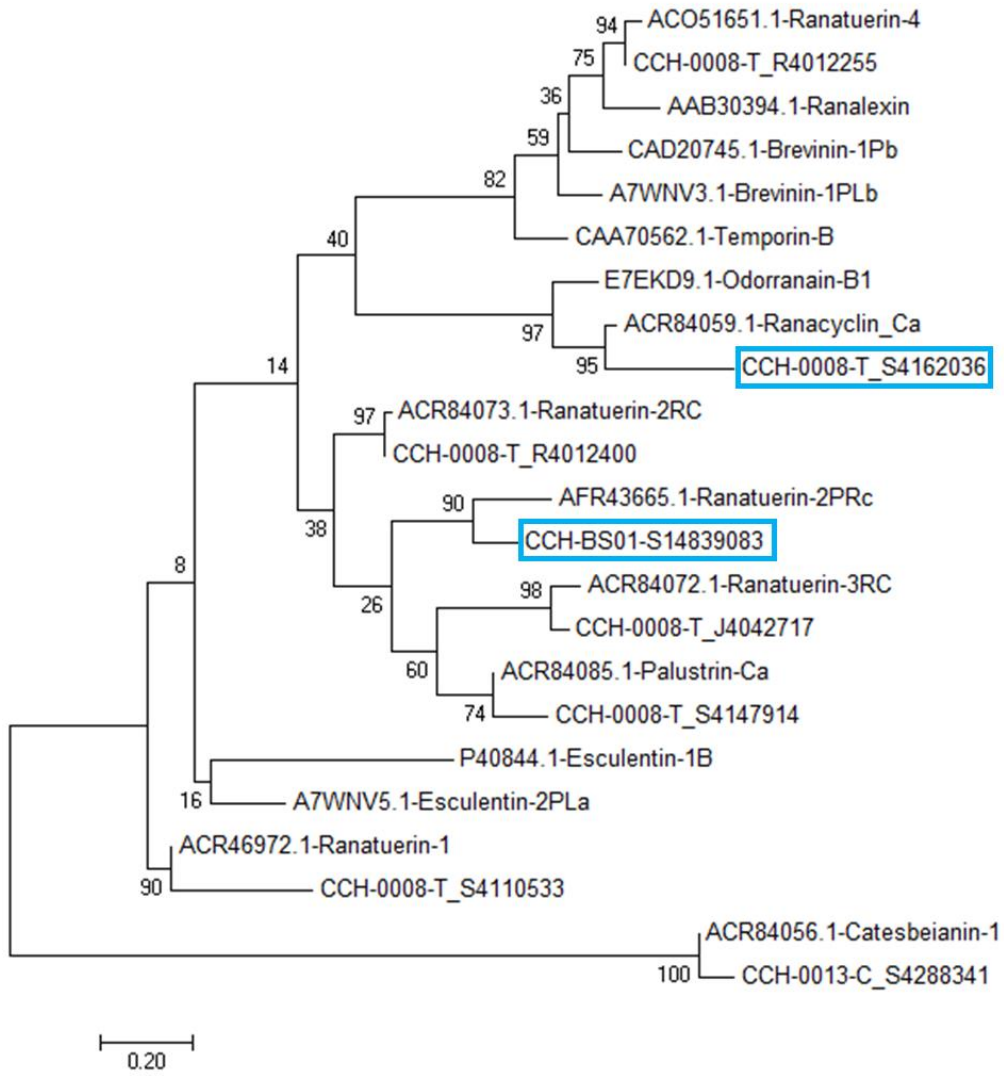


**Figure 3.1 Maximum likelihood tree of putative precursor AMP sequences from BART, known AMP sequences from NCBI that aligned best to the putatives, and additional outgroup characterized known AMP sequences from NCBI. Tested novel peptides are outlined in blue. Numbers at each node represent confidence values.**

SABLE protein prediction was used to predict the secondary structures of the putative peptides. In **Figure 3.2**, the structure predictions for known ranatuerin precursors are compared to the putative peptides that aligned closely to ranatuerin-like peptides, all of which contain a large common α-helix motif. Similarities in secondary structure are also observed in **Figure 3.3** between the other putative peptides and their best known AMP match. Although CCH-BS01-S16505513 did not align with any known AMPs, the secondary structure of this peptide also contains long stretches of α-helices; a common hallmark of AMPs (Bahar and Ren, 2013). .

### 3.3.1 Antimicrobial Peptide Expression in *R. catesbeiana* Tadpole Tissues

Transcript levels of these peptides was assessed in untreated premetamorphic back skin, tail fin, olfactory epithelium (OE), and liver using normalized RNA-seq data from previous studies (Hammond et al., 2017; Jackman et al., 2017; Partovi et al., 2017). Detection threshold of transcripts was applied for counts > 0. Generally, all contigs were approximately 2 orders of magnitude higher in the back skin compared to the other tissues. CCH-0008-T_R4012255 (encoding a Ranatuerin-4) and CCH-BS01-S14839083 (encoding a version of Ranatuerin-2PRc) were the most abundant in the back skin (**Figure 3.4A**). CCH-0013-C_S4288341 was the most abundant contig in the tail fin, OE, and liver (**Figure 3.4B-D**).

Of the two contigs encoding putative novel AMP peptides, CCH-0008-T_S4162036 was more abundant than CCH-BS01-S16505513 in all tissues except back skin (**Figure 3.4A**). Additionally, CCH-0008-T_S4162036 transcript expression was more abundant in all tissues than the Ranatuerin-1 transcript we identified (CCH-0008-T_S4110533).

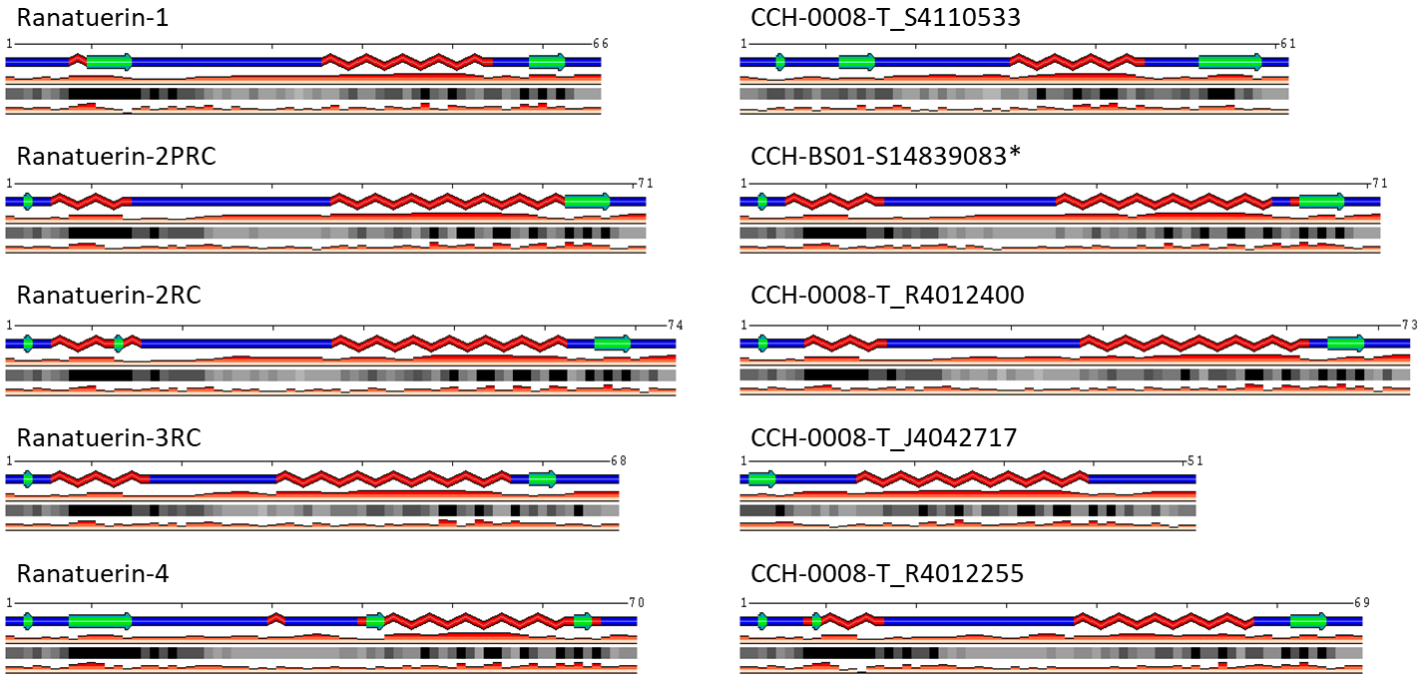


**Figure 3.2 SABLE protein prediction images of putative precursor ranatuerin-like AMP secondary structures and best BLASP AMP alignments. Red lines are alpha helices, green arrows are beta sheets, blue lines are extended coils. Relevant solvent accessibility (RSA) is denoted by black, white, and grey boxes below each secondary structure prediction, with black representing 0-9% RSA and white representing 90-100% RSA. Confidence level predictions are denoted by colored bars below secondary structure predictions. The length of the peptide is indicated above each image. Asterisks next to peptide IDs denote novel peptides.**

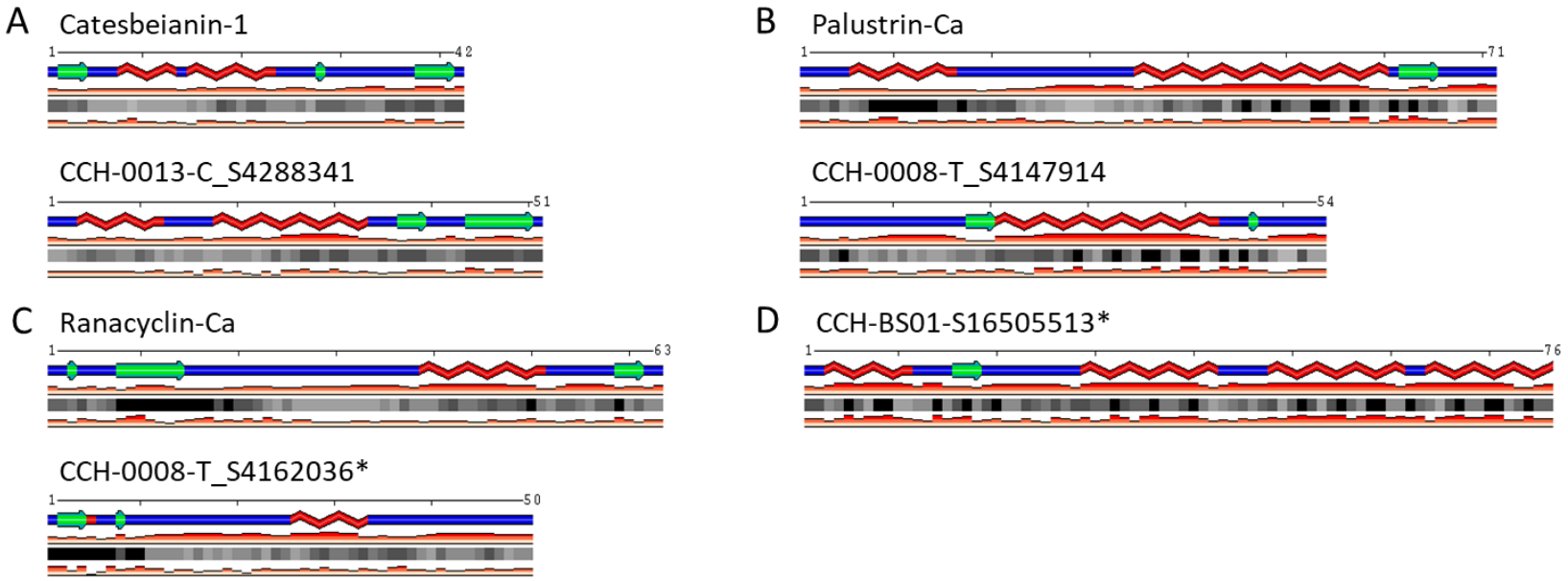


**Figure 3.3 SABLE protein prediction images of putative precursor catesbeianin (A), palustrin (B), and ranacyclin-like (C) AMP secondary structures best BLASP AMP alignments. CCH-BS01-S16505513 (D) does not align with any known AMPs in the NR database. Refer to Figure 3.2 legend for additional details.**

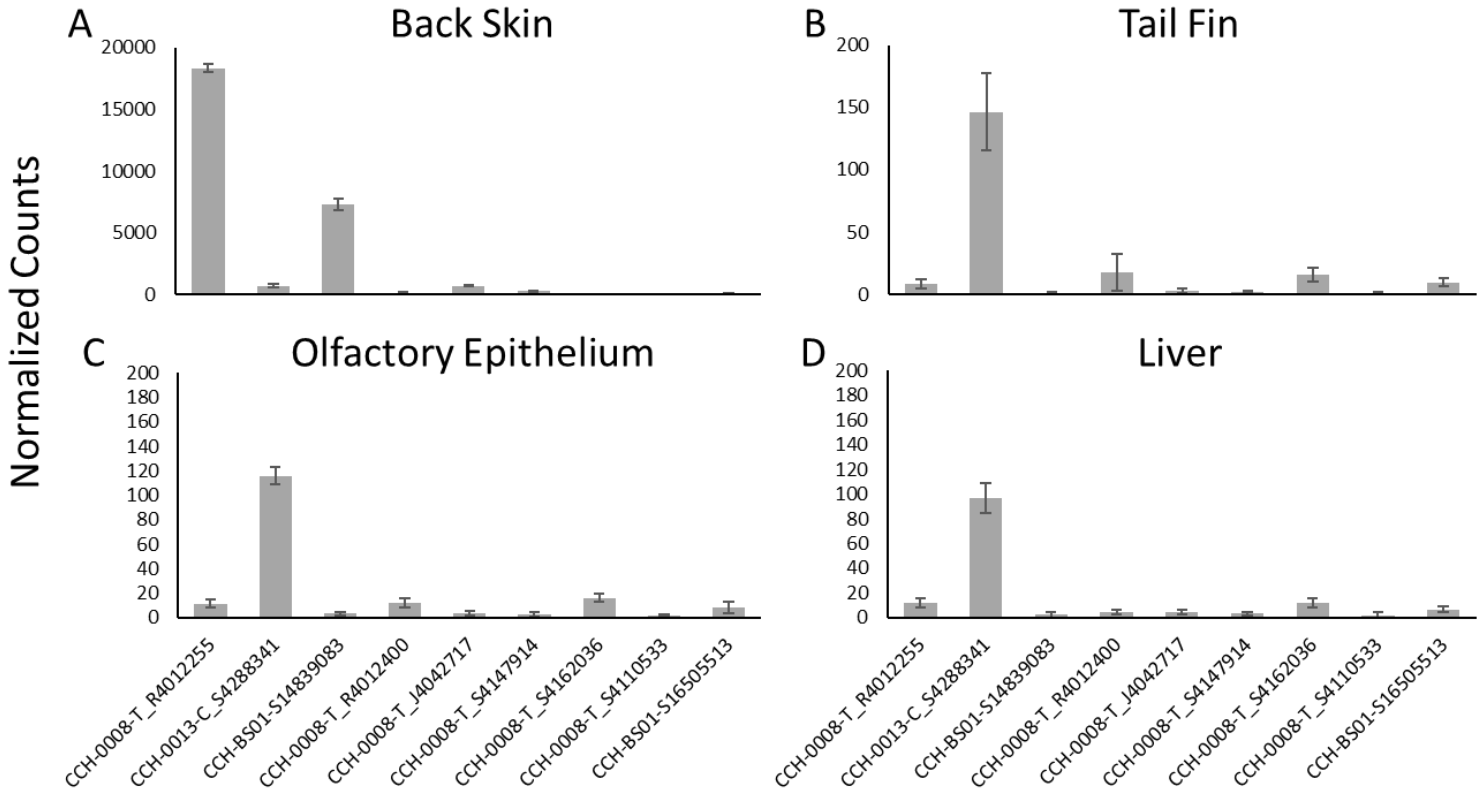


**Figure 3.4 Putative peptide expression in normalized read counts in tadpole back skin (A; n=3), tail fin (B; n=15), olfactory epithelium (C; n=15), and liver (D; n=15). The median of the raw read counts per peptide were plotted. Bars represent median read counts, and whiskers represent median absolute deviation (MAD). Note the differences in scales between the four graphs.**

### 3.1 MIC/MBC Determination

Of the five bacterial species tested, only *E. coli*, *S. aureus*, and *M. smegmatis* growth was affected by the 10x dilution series for the four tested peptides. Growth persisted in all wells of the plates containing *S. pyogenes* and *P. aeruginosa*. The two known peptides (identified as Ranatuerin-4 and Ranatuerin-1) exhibited inhibitory and bactericidal capabilities against *E. coli*, *S. aureus*, and *M. smegmatis* (**Table 3.2**). CCH-0008-T_R4012255 (Ranatuerin-4) exhibited the strongest antimicrobial activity against all three bacterial species, particularly *S. aureus* (MIC: 4 µg/mL; MBC: 8 µg/mL; **Table 3.2**). CCH-0008-T_S4110533 (Ranatuerin-1), by contrast, exhibited an MIC and MBC of 256 µg/mL against *E. coli*. Both putative peptides exhibited bacteriostatic activity against *M. smegmatis*, but only CCH-0008-T_S4162036 exhibited bactericidal activity. CCH-0008-T_S4162036 incubation with *M. smegmatis* resulted in an MIC and MBC of 16 µg/mL and 32 µg/mL, respectively (**Table 3.2**). CCH-BS01-S16505513 exhibited an MIC of 256 µg/mL against *M. smegmatis* but failed to exhibit bactericidal activity (**Table 3.2**). Interestingly, CCH-0008-T_S4162036 exhibited more potent antimicrobial activity than CCH-0008-T_R4012400 (Ranatuerin-1). No effect was observed by the negative control peptide on any bacteria tested, and no contamination was observed in column 12 (MHB sterility control with no added peptide or bacteria) in any of the five plates.

**Table 3.2 Broth microdilution assay results for tested known and putative AMPs. MIC and MBC values are in units of µg/µL.**

| | | MIC | MBC |
|---|---|---|---|
| *E. coli* | CCH-0008-T_R4012255 | 16 | 16 |
| | CCH-0008-T_S4110533 | 32 | 32 |
| | CCH-0008-T_S4162036 | N/A | N/A |
| | CCH-BS01-S16505513 | N/A | N/A |
| | [-] | N/A | N/A |
| *S. aureus* | CCH-0008-T_R4012255 | 4 | 8 |
| | CCH-0008-T_S4110533 | 256 | 256 |
| | CCH-0008-T_S4162036 | N/A | N/A |
| | CCH-BS01-S16505513 | N/A | N/A |
| | [-] | N/A | N/A |
| *M. smegmatis* | CCH-0008-T_R4012255 | 8 | 32 |
| | CCH-0008-T_S4110533 | 32 | 128 |
| | CCH-0008-T_S4162036 | 16 | 32 |
| | CCH-BS01-S16505513 | 256 | >256 |
| | [-] | N/A | N/A |

## 3.4 Discussion

By utilizing known homology and structural characteristics of AMPs, we have demonstrated the efficacy of computational identification and characterization of AMPs from an assembled bullfrog transcriptome via a bioinformatics approach by identifying two novel bullfrog AMPs. Sequence-based alignments, phylogenetic tree analyses, and secondary structure predictions presented herein demonstrate the utility of this approach to identify known and novel AMPs based on the shared sequence and structure characteristics of these peptides. Alignments of putative peptides with the reference peptides identified in BLASTP analyses provided us with the ability to categorize both known and novel peptides based on the sequence similarity in their signal and prosequence segments, and the strength of their mature peptide alignments. In the maximum likelihood tree analysis, the clustering of known reference AMPs and our list of putative peptides resulted in the ability to differentiate known candidates and novel candidates on the basis of their sequence similarities. The observed separate cluster of ranatuerins and ranatuerin-like peptides affirms that sequence similarities are maintained within AMP families, and the inclusion of outgroup AMP families within this cluster suggests that different families maintain some similarities. Secondary structure predictions presented herein indicate a similarity in structural characteristics that correlate with a similarity in amino acid sequence that is shared within families of AMPs.

We experimentally confirmed the antimicrobial activity of two identified known AMPs and two novel AMPs. Low MIC values for AMPs are most preferable as they translate to high antimicrobial activity, although cytotoxicity is another characteristic of these peptides that must be ascertained before they can be considered for use (Ebbensgaard et al., 2015). Antimicrobial activity of Ranatuerin-1 and Ranatuerin-4 has been assessed

minimally in previous research; although the MIC of Ranatuerin-1 against *S. aureus* is stronger in the present study than the values reported in previous literature, the MIC values reported for Ranatuerin-1 activity against *E. coli* are similar, as are the MIC values for Ranatuerin-4 against *S. aureus* (Goraya et al., 1998). However, comparisons of antimicrobial activity across studies is often difficult to compare due to the differences in assay conditions and peptide purities (Ebbensgaard et al., 2015). Activity against *M. smegmatis* was not assessed for these peptides previously. Novel peptides CCH-BS01-S16505513 exhibited bacteriostatic activity against *M. smegmatis*, while CCH-0008-T_S4162036 exhibited both bacteriostatic and bactericidal activity against *M. smegmatis* to a stronger degree than known peptide Ranatuerin-1. Previous functional analyses assessing AMP activity on *M. smegmatis* are minimal, with most studies focusing on the antimicrobial activity of synthetic peptides with weaker MIC values than what is reported in the present study for peptide CCH-0008-T_S4162036 (Gutsmann, 2016). Furthermore, this peptide exhibited MIC and MBC values competitive with those demonstrated in previous antimicrobial assay experiments (Ebbensgaard et al., 2015). Further investigation into the antimicrobial activities against *Mycobacteria* is warranted to determine the efficacy against more pathogenic strains, such as *M. tuberculosis*.

Successful functional testing of AMPs identified via the bioinformatics methods used in the present study affirms the value of the bioinformatics approach and bullfrog genome resources described herein. This presents the opportunity for further investigations into a previously untapped resource to discover more novel AMPs that may be useful for the discovery of therapeutics as antibiotic resistance continues to threaten global health.

Further research must be conducted to determine the possible modes of action employed by these tested peptides against the different bacterial strains involved in this study.

The high expression levels of these AMPs within the back skin of tadpoles and verified AMP expression in the other analyzed tissues confirms that bullfrog tissues, particularly the back skin, are plentiful sources of these peptides, and that our bullfrog genome resources are useful and relevant tools for further AMP research and experimentation. Additionally, this presents an opportunity to explore AMPs that target various pathogens in the context of conservation. Amphibians around the world are experiencing drastically decreased population numbers due to the emergence of pathogens that cause Ranavirus and chytrid fungal infection (Rosa et al., 2017). Previous research discovered a substilisin-like serine protease secreted by *Batrachochytrium dendrobatidis*, the causative agent of chytrid fungal infection, with the ability to cleave and disrupt amphibian AMPs (Thekkiniath et al., 2013). Because AMPs play a critical role in innate immunity (Bahar and Ren, 2013; Rollins-Smith, 2009), further examination of the circumstances of their expression, such as TH modulation, and factors that may disrupt their normal function can provide useful information for amphibian conservation studies.

We have demonstrated the strength of our computational approach for AMP prediction and characterization using our bullfrog genomic resources by identifying two novel AMPs with bacteriostatic and bactericidal capabilities. This approach may be used for future identification of additional novel peptides in the bullfrog and other organisms to further the field of antimicrobial therapeutics.

# 4 Conclusions and future directions

## 4.1 Conclusions

The first objective of this thesis was to examine differential TH responses in premetamorphic *R. catesbeiana* liver and tail fin tissue transcriptomes through RNA-seq and evaluate TH-modulation of immune system transcripts in the liver and tail fin. The effect of $E_2$ exposure was also evaluated to provide a contrast between estrogen and TH responses due to the similarity exhibited between TRs and ERs and the cross-talk potential of these hormones described in Chapter 1. Analysis of the transcriptomic profiles of these two outer ring deiodinase-poor tissues revealed distinct differences in response to $T_4$ and $T_3$, providing novel insight into differential tissue responsiveness following treatment with these two forms of TH, as well as validation of $T_4$ as a bioactive molecule in the absence of deiodinases, rather than the classical depiction of $T_4$ as a prohormone.

qPCR results of canonical TH-responsive genes revealed a preference for $T_3$ over $T_4$ in the tail fin. This finding differs from previous research that found that $T_4$ and $T_3$ elicited a superimposable response in these same genes in the tail fin (Maher et al., 2016). The water-bath immersion method used in the study described in Chapter 2 differs from the injection method implemented in Maher et al., (2016). The differences observed in these two studies may be the result of the differential kinetics of these methods, with immersion requiring more time to elicit the same response as injection. However, the preference for $T_3$ observed in qPCR analysis was exemplified in the various analyses performed on the corresponding RNA-seq data, which indicated that although the tissue responds to $T_4$, $T_3$ plays a more extensive role than $T_4$ in the overall modulation of the tail

fin transcriptome in developing tadpoles. The presence of $T_3$ specific transporter MCT10 within the tail fin transcriptome also provides additional support to the overall $T_3$ preference observed in the tail fin RNA-seq data after immersion.

Despite the outer ring deiodinase-poor status maintained by both tissues, qPCR results of canonical TH-responsive genes in the liver indicated that multiple modes TH binding are possible within the same tissue. *Thra* responded similarly to $T_4$ and $T_3$ treatment, which suggests that a direct mode of $T_4$ action is possible for certain genes. *Thrb* and *thibz* transcripts, however, exhibited a stronger response at the medium concentration of $T_4$ than the matched concentration of $T_3$. The presence of the transmembrane integrin αvβ3 within RNA-seq liver data indicates that non-genomic $T_4$ signaling may be at play in the liver for the expression of specific genes, which may explain the differences observed across the three TH-responsive canonical genes. In contrast to the results observed in the tail fin, RNA-seq examination of $T_4$ and $T_3$ response patterns in the liver suggests that $T_4$ may play a more extensive role than $T_3$ in modulating transcriptomic events. TH-affected contigs identified from the RNA-seq experiments suggest that while $T_4$ and $T_3$ both elicit a response in the liver, the preference for $T_4$ likely occurs via both genomic and non-genomic pathways. While LAT1/LAT2 transcripts encoding transporters with a slight preference for $T_3$ over $T_4$ are expressed in the tadpole liver, the integrin-mediated, $T_4$-preferring mechanism likely plays a more substantial role. Further investigation of $T_3$- and $T_4$-modulated aspects of the liver transcriptome, both genomic and non-genomic, is warranted to understand the differential aspects of both forms of TH.

We also demonstrated that classical TH-responsive genes *thra, thrb,* and *thibz* did not respond to $E_2$ treatment at physiological doses in either tissue. This finding is important

in evaluating the presence of EDCs based on perturbation of these genes in that a demonstrated effect in these transcripts would represent TH disruption rather than xenoestrogen disruption. Furthermore, transcriptomic analysis of $E_2$ treatment in the liver and tail fin indicate that although $E_2$ plays somewhat of a role in modulation of the liver transcriptome, it appears to have a negligible effect on the tail fin transcriptome. This indicates that while the liver may be a useful tissue to use to investigate the effect of $E_2$ exposure and xenoestrogen-based EDCs, the tail fin is not. On the other hand, the differential $T_4$ and $T_3$ transcriptomic response observed in the tail fin compared to the liver indicates that the tail fin may be a better tissue to utilize in studies focusing on differential susceptibilities to EDCs that effect $T_4$ or $T_3$ specifically.

Finally, qPCR analysis of two novel validated immune transcripts, as well as examination of RNA-seq data through gene ontology, revealed that elements of the immune system are modulated by both forms of TH in the liver and tail fin.

The second objective of this thesis was to identify, characterize, and functionally analyze putative AMPs using *R. catesbeiana* genomic resources. By utilizing known homology and structural characteristics of AMPs and applying this information as methodology, we identified and experimentally confirmed the antimicrobial activity of two identified known AMPs and two novel AMPs that demonstrated bactericidal and bacteriostatic properties against various bacterial species. Successful functional testing of AMPs identified via the bioinformatics methods outlined in Chapter 3 presents the opportunity for further investigations into a previously untapped resource to discover more novel AMPs that may be useful for the discovery of therapeutics. Furthermore, the high expression levels of these AMPs within the back skin of tadpoles and verified AMP

expression in the other analyzed tissues confirms the value of bullfrog genome resources for further AMP research and experimentation, including research endeavors involving the investigation of immunity in amphibians.

The findings presented herein shed light on the differential and extensive modulatory effects of both forms of TH on a transcriptomic level, as well as the utility of the bullfrog transcriptome in identifying novel bullfrog-derived AMPs and elucidating aspects of AMP expression. The assembled bullfrog transcriptome described in these chapters enables further investigation of the impact of these critical hormones on specific pathways and systems in a way that has not yet been explored, such as TH-modulation of the immune system and vital immune components like AMPs in developing *R. catesbeiana* tadpoles.

## 4.2 Future directions

The results and methods presented in this thesis represent the first transcriptomic analyses comparing $T_4$ and $T_3$ responsiveness in premetamorphic *R. catesbeiana* liver and tail fin tissues, with an additional comparison of $E_2$ treatment. This work also illuminates the potential to utilize novel bullfrog genomics resources for AMP identification and characterization. The methodology and findings described herein present the opportunity for further experiments and investigations regarding TH-modulation of specific pathways and individual components that have not yet been examined.

The immune system is extensively remodeled by THs in bullfrog tadpole liver and the tail fin tissues. The creation of a TH-responsive immune system qPCR panel using RNA-seq data would be useful in evaluating potential disruption of these transcripts under a variety of conditions, such as EDC exposure due to anthropogenic pollutants. The

generation and use of $T_4$ and $T_3$-specific immune-associated qPCR tools would elucidate the effect of certain polluting chemicals on a developing immune system as certain EDCs may affect one form of TH over the other. This would provide a greater understanding of the interplay between THs and immunity. Furthermore, this experimentation would provide insights into the factors that contribute to the current devastation of amphibian populations around the world since EDC exposure has been shown to modulate the immune systems of vertebrates (Qiu et al., 2016; Regnault et al., 2016)

Examination of the infectivity of ranaviruses in previous research suggests that tadpoles are more likely to succumb to Ranavirus infection than adult frogs (Gantress et al., 2003; Robert et al., 2011). Evaluating the response of TH-affected immune transcripts in tadpoles through qPCR-based methods following exposure to frog virus 3 (FV3), a commonly researched and prevalent ranavirus strain (Gantress et al., 2003), could identify specific immune genes that are negatively affected by this virus during metamorphosis.

Use of the improved bullfrog transcriptome to perform the computational approach for the identification of AMPs could enable the discovery and characterization of additional, novel AMPs with therapeutic potential that could also be evaluated for TH-responsiveness in the tissues available within the transcriptome. Furthermore, AMP cDNA sequences could be used to generate novel qPCR tools for analysis of AMP expression in several different conditions. Evaluation of AMP expression throughout metamorphosis in the back skin of *R. catesbeiana* tadpoles would not only present a clearer picture of the role of AMPs throughout metamorphosis, but it may also shed light on the role of TH in the synthesis and regulation of these peptides. Using these qPCR

tools, AMP expression could also be evaluated in the context of FV3 challenge to further our understanding of the role of AMPs in immune responses and the devastation caused by these diseases and pathogens. Finally, the newly curated bullfrog genome (Hammond et al., 2017) may also provide novel information regarding details of the genomic structures of AMPs within the bullfrog genome that may shed light on unknown regulatory aspects of these important antimicrobial agents.

# Bibliography

Aittomäki, S., Valanne, S., Lehtinen, T., Matikainen, S., Nyman, T.A., Rämet, M., Pesu, M., 2017. Proprotein convertase *Furin1* expression in the *Drosophila* fat body is essential for a normal antimicrobial peptide response and bacterial host defense. FASEB J. fj.201700296R. https://doi.org/10.1096/fj.201700296R

Altschul, S.F., Gish, W., Miller, W., Myers, E.W., Lipman, D.J., 1990. Basic local alignment search tool. J. Mol. Biol. 215, 403–410. https://doi.org/10.1016/S0022-2836(05)80360-2

Andersson, D.I., Hughes, D., Kubicek-Sutherland, J.Z., 2016. Mechanisms and consequences of bacterial resistance to antimicrobial peptides. Drug Resist. Updat. 26, 43–57. https://doi.org/10.1016/j.drup.2016.04.002

Atkinson, B.G., Warkman, A.S., Chen, Y., 1998. Thyroid hormone induces a reprogramming of gene expression in the liver of premetamorphic Rana catesbeiana tadpoles. Wound Repair Regen. 6, S-323-S-336. https://doi.org/10.1046/j.1524-475X.1998.60408.x

Austin Hammond, S., Jackman, K.W., Partovi, S.H., Veldhoen, N., Helbing, C.C., 2016. Identification of organ-autonomous constituents of the molecular memory conferred by thyroid hormone exposure in cold temperature-arrested metamorphosing *Rana (Lithobates)* catesbeiana tadpoles. Comp. Biochem. Physiol. Part D Genomics Proteomics 17, 58–65. https://doi.org/10.1016/j.cbd.2016.01.002

Bahar, A., Ren, D., 2013. Antimicrobial Peptides. Pharmaceuticals 6, 1543–1575. https://doi.org/10.3390/ph6121543

Batista, C.V.., Scaloni, A., Rigden, D.J., Silva, L.R., Rodrigues Romero, A., Dukor, R., Sebben, A., Talamo, F., Bloch, C., 2001. A novel heterodimeric antimicrobial peptide from the tree-frog *Phyllomedusa distincta*. FEBS Lett. 494, 85–89. https://doi.org/10.1016/S0014-5793(01)02324-9

Bergh, J.J., Lin, H.-Y., Lansing, L., Mohamed, S.N., Davis, F.B., Mousa, S., Davis, P.J., 2005. Integrin $\alpha_V \beta_3$ Contains a Cell Surface Receptor Site for Thyroid Hormone that Is Linked to Activation of Mitogen-Activated Protein Kinase and Induction of Angiogenesis. Endocrinology 146, 2864–2871. https://doi.org/10.1210/en.2005-0102

Berry, D.L., Rose, C.S., Remo, B.F., Brown, D.D., 1998. The Expression Pattern of Thyroid Hormone Response Genes in Remodeling Tadpole Tissues Defines Distinct Growth and Resorption Gene Expression Programs. Dev. Biol. 203, 24–35. https://doi.org/10.1006/dbio.1998.8975

Birol, I., Behsaz, B., Hammond, S.A., Kucuk, E., Veldhoen, N., Helbing, C.C., 2015. De novo transcriptome assemblies of *Rana (Lithobates) catesbeiana* and *Xenopus laevis* tadpole livers for comparative genomics without reference genomes. PLOS ONE 10, e0130720. https://doi.org/10.1371/journal.pone.0130720

Boehm, T., 2012. Evolution of Vertebrate Immunity. Curr. Biol. 22, R722–R732. https://doi.org/10.1016/j.cub.2012.07.003

Boland, M.P., Separovic, F., 2006. Membrane interactions of antimicrobial peptides from Australian tree frogs. Biochim. Biophys. Acta BBA - Biomembr. 1758, 1178–1183. https://doi.org/10.1016/j.bbamem.2006.02.010

Brandenburg, K., Heinbockel, L., Correa, W., Lohner, K., 2016. Peptides with dual mode of action: Killing bacteria and preventing endotoxin-induced sepsis. Biochim. Biophys. Acta BBA - Biomembr. 1858, 971–979. https://doi.org/10.1016/j.bbamem.2016.01.011

Brent, G.A., 2012. Mechanisms of thyroid hormone action. J. Clin. Invest. 122, 3035–3043. https://doi.org/10.1172/JCI60047

Brown, D.D., Cai, L., 2007a. Amphibian metamorphosis. Dev. Biol. 306, 20–33. https://doi.org/10.1016/j.ydbio.2007.03.021

Brown, D.D., Cai, L., 2007b. Amphibian metamorphosis. Dev. Biol. 306, 20–33. https://doi.org/10.1016/j.ydbio.2007.03.021

Cameron, C.E., Brouwer, N.L., Tisch, L.M., Kuroiwa, J.M.Y., 2005. Defining the Interaction of the Treponema pallidum Adhesin Tp0751 with Laminin. Infect. Immun. 73, 7485–7494. https://doi.org/10.1128/IAI.73.11.7485-7494.2005

Cao, X., Kambe, F., Moeller, L.C., Refetoff, S., Seo, H., 2005. Thyroid Hormone Induces Rapid Activation of Akt/Protein Kinase B-Mammalian Target of Rapamycin-p70 $^{S6K}$ Cascade through Phosphatidylinositol 3-Kinase in Human Fibroblasts. Mol. Endocrinol. 19, 102–112. https://doi.org/10.1210/me.2004-0093

Cardoso, M.H., 2014. Insights into the Antimicrobial Activities of Unusual Antimicrobial Peptide Families from Amphibian Skin. J. Clin. Toxicol. 04. https://doi.org/10.4172/2161-0495.1000205

Chen, T., Zhou, M., Chen, W., Lorimer, J., Rao, P., Walker, B., Shaw, C., 2006. Cloning from tissue surrogates: Antimicrobial peptide (esculentin) cDNAs from the

defensive skin secretions of Chinese ranid frogs. Genomics 87, 638–644. https://doi.org/10.1016/j.ygeno.2005.12.002

Cheng, S.-Y., Leonard, J.L., Davis, P.J., 2010. Molecular Aspects of Thyroid Hormone Actions. Endocr. Rev. 31, 139–170. https://doi.org/10.1210/er.2009-0007

Choi, J., Suzuki, K.T., Sakuma, T., Shewade, L., Yamamoto, T., Buchholz, D.R., 2015. Unliganded Thyroid Hormone Receptor α Regulates Developmental Timing via Gene Repression in *Xenopus tropicalis*. Endocrinology 156, 735–744. https://doi.org/10.1210/en.2014-1554

Choksi, N.Y., Jahnke, G.D., St. Hilaire, C., Shelby, M., 2003. Role of thyroid hormones in human and laboratory animal reproductive health. Birth Defects Res. B. Dev. Reprod. Toxicol. 68, 479–491. https://doi.org/10.1002/bdrb.10045

Clark, D.P., Durell, S., Maloy, W.L., Zasloff, M., 1994. A novel antimicrobial peptide from bullfrog (*Rana catesbeiana*) skin, structurally related to the bacterial antibiotic, polymixin. J. Biol. Chem. 269, 10849–10855.

Cockerill, F., Clinical and Laboratory Standards Institute, 2015. Methods for dilution antimicrobial susceptibility tests for bacteria that grow aerobically: approved standard. Clinical and Laboratory Standards Institute, Wayne, Pa.

Colombo, B.M., Scalvenzi, T., Benlamara, S., Pollet, N., 2015. Microbiota and Mucosal Immunity in Amphibians. Front. Immunol. 6. https://doi.org/10.3389/fimmu.2015.00111

Conlon, J.M., 2012. The Potential of Frog Skin Antimicrobial Peptides for Development into Therapeutically Valuable Anti-Infective Agents, in: Rajasekaran, K., Cary, J.W., Jaynes, J.M., Montesinos, E. (Eds.), Small Wonders: Peptides for Disease

Control. American Chemical Society, Washington, DC, pp. 47–60. https://doi.org/10.1021/bk-2012-1095.ch003

Conlon, J.M., 2011. The contribution of skin antimicrobial peptides to the system of innate immunity in anurans. Cell Tissue Res. 343, 201–212. https://doi.org/10.1007/s00441-010-1014-4

Conlon, J.M., Mechkarska, M., 2014. Host-Defense Peptides with Therapeutic Potential from Skin Secretions of Frogs from the Family Pipidae. Pharmaceuticals 7, 58–77. https://doi.org/10.3390/ph7010058

Das, B., Heimeier, R.A., Buchholz, D.R., Shi, Y.-B., 2009. Identification of Direct Thyroid Hormone Response Genes Reveals the Earliest Gene Regulation Programs during Frog Metamorphosis. J. Biol. Chem. 284, 34167–34178. https://doi.org/10.1074/jbc.M109.066084

Database resources of the National Center for Biotechnology Information, 2016. . Nucleic Acids Res. 44, D7–D19. https://doi.org/10.1093/nar/gkv1290

Davis, F.B., Tang, H.-Y., Shih, A., Keating, T., Lansing, L., Hercbergs, A., Fenstermaker, R.A., Mousa, A., Mousa, S.A., Davis, P.J., Lin, H.-Y., 2006. Acting via a Cell Surface Receptor, Thyroid Hormone Is a Growth Factor for Glioma Cells. Cancer Res. 66, 7270–7275. https://doi.org/10.1158/0008-5472.CAN-05-4365

Davis, P.J., Davis, F.B., Lin, H.-Y., Mousa, S.A., Zhou, M., Luidens, M.K., 2009. Translational implications of nongenomic actions of thyroid hormone initiated at its integrin receptor. AJP Endocrinol. Metab. 297, E1238–E1246. https://doi.org/10.1152/ajpendo.00480.2009

De Jesús Andino, F., Chen, G., Li, Z., Grayfer, L., Robert, J., 2012. Susceptibility of *Xenopus laevis* tadpoles to infection by the ranavirus Frog-Virus 3 correlates with a reduced and delayed innate immune response in comparison with adult frogs. Virology 432, 435–443. https://doi.org/10.1016/j.virol.2012.07.001

Denver, R.J., 2013. Neuroendocrinology of amphibian metamorphosis, in: Current Topics in Developmental Biology. Elsevier, pp. 195–227. https://doi.org/10.1016/B978-0-12-385979-2.00007-1

Dürr, U.H.N., Sudheendra, U.S., Ramamoorthy, A., 2006. LL-37, the only human member of the cathelicidin family of antimicrobial peptides. Biochim. Biophys. Acta BBA - Biomembr. 1758, 1408–1425. https://doi.org/10.1016/j.bbamem.2006.03.030

Dutton, C.J. (Ed.), 2002. Peptide antibiotics: discovery, modes of action, and applications. Marcel Dekker, New York.

Ebbensgaard, A., Mordhorst, H., Overgaard, M.T., Nielsen, C.G., Aarestrup, F.M., Hansen, E.B., 2015. Comparative evaluation of the antimicrobial activity of different antimicrobial peptides against a range of pathogenic bacteria. PLOS ONE 10, e0144611. https://doi.org/10.1371/journal.pone.0144611

Ellison, A.R., DiRenzo, G.V., McDonald, C.A., Lips, K.R., Zamudio, K.R., 2017. First *in vivo Batrachochytrium dendrobatidis* transcriptomes reveal mechanisms of host exploitation, host-specific gene expression, and expressed genotype shifts. Genes Genomes Genetics 7, 269–278. https://doi.org/10.1534/g3.116.035873

Fagerberg, L., Hallström, B.M., Oksvold, P., Kampf, C., Djureinovic, D., Odeberg, J., Habuka, M., Tahmasebpoor, S., Danielsson, A., Edlund, K., Asplund, A.,

Sjöstedt, E., Lundberg, E., Szigyarto, C.A.-K., Skogs, M., Takanen, J.O., Berling, H., Tegel, H., Mulder, J., Nilsson, P., Schwenk, J.M., Lindskog, C., Danielsson, F., Mardinoglu, A., Sivertsson, Å., von Feilitzen, K., Forsberg, M., Zwahlen, M., Olsson, I., Navani, S., Huss, M., Nielsen, J., Ponten, F., Uhlén, M., 2014. Analysis of the human tissue-specific expression by genome-wide integration of transcriptomics and antibody-based proteomics. Mol. Cell. Proteomics 13, 397–406. https://doi.org/10.1074/mcp.M113.035600

Finn, R.D., Coggill, P., Eberhardt, R.Y., Eddy, S.R., Mistry, J., Mitchell, A.L., Potter, S.C., Punta, M., Qureshi, M., Sangrador-Vegas, A., Salazar, G.A., Tate, J., Bateman, A., 2016. The Pfam protein families database: towards a more sustainable future. Nucleic Acids Res. 44, D279–D285. https://doi.org/10.1093/nar/gkv1344

Freindorf, M., Furlani, T.R., Kong, J., Cody, V., Davis, F.B., Davis, P.J., 2012. Combined QM/MM Study of thyroid and steroid hormone analogue interactions with integrin. J. Biomed. Biotechnol. 2012, 1–12. https://doi.org/10.1155/2012/959057

Frieden, E., Westmark, G.W., 1961. On the anomalous activity mf thyroxin analogs in tadpoles. Science 133, 1487–1489.

Friesema, E.C.H., Jansen, J., Visser, T.., 2005. Thyroid hormone transporters. Biochem. Soc. Trans. 33, 228–232. https://doi.org/10.1042/BST0330228

Fu, L., Das, B., Matsuura, K., Fujimoto, K., Heimeier, R.A., Shi, Y.-B., 2017. Genome-wide identification of thyroid hormone receptor targets in the remodeling intestine

during Xenopus tropicalis metamorphosis. Sci. Rep. 7. https://doi.org/10.1038/s41598-017-06679-x

Fujimoto, N., 2004. Activation of estrogen response element dependent transcription by thyroid hormone with increase in estrogen receptor levels in a rat pituitary cell line, GH3. J. Endocrinol. 181, 77–83. https://doi.org/10.1677/joe.0.1810077

Galton, V.A., Cohen, J.S., 1980. Action of thyroid hormones in premetamorphic tadpoles: an important role for thyroxine?. Endocrinology 107, 1820–1826. https://doi.org/10.1210/endo-107-6-1820

Galton, V.A., de Waard, E., Parlow, A.F., St Germain, D.L., Hernandez, A., 2014. Life without the iodothyronine deiodinases. Endocrinology 155, 4081–4087. https://doi.org/10.1210/en.2014-1184

Galton, V.A., Schneider, M.J., Clark, A.S., St. Germain, D.L., 2009. Life without thyroxine to 3,5,3′-triiodothyronine conversion: Studies in mice devoid of the 5′-deiodinases. Endocrinology 150, 2957–2963. https://doi.org/10.1210/en.2008-1572

Gantress, J., Maniero, G.D., Cohen, N., Robert, J., 2003. Development and characterization of a model system to study amphibian immune responses to iridoviruses. Virology 311, 254–262. https://doi.org/10.1016/S0042-6822(03)00151-X

Ge, L., Chen, X., Ma, C., Zhou, M., Xi, X., Wang, L., Ding, A., Duan, J., Chen, T., Shaw, C., 2014. Balteatide: A novel antimicrobial decapeptide from the skin secretion of the purple-sided leaf frog, *Phyllomedusa baltea*. Sci. World J. 2014, 1–8. https://doi.org/10.1155/2014/176214

Gereben, B., Zavacki, A.M., Ribich, S., Kim, B.W., Huang, S.A., Simonides, W.S., Zeöld, A., Bianco, A.C., 2008. Cellular and Molecular basis of deiodinase-regulated thyroid hormone signaling. Endocr. Rev. 29, 898–938. https://doi.org/10.1210/er.2008-0019

Gilbert, L.I., Tata, J.R., Atkinson, B.G. (Eds.), 1996. Metamorphosis: Postembryonic reprogramming of gene expression in amphibian and insect cells. Academic Press, San Diego.

Gilbert, S.F., 2006. Developmental biology, 8th ed. ed. Sinauer Associates, Inc. Publishers, Sunderland, Mass.

Gilbert, S.F., 2000. Developmental biology, 6th ed. ed. Sinauer Associates, Sunderland, Mass.

Glinoer, D., 1997. The regulation of thyroid function in pregnancy: pathways of endocrine adaptation from physiology to pathology. Endocr. Rev. 18, 404–433. https://doi.org/10.1210/edrv.18.3.0300

Goraya, J., Knoop, F.C., Conlon, J.M., 1998. Ranatuerins: Antimicrobial peptides isolated from the skin of the American bullfrog, *Rana catesbeiana*. Biochem. Biophys. Res. Commun. 250, 589–592. https://doi.org/10.1006/bbrc.1998.9362

Gosner, K.L., 1960. A simplified table for staging anuran embryos and larvae with notes on identification. Herpetologica 16, 183–190.

Grayfer, L., Andino, F.D.J., Chen, G., Chinchar, G.V., Robert, J., 2012. Immune evasion strategies of ranaviruses and innate immune responses to these emerging pathogens. Viruses 4, 1075–1092. https://doi.org/10.3390/v4071075

Grimaldi, A., Buisine, N., Miller, T., Shi, Y.-B., Sachs, L.M., 2013. Mechanisms of thyroid hormone receptor action during development: Lessons from amphibian studies. Biochim. Biophys. Acta BBA - Gen. Subj. 1830, 3882–3892. https://doi.org/10.1016/j.bbagen.2012.04.020

Guilhelmelli, F., Vilela, N., Albuquerque, P., Derengowski, L. da S., Silva-Pereira, I., Kyaw, C.M., 2013. Antibiotic development challenges: the various mechanisms of action of antimicrobial peptides and of bacterial resistance. Front. Microbiol. 4. https://doi.org/10.3389/fmicb.2013.00353

Gutsmann, T., 2016. Interaction between antimicrobial peptides and mycobacteria. Biochim. Biophys. Acta BBA - Biomembr. 1858, 1034–1043. https://doi.org/10.1016/j.bbamem.2016.01.031

Hammes, S.R., Davis, P.J., 2015. Overlapping nongenomic and genomic actions of thyroid hormone and steroids. Best Pract. Res. Clin. Endocrinol. Metab. 29, 581–593. https://doi.org/10.1016/j.beem.2015.04.001

Hammond, S.A., Veldhoen, N., Helbing, C.C., 2015. Influence of temperature on thyroid hormone signaling and endocrine disruptor action in *Rana (Lithobates)* catesbeiana tadpoles. Gen. Comp. Endocrinol. 219, 6–15. https://doi.org/10.1016/j.ygcen.2014.12.001

Hammond, S.A., Warren, R.L., Vanderwalk, B.P., Kucuk, E., Khan, H., Gibb, E.A., Pandoh, P., Kirk, H., Zhao, Y., Jones, M., Mungall, A.J., Coope, R., Pleasance, S., Moore, R.A., Holt, R.A., Round, J.M., Ohora, S., Walle, B.V., Veldhoen, N., Helbing, C.C., Birol, I., 2017. The North American bullfrog draft genome

provides insight into hormonal regulation of long noncodomg RNA. Nature Commun. 8, 1433. https://doi.org/doi:10.1101/100149

Hancock, R.E.W., 1999. Modified MIC method for cationic antimicrobial peptides [WWW Document]. URL http://cmdr.ubc.ca/bobh/method/modified-mic-method-for-cationic-antimicrobial-peptides/ (accessed 9.22.17).

Haney, E.F., Petersen, A.P., Lau, C.K., Jing, W., Storey, D.G., Vogel, H.J., 2013. Mechanism of action of puroindoline derived tryptophan-rich antimicrobial peptides. Biochim. Biophys. Acta BBA - Biomembr. 1828, 1802–1813. https://doi.org/10.1016/j.bbamem.2013.03.023

Heerema, J.L., Jackman, K.W., Miliano, R.C., Li, L., Zaborniak, T.S.M., Veldhoen, N., Van Aggelen, G., Parker, W.J., Pyle, G.G., Helbing, C.C., 2017. Behavioral and molecular analyses of olfaction-mediated avoidance responses of *Rana (Lithobates)* catesbeiana tadpoles: Sensitivity to thyroid hormones, estrogen, and treated municipal wastewater effluent. Horm. Behav. pii: S0018-506X(17) 30331-8. doi: 10.1016/j.yhbeh.2017.09.016

Helbing, C., Gergely, G., Atkinson, B.G., 1992. Sequential up-regulation of thyroid hormone β receptor, ornithine transcarbamylase, and carbamyl phosphate synthetase mRNAs in the liver of *Rana catesbeiana* tadpoles during spontaneous and thyroid hormone-induced metamorphosis. Dev. Genet. 13, 289–301. https://doi.org/10.1002/dvg.1020130406

Helbing, C.C., 2012. The metamorphosis of amphibian toxicogenomics. Front. Genet. 3. https://doi.org/10.3389/fgene.2012.00037

Hiemstra, P.S., Zaat, S.A.J. (Eds.), 2013. Antimicrobial peptides and innate immunity, Progress in inflammation research. Springer, Basel ; New York.

Hogan, N.S., Duarte, P., Wade, M.G., Lean, D.R.S., Trudeau, V.L., 2008. Estrogenic exposure affects metamorphosis and alters sex ratios in the northern leopard frog *(Rana pipiens)* : Identifying critically vulnerable periods of development. Gen. Comp. Endocrinol. 156, 515–523. https://doi.org/10.1016/j.ygcen.2008.03.011

Holden, W.M., Reinert, L.K., Hanlon, S.M., Parris, M.J., Rollins-Smith, L.A., 2015. Development of antimicrobial peptide defenses of southern leopard frogs, *Rana sphenocephala*, against the pathogenic chytrid fungus, *Batrachochytrium dendrobatidis*. Dev. Comp. Immunol. 48, 65–75. https://doi.org/10.1016/j.dci.2014.09.003

Huang, L., Li, J., Anboukaria, H., Luo, Z., Zhao, M., Wu, H., 2016. Comparative transcriptome analyses of seven anurans reveal functions and adaptations of amphibian skin. Sci. Rep. 6. https://doi.org/10.1038/srep24069

Ishizuya-Oka, A., 2011. Amphibian organ remodeling during metamorphosis: Insight into thyroid hormone-induced apoptosis: Apoptosis during amphibian metamorphosis. Dev. Growth Differ. 53, 202–212. https://doi.org/10.1111/j.1440-169X.2010.01222.x

Ishizuya-Oka, A., Hasebe, T., Shi, Y.-B., 2010. Apoptosis in amphibian organs during metamorphosis. Apoptosis 15, 350–364. https://doi.org/10.1007/s10495-009-0422-y

Jackman, K.W., Veldhoen, N., Miliano, R.C., Robert, B.J., Li, L., Khojasteh, A., Zheng, X., Zaborniak, T.S.M., Van Aggelen, G., Lesperance, M., Parker, W.J., Hall,

E.R., Pyle, G.G., Helbing, C.C., 2017. Transcriptomic analysis of the *Rana (Lithobates) catesbeiana* tadpole olfactory epithelium in response to thyroid hormones, estrogen, and treated municipal wastewater effluent exposure. In preparation.

Jantaruk, P., Roytrakul, S., Sitthisak, S., Kunthalert, D., 2017. Potential role of an antimicrobial peptide, KLK in inhibiting lipopolysaccharide-induced macrophage inflammation. PLOS ONE 12, e0183852. https://doi.org/10.1371/journal.pone.0183852

Jones, P., Binns, D., Chang, H.-Y., Fraser, M., Li, W., McAnulla, C., McWilliam, H., Maslen, J., Mitchell, A., Nuka, G., Pesseat, S., Quinn, A.F., Sangrador-Vegas, A., Scheremetjew, M., Yong, S.-Y., Lopez, R., Hunter, S., 2014. InterProScan 5: genome-scale protein function classification. Bioinformatics 30, 1236–1240. https://doi.org/10.1093/bioinformatics/btu031

Joo, H.-S., Fu, C.-I., Otto, M., 2016. Bacterial strategies of resistance to antimicrobial peptides. Philos. Trans. R. Soc. B Biol. Sci. 371, 20150292. https://doi.org/10.1098/rstb.2015.0292

Katzenback, B.A., Holden, H.A., Falardeau, J., Childers, C., Hadj-Moussa, H., Avis, T.J., Storey, K.B., 2014. Regulation of the Rana sylvatica brevinin-1SY antimicrobial peptide during development and in dorsal and ventral skin in response to freezing, anoxia and dehydration. J. Exp. Biol. 217, 1392–1401. https://doi.org/10.1242/jeb.092288

Kent, W.J., 2002. BLAT---The BLAST-Like Alignment Tool. Genome Res. 12, 656–664. https://doi.org/10.1101/gr.229202

Khamis, A.M., Essack, M., Gao, X., Bajic, V.B., 2015. Distinct profiling of antimicrobial peptide families. Bioinformatics 31, 849–856. https://doi.org/10.1093/bioinformatics/btu738

Kiemnec-Tyburczy, K.M., Richmond, J.Q., Savage, A.E., Lips, K.R., Zamudio, K.R., 2012. Genetic diversity of MHC class I loci in six non-model frogs is shaped by positive selection and gene duplication. Heredity 109, 146–155. https://doi.org/10.1038/hdy.2012.22

Kinne, A., Schülein, R., Krause, G., 2011. Primary and secondary thyroid hormone transporters. Thyroid Res. 4, S7. https://doi.org/10.1186/1756-6614-4-S1-S7

Kulikova, T., Akhtar, R., Aldebert, P., Althorpe, N., Andersson, M., Baldwin, A., Bates, K., Bhattacharyya, S., Bower, L., Browne, P., Castro, M., Cochrane, G., Duggan, K., Eberhardt, R., Faruque, N., Hoad, G., Kanz, C., Lee, C., Leinonen, R., Lin, Q., Lombard, V., Lopez, R., Lorenc, D., McWilliam, H., Mukherjee, G., Nardone, F., Pastor, M.P.G., Plaister, S., Sobhany, S., Stoehr, P., Vaughan, R., Wu, D., Zhu, W., Apweiler, R., 2007. EMBL Nucleotide Sequence Database in 2006. Nucleic Acids Res. 35, D16–D20. https://doi.org/10.1093/nar/gkl913

Kumar, S., Stecher, G., Tamura, K., 2016. MEGA7: Molecular Evolutionary Genetics Analysis Version 7.0 for Bigger Datasets. Mol. Biol. Evol. 33, 1870–1874. https://doi.org/10.1093/molbev/msw054

Lei, J., Mariash, C.N., Bhargava, M., Wattenberg, E.V., Ingbar, D.H., 2008. T3 increases Na-K-ATPase activity via a MAPK/ERK1/2-dependent pathway in rat adult alveolar epithelial cells. AJP Lung Cell. Mol. Physiol. 294, L749–L754. https://doi.org/10.1152/ajplung.00335.2007

Liu, H., Lei, M., Du, X., Cui, P., Zhang, S., 2016. Identification of a novel antimicrobial peptide from amphioxus Branchiostoma japonicum by in silico and functional analyses. Sci. Rep. 5. https://doi.org/10.1038/srep18355

Love, M.I., Huber, W., Anders, S., 2014. Moderated estimation of fold change and dispersion for RNA-seq data with DESeq2. Genome Biol. 15. https://doi.org/10.1186/s13059-014-0550-8

Luca, V., Stringaro, A., Colone, M., Pini, A., Mangoni, M.L., 2013. Esculentin(1-21), an amphibian skin membrane-active peptide with potent activity on both planktonic and biofilm cells of the bacterial pathogen Pseudomonas aeruginosa. Cell. Mol. Life Sci. 70, 2773–2786. https://doi.org/10.1007/s00018-013-1291-7

Maher, S.K., Wojnarowicz, P., Ichu, T.-A., Veldhoen, N., Lu, L., Lesperance, M., Propper, C.R., Helbing, C.C., 2016a. Rethinking the biological relationships of the thyroid hormones, l-thyroxine and 3,5,3′-triiodothyronine. Comp. Biochem. Physiol. Part D Genomics Proteomics 18, 44–53. https://doi.org/10.1016/j.cbd.2016.04.002

Maher, S.K., Wojnarowicz, P., Ichu, T.-A., Veldhoen, N., Lu, L., Lesperance, M., Propper, C.R., Helbing, C.C., 2016b. Rethinking the biological relationships of the thyroid hormones, l-thyroxine and 3,5,3′-triiodothyronine. Comp. Biochem. Physiol. Part D Genomics Proteomics 18, 44–53. https://doi.org/10.1016/j.cbd.2016.04.002

Malanovic, N., Lohner, K., 2016. Antimicrobial Peptides Targeting Gram-Positive Bacteria. Pharmaceuticals 9, 59. https://doi.org/10.3390/ph9030059

Mangoni, M.L., 2001. The synthesis of antimicrobial peptides in the skin of Rana esculenta is stimulated by microorganisms. FASEB J. https://doi.org/10.1096/fj.00-0695fje

Mangoni, M.L., Saugar, J.M., Dellisanti, M., Barra, D., Simmaco, M., Rivas, L., 2005. Temporins, small antimicrobial peptides with leishmanicidal activity. J. Biol. Chem. 280, 984–990. https://doi.org/10.1074/jbc.M410795200

Mistry, J., Finn, R.D., Eddy, S.R., Bateman, A., Punta, M., 2013. Challenges in homology search: HMMER3 and convergent evolution of coiled-coil regions. Nucleic Acids Res. 41, e121–e121. https://doi.org/10.1093/nar/gkt263

Miyata, K., Ose, K., 2012. Thyroid hormone-disrupting effects and the amphibian metamorphosis assay. J. Toxicol. Pathol. 25, 1–9. https://doi.org/10.1293/tox.25.1

Mochizuki, K., Goda, T., Yamauchi, K., 2012. Gene expression profile in the liver of *Rana catesbeiana* tadpoles exposed to low temperature in the presence of thyroid hormone. Biochem. Biophys. Res. Commun. 420, 845–850. https://doi.org/10.1016/j.bbrc.2012.03.085

Morales, H.D., Abramowitz, L., Gertz, J., Sowa, J., Vogel, A., Robert, J., 2010. Innate immune responses and permissiveness to ranavirus infection of peritoneal leukocytes in the frog *Xenopus laevis*. J. Virol. 84, 4912–4922. https://doi.org/10.1128/JVI.02486-09

Mullur, R., Liu, Y.-Y., Brent, G.A., 2014. Thyroid hormone regulation of metabolism. Physiol. Rev. 94, 355–382. https://doi.org/10.1152/physrev.00030.2013

Munita, J.M., Arias, C.A., 2016. Mechanisms of Antibiotic Resistance, in: Kudva, I.T., Cornick, N.A., Plummer, P.J., Zhang, Q., Nicholson, T.L., Bannantine, J.P.,

Bellaire, B.H. (Eds.), Virulence mechanisms of bacterial pathogens, Fifth Edition. American Society of Microbiology, pp. 481–511. https://doi.org/10.1128/microbiolspec.VMBF-0016-2015

Nathan, C., Cars, O., 2014. Antibiotic resistance — Problems, progress, and prospects. N. Engl. J. Med. 371, 1761–1763. https://doi.org/10.1056/NEJMp1408040

Nguyen, L.T., Haney, E.F., Vogel, H.J., 2011. The expanding scope of antimicrobial peptide structures and their modes of action. Trends Biotechnol. 29, 464–472. https://doi.org/10.1016/j.tibtech.2011.05.001

Nijnik, A., Hancock, R., 2009. Host defence peptides: antimicrobial and immunomodulatory activity and potential applications for tackling antibiotic-resistant infections. Emerg. Health Threats J. 2. https://doi.org/10.3134/ehtj.09.001

Nussey, S.S., Whitehead, S.A., 2001. Endocrinology: an integrated approach. Bios Scientific Publ, Oxford.

Oetting, A., Yen, P.M., 2007. New insights into thyroid hormone action. Best Pract. Res. Clin. Endocrinol. Metab. 21, 193–208. https://doi.org/10.1016/j.beem.2007.04.004

Ohnuma, A., Conlon, J.M., Iwamuro, S., 2009. Developmental and thyroid hormone-induced expression of preprotemporin genes in the skin of japanese mountain brown frog *Rana ornativentris*. Ann. N. Y. Acad. Sci. 1163, 494–496. https://doi.org/10.1111/j.1749-6632.2008.03665.x

Ortiga-Carvalho, T.M., Chiamolera, M.I., Pazos-Moura, C.C., Wondisford, F.E., 2016. Hypothalamus-pituitary-thyroid axis, in: Terjung, R. (Ed.), Comprehensive

Physiology. John Wiley & Sons, Inc., Hoboken, NJ, USA, pp. 1387–1428. https://doi.org/10.1002/cphy.c150027

Otvos Jr., L., 2016. Immunomodulatory effects of anti-microbial peptides. Acta Microbiol. Immunol. Hung. 63, 257–277. https://doi.org/10.1556/030.63.2016.005

Pan, C.-Y., Chen, J.-C., Sheen, J.-F., Lin, T.-L., Chen, J.-Y., 2014. Epinecidin-1 has immunomodulatory effects, facilitating its therapeutic use in a mouse model of *Pseudomonas aeruginosa* sepsis. Antimicrob. Agents Chemother. 58, 4264–4274. https://doi.org/10.1128/AAC.02958-14

Paquette, M.A., Atlas, E., Wade, M.G., Yauk, C.L., 2014. Thyroid hormone response element half-site organization and its effect on thyroid hormone mediated transcription. PLoS ONE 9, e101155. https://doi.org/10.1371/journal.pone.0101155

Partovi, S.H., Miliano, R.C., Robert, B., Veldhoen, N., Lesperance, M., Pyle, G.G., Van Aggelen, G., Helbing, C.C., 2017. Transcriptomic analysis of *Rana [Lithobates] catesbeiana* tadpole tail fin and liver tissues following exposure to thyroid hormones and estrogen. In preparation.

Pfaffl, M.W., Tichopad, A., Prgomet, C., Neuvians, T.P., 2004. Determination of stable housekeeping genes, differentially regulated target genes and sample integrity: BestKeeper – Excel-based tool using pair-wise correlations. Biotechnol. Lett. 26, 509–515.

Pietiäinen, M., François, P., Hyyryläinen, H.-L., Tangomo, M., Sass, V., Sahl, H.-G., Schrenzel, J., Kontinen, V.P., 2009. Transcriptome analysis of the responses of

Staphylococcus aureus to antimicrobial peptides and characterization of the roles of vraDE and vraSR in antimicrobial resistance. BMC Genomics 10, 429. https://doi.org/10.1186/1471-2164-10-429

Qiu, W., Shen, Y., Pan, C., Liu, S., Wu, M., Yang, M., Wang, K.-J., 2016. The potential immune modulatory effect of chronic bisphenol A exposure on gene regulation in male medaka (*Oryzias latipes*) liver. Ecotoxicol. Environ. Saf. 130, 146–154. https://doi.org/10.1016/j.ecoenv.2016.04.015

Quesada-García, A., Encinas, P., Valdehita, A., Baumann, L., Segner, H., Coll, J.M., Navas, J.M., 2016. Thyroid active agents $T_3$ and PTU differentially affect immune gene transcripts in the head kidney of rainbow trout (*Oncorhynchus mykiss*). Aquat. Toxicol. 174, 159–168. https://doi.org/10.1016/j.aquatox.2016.02.016

R Core Team, 2017. R: A language and environment for statistical computing. Foundation for Statistical Computing, Vienna, Austria.

Regnault, C., Willison, J., Veyrenc, S., Airieau, A., Méresse, P., Fortier, M., Fournier, M., Brousseau, P., Raveton, M., Reynaud, S., 2016. Metabolic and immune impairments induced by the endocrine disruptors benzo[ a ]pyrene and triclosan in *Xenopus tropicalis*. Chemosphere 155, 519–527. https://doi.org/10.1016/j.chemosphere.2016.04.047

Reilly, D.S., Tomassini, N., Zasloff, M., 1994. Expression of magainin antimicrobial peptide genes in the developing granular glands of *Xenopus* skin and induction by thyroid hormone. Dev. Biol. 162, 123–133. https://doi.org/10.1006/dbio.1994.1072

Robert, J., George, E., De Jesús Andino, F., Chen, G., 2011. Waterborne infectivity of the Ranavirus frog virus 3 in *Xenopus laevis*. Virology 417, 410–417. https://doi.org/10.1016/j.virol.2011.06.026

Robert, J., Ohta, Y., 2009. Comparative and developmental study of the immune system in *Xenopus*. Dev. Dyn. 238, 1249–1270. https://doi.org/10.1002/dvdy.21891

Robertson, G., Schein, J., Chiu, R., Corbett, R., Field, M., Jackman, S.D., Mungall, K., Lee, S., Okada, H.M., Qian, J.Q., Griffith, M., Raymond, A., Thiessen, N., Cezard, T., Butterfield, Y.S., Newsome, R., Chan, S.K., She, R., Varhol, R., Kamoh, B., Prabhu, A.-L., Tam, A., Zhao, Y., Moore, R.A., Hirst, M., Marra, M.A., Jones, S.J.M., Hoodless, P.A., Birol, I., 2010. De novo assembly and analysis of RNA-seq data. Nat. Methods 7, 909–912. https://doi.org/10.1038/nmeth.1517

Rollins-Smith, L.A., 2009. The role of amphibian antimicrobial peptides in protection of amphibians from pathogens linked to global amphibian declines. Biochim. Biophys. Acta BBA - Biomembr. 1788, 1593–1599. https://doi.org/10.1016/j.bbamem.2009.03.008

Rollins-Smith, L.A., 2005. Antimicrobial Peptide Defenses in Amphibian Skin. Integr. Comp. Biol. 45, 137–142. https://doi.org/10.1093/icb/45.1.137

Rollins-Smith, L.A., 1998. Metamorphosis and the amphibian immune system. Immunol. Rev. 166, 221–230. https://doi.org/10.1111/j.1600-065X.1998.tb01265.x

Rollins-Smith, L.A., Parsons, S.C.V., Cohen, N., 1988. Effects of thyroxine-driven precocious metamorphosis on maturation of adult-type allograft rejection

responses in early thyroidectomized frogs. Differentiation 37, 180–185. https://doi.org/10.1111/j.1432-0436.1988.tb00719.x

Rosa, G.M., Sabino-Pinto, J., Laurentino, T.G., Martel, A., Pasmans, F., Rebelo, R., Griffiths, R.A., Stöhr, A.C., Marschang, R.E., Price, S.J., Garner, T.W.J., Bosch, J., 2017. Impact of asynchronous emergence of two lethal pathogens on amphibian assemblages. Sci. Rep. 7, 43260. https://doi.org/10.1038/srep43260

Schadich, E., Cole, A.L.J., Squire, M., Mason, D., 2009. Skin peptides of different life stages of Ewing's tree frog. J. Exp. Zool. Part Ecol. Genet. Physiol. 313A, 532–537. https://doi.org/10.1002/jez.582

Schroeder, A., Jimenez, R., Young, B., Privalsky, M.L., 2014. The ability of thyroid hormone receptors to sense t $_4$ as an agonist depends on receptor isoform and on cellular cofactors. Mol. Endocrinol. 28, 745–757. https://doi.org/10.1210/me.2013-1335

Sengupta, S., Sharma, C.G.N., Jordan, V.C., 2010. Estrogen regulation of X-box binding protein-1 and its role in estrogen induced growth of breast and endometrial cancer cells. Horm. Mol. Biol. Clin. Investig. 2. https://doi.org/10.1515/hmbci.2010.025

Shi, Y.-B., 2013. Unliganded thyroid hormone receptor regulates metamorphic timing via the recruitment of histone deacetylase complexes, in: Current Topics in Developmental Biology. Elsevier, pp. 275–297. https://doi.org/10.1016/B978-0-12-396968-2.00010-5

Shi, Y.-B., 2009. Dual functions of thyroid hormone receptors in vertebrate development: The roles of histone-modifying cofactor complexes. Thyroid 19, 987–999. https://doi.org/10.1089/thy.2009.0041

Shi, Y.-B., 2000. Amphibian metamorphosis: from morphology to molecular biology. Wiley-Liss, New York.

Shi, Y.-B., Hasebe, T., Fu, L., Fujimoto, K., Ishizuya-Oka, A., 2011. The development of the adult intestinal stem cells: Insights from studies on thyroid hormone-dependent amphibian metamorphosis. Cell Biosci. 1, 30. https://doi.org/10.1186/2045-3701-1-30

Sievers, F., Wilm, A., Dineen, D., Gibson, T.J., Karplus, K., Li, W., Lopez, R., McWilliam, H., Remmert, M., Soding, J., Thompson, J.D., Higgins, D.G., 2014. Fast, scalable generation of high-quality protein multiple sequence alignments using Clustal Omega. Mol. Syst. Biol. 7, 539–539. https://doi.org/10.1038/msb.2011.75

Soloviev, M., Shaw, C., Andrén, P., 2008. Peptidomics: methods and applications. Wiley-Interscience, Hoboken, N.J.

Song, Y., Yao, X., Ying, H., 2011. Thyroid hormone action in metabolic regulation. Protein Cell 2, 358–368. https://doi.org/10.1007/s13238-011-1046-x

Tata, J.R., 2006. Amphibian metamorphosis as a model for the developmental actions of thyroid hormone. Mol. Cell. Endocrinol. 246, 10–20. https://doi.org/10.1016/j.mce.2005.11.024

Tatiersky, L., Rollins-Smith, L.A., Lu, R., Jardine, C., Barker, I.K., Clark, M.E., Caswell, J.L., 2015. Effect of glucocorticoids on expression of cutaneous antimicrobial peptides in northern leopard frogs (Lithobates pipiens). BMC Vet. Res. 11. https://doi.org/10.1186/s12917-015-0506-6

Taylor, A.C., Kollros, J.J., 1946. Stages in the normal development of *Rana pipiens* larvae. Anat. Rec. 94, 7–13.

Thekkiniath, J.C., Zabet-Moghaddam, M., San Francisco, S.K., San Francisco, M.J., 2013. A novel subtilisin-like serine protease of Batrachochytrium dendrobatidis is induced by thyroid hormone and degrades antimicrobial peptides. Fungal Biol. 117, 451–461. https://doi.org/10.1016/j.funbio.2013.05.002

Valore, E.V., Ganz, T., 2008. Posttranslational processing of hepcidin in human hepatocytes is mediated by the prohormone convertase furin. Blood Cells. Mol. Dis. 40, 132–138. https://doi.org/10.1016/j.bcmd.2007.07.009

Van Rooij, P., Martel, A., Haesebrouck, F., Pasmans, F., 2015. Amphibian chytridiomycosis: a review with focus on fungus-host interactions. Vet. Res. 46. https://doi.org/10.1186/s13567-015-0266-0

VanCompernolle, S.E., Taylor, R.J., Oswald-Richter, K., Jiang, J., Youree, B.E., Bowie, J.H., Tyler, M.J., Conlon, J.M., Wade, D., Aiken, C., Dermody, T.S., KewalRamani, V.N., Rollins-Smith, L.A., Unutmaz, D., 2005. Antimicrobial peptides from amphibian skin potently inhibit human immunodeficiency virus infection and transfer of virus from dendritic cells to T cells. J. Virol. 79, 11598–11606. https://doi.org/10.1128/JVI.79.18.11598-11606.2005

Vanhoye, D., Bruston, F., Nicolas, P., Amiche, M., 2003. Antimicrobial peptides from hylid and ranin frogs originated from a 150-million-year-old ancestral precursor with a conserved signal peptide but a hypermutable antimicrobial domain. Eur. J. Biochem. 270, 2068–2081. https://doi.org/10.1046/j.1432-1033.2003.03584.x

Vasudevan, N., Ogawa, S., Pfaff, D., 2002. Estrogen and thyroid hormone receptor interactions: Physiological flexibility by molecular specificity. Physiol. Rev. 82, 923–944. https://doi.org/10.1152/physrev.00014.2002

Veldhoen, N., Propper, C.R., Helbing, C.C., 2014. Enabling comparative gene expression studies of thyroid hormone action through the development of a flexible real-time quantitative PCR assay for use across multiple anuran indicator and sentinel species. Aquat. Toxicol. 148, 162–173. https://doi.org/10.1016/j.aquatox.2014.01.008

Visser, W.E., Friesema, E.C.H., Jansen, J., Visser, T.J., 2007. Thyroid hormone transport by monocarboxylate transporters. Best Pract. Res. Clin. Endocrinol. Metab. 21, 223–236. https://doi.org/10.1016/j.beem.2007.03.008

Waghu, F.H., Barai, R.S., Gurung, P., Idicula-Thomas, S., 2016. CAMP $_{R3}$ : a database on sequences, structures and signatures of antimicrobial peptides: Table 1. Nucleic Acids Res. 44, D1094–D1097. https://doi.org/10.1093/nar/gkv1051

Wang, Z., 2004. APD: the Antimicrobial Peptide Database. Nucleic Acids Res. 32, 590D–592. https://doi.org/10.1093/nar/gkh025

Wen, L., Shi, Y.-B., 2015. Unliganded Thyroid Hormone Receptor α Controls Developmental Timing in *Xenopus tropicalis*. Endocrinology 156, 721–734. https://doi.org/10.1210/en.2014-1439

Wernersson, R., 2006. Virtual Ribosome--a comprehensive DNA translation tool with support for integration of sequence feature annotation. Nucleic Acids Res. 34, W385–W388. https://doi.org/10.1093/nar/gkl252

World Health Organization, 2015. Global action plan on antimicrobial resistance.

World Health Organization (Ed.), 2014. Antimicrobial resistance: global report on surveillance. World Health Organization, Geneva, Switzerland.

Yang, S.-J., Xiao, X.-H., Xu, Y.-G., Li, D.-D., Chai, L.-H., Zhang, J.-Y., 2012. Induction of antimicrobial peptides from *Rana dybowskii* under Rana grylio virus stress, and bioactivity analysis. Can. J. Microbiol. 58, 848–855. https://doi.org/10.1139/w2012-055

Yaoita, Y., Brown, D.D., 1990. A correlation of thyroid hormone receptor gene expression with amphibian metamorphosis. Genes Dev. 4, 1917–1924.

Yen, P.M., 2015. Unliganded TRs regulate growth and developmental timing during early embryogenesis: evidence for a dual function mechanism of TR action. Cell Biosci. 5, 8. https://doi.org/10.1186/2045-3701-5-8

Yen, P.M., 2001. Physiological and molecular basis of thyroid hormone action. Am. Physiol. Soc. 81, 1097–1142.

Yen, P.M., Feng, X., Flamant, F., Chen, Y., Walker, R.L., Weiss, R.E., Chassande, O., Samarut, J., Refetoff, S., Meltzer, P.S., 2003. Effects of ligand and thyroid hormone receptor isoforms on hepatic gene expression profiles of thyroid hormone receptor knockout mice. EMBO Rep. 4, 581–587. https://doi.org/10.1038/sj.embor.embor862

Yoshizato, K., Kistler, A., Frieden, E., 1975. Binding of Thyroid Hormones by Nuclei of Cells from Bullfrog Tadpole Tail Fins [1]. Endocrinology 97, 1030–1035. https://doi.org/10.1210/endo-97-4-1030

Zhang, D., Li, Y., Liu, S., Wang, Y., Guo, F., Zhai, Q., Jiang, J., Ying, H., 2017. microRNA and thyroid hormone signaling in cardiac and skeletal muscle. Cell Biosci. 7. https://doi.org/10.1186/s13578-017-0141-y

Zhao, X., Lorenc, H., Stephenson, H., Wang, Y.J., Witherspoon, D., Katzenellenbogen, B., Pfaff, D., Vasudevan, N., 2005. Thyroid hormone can increase estrogen-mediated transcription from a consensus estrogen response element in neuroblastoma cells. Proc. Natl. Acad. Sci. 102, 4890–4895. https://doi.org/10.1073/pnas.0501042102

Zimmerman, L.M., Vogel, L.A., Bowden, R.M., 2010. Understanding the vertebrate immune system: insights from the reptilian perspective. J. Exp. Biol. 213, 661–671. https://doi.org/10.1242/jeb.038315

# Appendix

## Appendix A Summary of tail fin and liver RNA-seq read counts following alignment to BART

| Tail Fin - $E_2$ | | | | |
|---|---|---|---|---|
| Sample | Reads in Input File | Unmapped | % Aligned | % BART Contigs w/ at least 1 aligned read |
| Vehicle | | | | |
| Solvent 1 | 101783863 | 232124 | 99.8 | 82.5 |
| Solvent 2 | 90132212 | 279035 | 99.7 | 86.8 |
| Solvent 3 | 97543035 | 296365 | 99.7 | 85.9 |
| Solvent 4 | 91984980 | 253176 | 99.7 | 85.9 |
| Solvent 5 | 101292806 | 273376 | 99.7 | 86.6 |
| | | | | |
| **Mean** | **96547379** | **266815** | **99.7** | **85.5** |
| **SD** | **5312745** | **24774** | **0.0** | **1.8** |
| $E_2H$ | | | | |
| High Conc. 1 | 104732909 | 269724 | 99.7 | 86.7 |
| High Conc. 2 | 104925993 | 306222 | 99.7 | 87.0 |
| High Conc. 3 | 99900720 | 289838 | 99.7 | 86.3 |
| High Conc. 4 | 84556224 | 230614 | 99.7 | 84.5 |
| High Conc. 5 | 97166609 | 272501 | 99.7 | 86.1 |
| | | | | |
| **Mean** | **98256491** | **273780** | **99.7** | **86.1** |
| **SD** | **8336889** | **28248** | **0.0** | **1.0** |

| Tail Fin - $T_4$ | | | | |
|---|---|---|---|---|
| Sample | Reads in Input File | Unmapped | % Aligned | % BART Contigs w/ at least 1 aligned read |
| Vehicle | | | | |
| Solvent 1 | 107972018 | 316975 | 99.7 | 86.8 |
| Solvent 2 | 95324726 | 285227 | 99.7 | 86.3 |
| Solvent 3 | 93483024 | 253021 | 99.7 | 85.6 |
| Solvent 4 | 105389468 | 273448 | 99.7 | 87.2 |
| Solvent 5 | 107486919 | 309929 | 99.7 | 87.4 |
| | | | | |
| **Mean** | **101931231** | **287720** | **99.7** | **86.6** |
| **SD** | **6970192** | **26282** | **0.0** | **0.7** |

| $T_4H$ | | | | |
|---|---|---|---|---|
| High Conc. 1 | 99259965 | 316975 | 99.7 | 87.1 |
| High Conc. 2 | 90155233 | 299781 | 99.7 | 86.7 |
| High Conc. 3 | 96361483 | 283760 | 99.7 | 86.8 |
| High Conc. 4 | 101337702 | 328575 | 99.7 | 87.6 |
| High Conc. 5 | 85585541 | 257653 | 99.7 | 86.3 |
| | | | | |
| **Mean** | **94539985** | **297349** | **99.7** | **86.9** |
| **SD** | **6542422** | **27958** | **0.0** | **0.5** |

| Tail Fin - $T_3$ | | | | |
|---|---|---|---|---|
| Sample | Reads in Input File | Unmapped | % Aligned | % BART Contigs w/ at least 1 aligned read |
| Vehicle | | | | |
| Solvent 1 | 96759492 | 241884 | 99.8 | 85.8 |
| Solvent 2 | 102788141 | 257173 | 99.7 | 86.6 |
| Solvent 3 | 101910995 | 266161 | 99.7 | 86.4 |
| Solvent 4 | 97153525 | 243711 | 99.7 | 85.2 |
| Solvent 5 | 96306553 | 275138 | 99.7 | 86.6 |
| | | | | |
| **Mean** | **98983741** | **256813** | **99.7** | **86.1** |
| **SD** | **3102684** | **14299** | **0.0** | **0.6** |
| $T_3H$ | | | | |
| High Conc. 1 | 95227043 | 251655 | 99.7 | 86.4 |
| High Conc. 2 | 94379039 | 245221 | 99.7 | 85.9 |
| High Conc. 3 | 94389390 | 246988 | 99.7 | 86.2 |
| High Conc. 4 | 100646664 | 264406 | 99.7 | 87.2 |
| High Conc. 5 | 100990252 | 245333 | 99.8 | 85.5 |
| | | | | |
| **Mean** | **97126478** | **250721** | **99.7** | **86.3** |
| **SD** | **3389999** | **8083** | **0.0** | **0.6** |

| Liver - $E_2$ | | | | |
|---|---|---|---|---|
| Sample | Reads in Input File | Unmapped | % Aligned | % BART Contigs w/ at least 1 aligned read |
| Vehicle | | | | |
| Solvent 1 | 110311686 | 292141 | 99.7 | 75.6 |
| Solvent 2 | 94173329 | 200550 | 99.8 | 68.9 |
| Solvent 3 | 91796761 | 472421 | 99.5 | 67.1 |
| Solvent 4 | 100871620 | 179190 | 99.8 | 73.6 |
| Solvent 5 | 93925502 | 217617 | 99.8 | 77.1 |
| | | | | |
| **Mean** | **98215780** | **272384** | **99.7** | **72.5** |
| **SD** | **7571594** | **119635** | **0.1** | **4.3** |

| $E_2H$ | | | | |
|---|---|---|---|---|
| High Conc. 1 | 87927912 | 147961 | 99.8 | 72.1 |
| High Conc. 2 | 100778765 | 178012 | 99.8 | 72.4 |
| High Conc. 3 | 97982404 | 204684 | 99.8 | 73.1 |
| High Conc. 4 | 102338061 | 230712 | 99.8 | 72.9 |
| High Conc. 5 | 103090416 | 209296 | 99.8 | 74.7 |
| | | | | |
| **Mean** | **98423512** | **194133** | **99.8** | **73.1** |
| **SD** | **6184721** | **31902** | **0.0** | **1.0** |

| Liver - $T_4$ | | | | |
|---|---|---|---|---|
| Sample | Reads in Input File | Unmapped | % Aligned | % BART Contigs w/ at least 1 aligned read |
| Vehicle | | | | |
| Solvent 1 | 92845041 | 158265 | 99.8 | 71.5 |
| Solvent 2 | 91118081 | 177845 | 99.8 | 72.8 |
| Solvent 3 | 96926090 | 187618 | 99.8 | 71.5 |
| Solvent 4 | 92202158 | 198502 | 99.8 | 74.3 |
| Solvent 5 | 95456497 | 181124 | 99.8 | 71.0 |
| | | | | |
| **Mean** | **93709573** | **180671** | **99.8** | **72.2** |
| **SD** | **2404853** | **14802** | **0.0** | **1.3** |
| $T_4H$ | | | | |
| High Conc. 1 | 100838494 | 222048 | 99.8 | 76.6 |
| High Conc. 2 | 101756944 | 206213 | 99.8 | 72.8 |
| High Conc. 3 | 98431072 | 211557 | 99.8 | 71.6 |
| High Conc. 4 | 91156764 | 230704 | 99.7 | 70.3 |
| High Conc. 5 | 96455702 | 180261 | 99.8 | 72.5 |
| | | | | |
| **Mean** | **97727795** | **210157** | **99.8** | **72.8** |
| **SD** | **4219057** | **19202** | **0.0** | **2.4** |

| Liver - $T_3$ | | | | |
|---|---|---|---|---|
| Sample | Reads in Input File | Unmapped | % Aligned | % BART Contigs w/ at least 1 aligned read |
| Vehicle | | | | |
| Solvent 1 | 98114214 | 219168 | 99.8 | 74.0 |
| Solvent 2 | 88346444 | 178265 | 99.8 | 73.8 |
| Solvent 3 | 90113214 | 184595 | 99.8 | 71.5 |
| Solvent 4 | 98981025 | 201654 | 99.8 | 73.4 |
| Solvent 5 | 83317497 | 153161 | 99.8 | 72.4 |
| | | | | |
| **Mean** | **91774479** | **187369** | **99.8** | **73.0** |
| **SD** | **6673798** | **24880** | **0.0** | **1.1** |

| $T_3H$ | | | | |
|---|---|---|---|---|
| High Conc. 1 | 92483873 | 235609 | 99.7 | 70.1 |
| High Conc. 2 | 84021587 | 216946 | 99.7 | 70.1 |
| High Conc. 3 | 94401304 | 166637 | 99.8 | 72.0 |
| High Conc. 4 | 93083212 | 133843 | 99.9 | 69.6 |
| High Conc. 5 | 85832761 | 141496 | 99.4 | 66.6 |
| | | | | |
| **Mean** | **89964547** | **178906** | **99.7** | **69.7** |
| **SD** | **4694367** | **45395** | **0.2** | **1.9** |

**Appendix B Biological process GO Panther-Slim bar chart of difference of A) $T_4$-treated or B) $T_3$-treated differentially expressed tail fin contigs.**

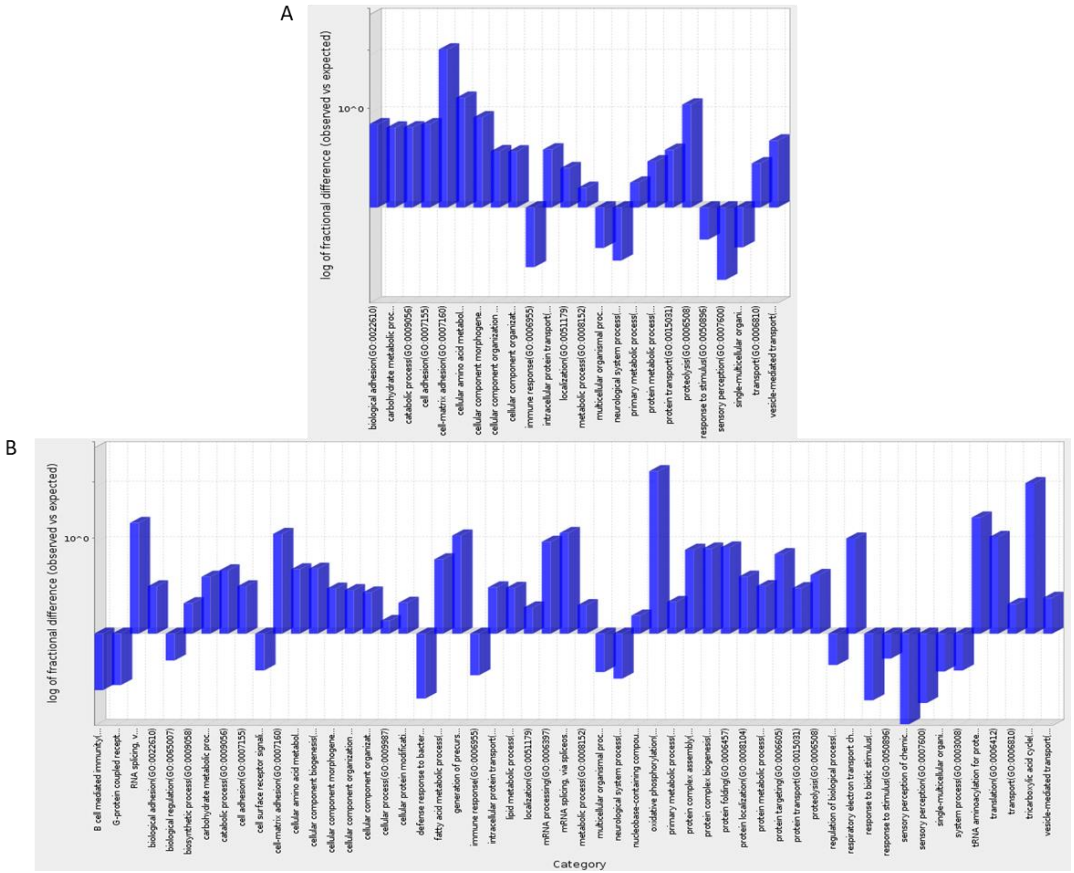

**Appendix C Biological process GO Panther-Slim bar chart of difference of A) $E_2$-treated, B) $T_4$-treated or C) $T_3$-treated differentially expressed liver contigs.**

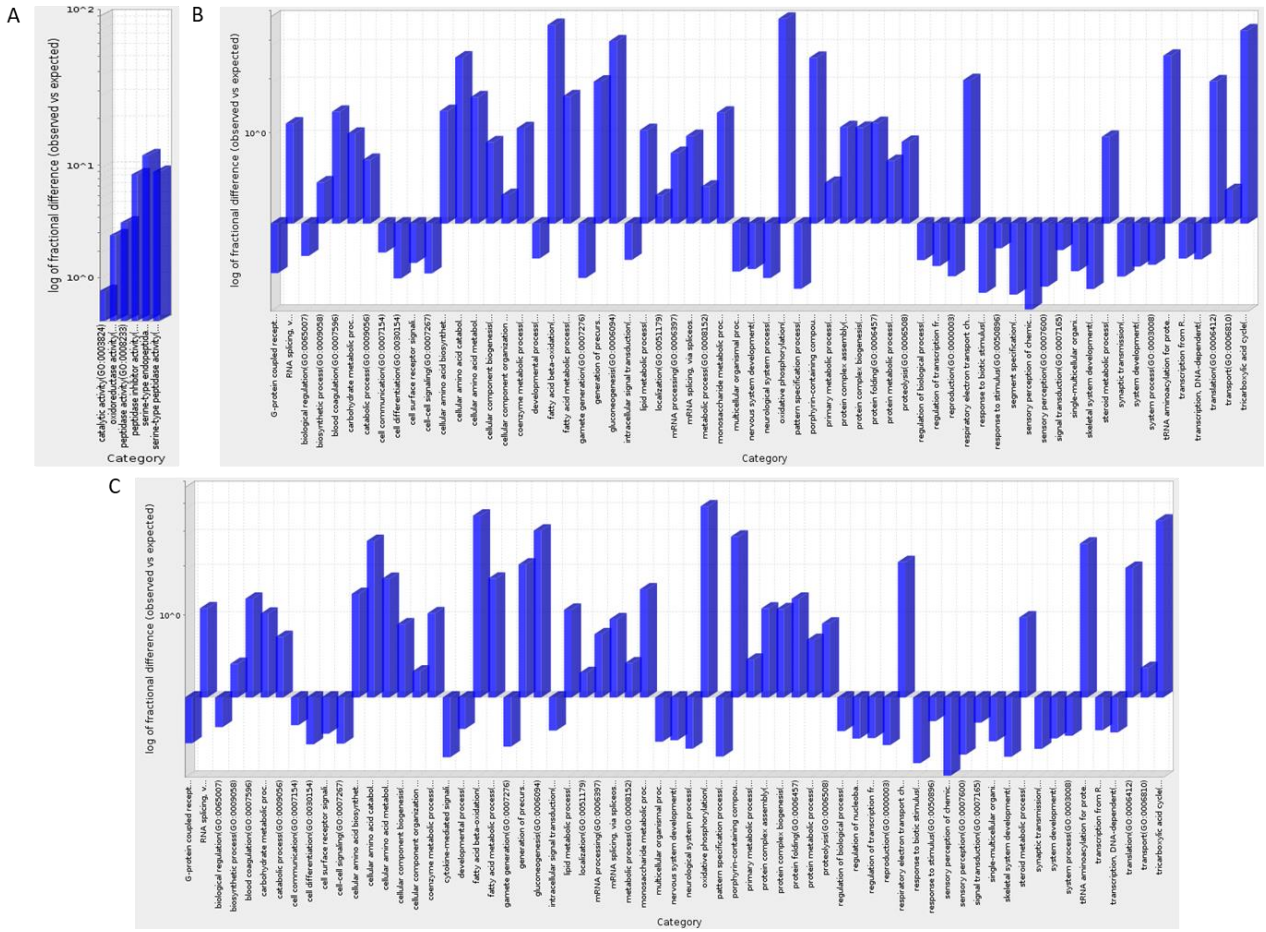

**Appendix D Putative precursor peptide alignments with top BLASTP aligned reference AMPs. The cleavage site (KR) for generating the mature peptide is underlined.**

```
A   ACO51651.1-Ranatuerin-4      MFTSKKSLLLLFFLGTINLSFCEEERDAEEERRDNPDERDVEVEKRFLPFIARLAAKVFP
    CCH-0008-T_R4012255          MFTLKKSLLLLFFLGTINLSLCEEERDAEEERRDNPDERDVEVEKRFLPFIA-LAAKVFP
                                 *** ****************:****************************** *******

    ACO51651.1-Ranatuerin-4      SIICSVTKKC
    CCH-0008-T_R4012255          SIICSVTKKC
                                 **********

B   ACR46972.1-Ranatuerin-1      MFTLKKSLLLLFFLGTITLSLCEQERGADEEEGNGEKEIKRSMLSVLKNLGKVGLGFVAC
    CCH-0008-T_S4110533          -----MSSFCEITNVALTISLSSPRRGADEEEGNGEKEIKRSMLSVLKNLGKVGLGFVAC
                                       * :  :   ::*:**.. .**********************************

    ACR46972.1-Ranatuerin-1      KINKQC
    CCH-0008-T_S4110533          KINKQC
                                 ******

C   ACR84056.1-Catesbeianin-1    ---------MFTMKKSEKERRERGKRMMRVMRRKTKVIWEKKDFIGLYSID
    CCH-0013-C_S4288341          MRKRMTMRRMMKKKKSEKERRERGKRMMRVMRRKTKVIWEKKDFIGLYSID
                                         *:. ************************************

D   ACR84073.1-Ranatuerin-2RC    MFTVKKSLLLLFFLGTITLSLCEQERGADEDNGGEMTEEEVKRGLFLDTLKGAAKDVAGK
    CCH-0008-T_R4012400          MFTLKKSLLLLFFLGTITLSLCEQERGADEDNGGEMTEEEVKRGLFLDTLKGA-KDVAGK
                                 ***:********************************************** ******

    ACR84073.1-Ranatuerin-2RC    LLEGLKCKITGCKP
    CCH-0008-T_R4012400          LLEGLKCKITGCKP
                                 **************

E   ACR84072.1-Ranatuerin-3RC    MFTMKKSLLLLFFLGTISLSLCEPQRDADEVKEVKRGFLDIIKNLGKTFAGHMLDKIKCT
    CCH-0008-T_J4042717          -----------------MFFMSSPRRDADEVKEVKRGFLDIIKNLGKTFAGHMLDKIKCT
                                                 : :..*:**********************************

    ACR84072.1-Ranatuerin-3RC    IGTCPPSP
    CCH-0008-T_J4042717          IGTCPPSP
                                 ********

F   ACR84085.1-Palustrin-Ca      MFTMKKSLLLLFFLGTISLSLCEQERDADGDEGEVEEVKRGFLDIIKDTGKEFAVKILNN
    CCH-0008-T_S4147914          -----------------MITVSSPRRDADGDEGEVEEVKRGFLDIIKDTGKEFAVKILNN
                                               ::::.. .**********************************

    ACR84085.1-Palustrin-Ca      LKCKLAGGCPP
    CCH-0008-T_S4147914          LKCKLAGGCPP
                                 ***********

G   ACR84059.1-Ranacyclin-Ca
    CCH-0008-T_S4162036          embargoed

H   AFR43665.1-Ranatuerin-2PRc
    CCH-BS01-S14839083           embargoed
```

**Appendix E ClustalW alignment of BART-derived peptides, known NCBI AMPs, and outgroup NCBI AMPs. Alignment was performed using default parameters on MEGA 7.0.**